FUEL CELLS FOR TRANSPORTATION

2001
ANNUAL
PROGRESS
REPORT

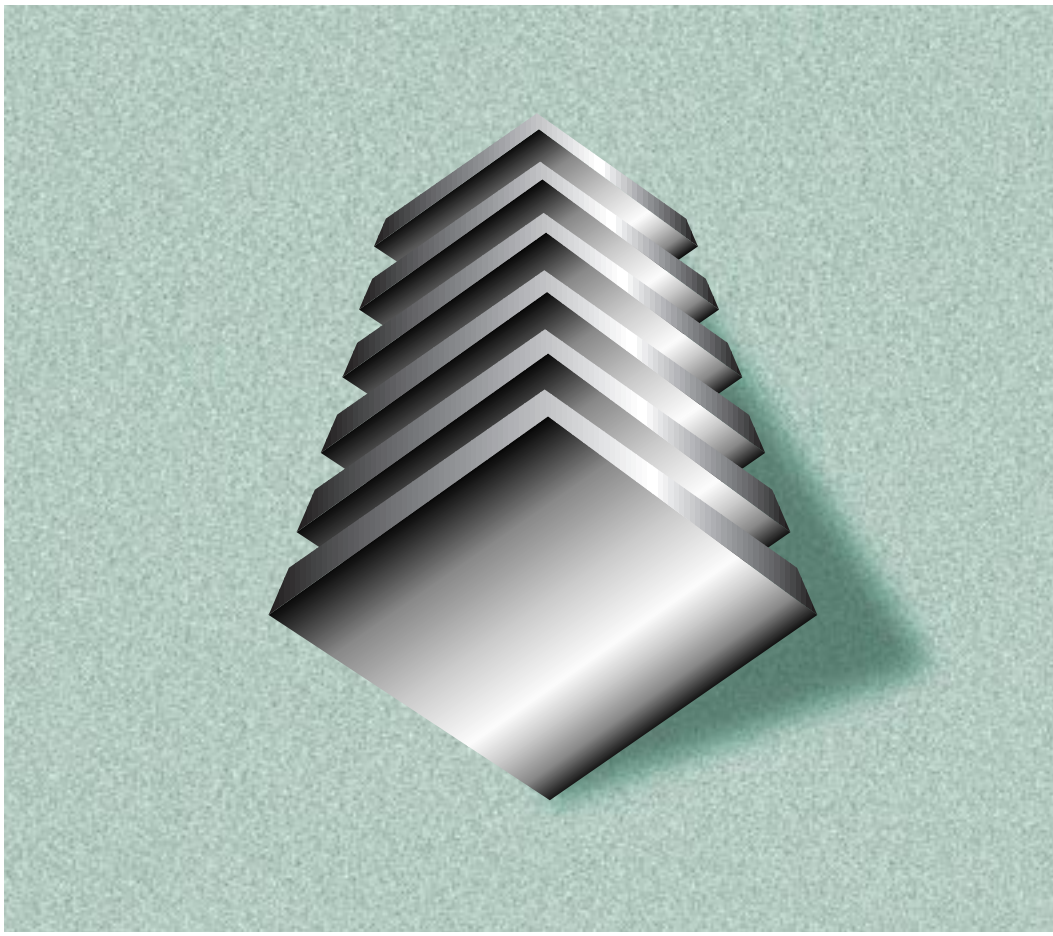

U.S. Department of Energy

Energy Efficiency and Renewable Energy

Office of Transportation Technologies

ACKNOWLEDGEMENT

We would like to express our sincere appreciation to Argonne National Laboratory for its artistic and technical contributions in preparing and publishing this report.

In addition, we would like to thank all our program participants for their contributions to the programs and all the authors who prepared the project abstracts that comprise this report.

U.S. Department of Energy
Office of Advanced Automotive Technologies
1000 Independence Avenue, S.W.
Washington, D.C. 20585-0121

FY 2001

Progress Report for Fuel Cells for Transportation

Energy Efficiency and Renewable Energy
Office of Transportation Technologies

Approved by Steven Chalk Energy Conversion Team Leader

December 2001

CONTENTS

CONTENTS (Cont.)

I. INTRODUCTION

Developing Advanced PEM Fuel Cell Technologies for Transportation Power Systems

We are pleased to present the Fiscal Year (FY) 2001 Annual Progress Report for the Fuel Cells for Transportation Program. Every year, we provide an overview of the nature, objectives, and progress of the program; examine the remaining technical barriers to commercialization of the technology; and highlight the program's future directions. The reader is also referred to the FY 2001 Annual Progress Reports on "Fuels for Advanced CIDI Engines and Fuel Cells," "Automotive Propulsion Materials," and "Snapshots of CARAT Projects (September 2001)" for additional information on the Office of Transportation Technologies' (OTT's) R&D activities supporting the development of fuel cell technology.

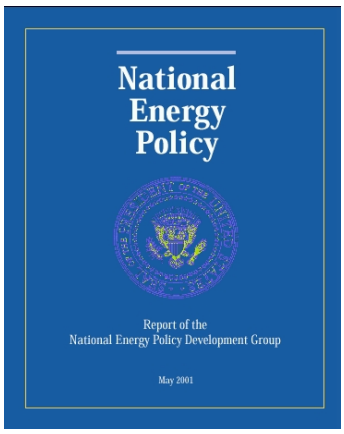

In May 2001, the president's National Energy Policy Development Group published the National Energy Policy (NEP). This comprehensive energy policy specifically recommended the development of energy-efficient vehicle technologies, including hybrid systems, fuel cells, and hydrogen-based systems. The NEP is a strong indicator of the continuing federal support for fuel cell technologies in the transportation sector.

Worldwide interest in fuel cell technology remains very strong for a broad range of transportation, stationary, and portable power applications. In the transportation sector, U.S. automotive and fuel cell companies continue to announce major breakthroughs in the technology, introduce new development vehicles, and form new partnerships. The major energy providers of both conventional and alternative fuels are playing an increasing role in addressing important fuel infrastructure issues. The U.S. Department of Energy (DOE) remains committed to contributing to this progress in a significant way by supporting R&D activities that address the most critical barriers to the introduction of commercially viable polymer-electrolyte-membrane (PEM) fuel cell systems.

The mission of the Fuel Cells for Transportation Program is to support fuel cell R&D activities that will lead to the private-sector development of highly efficient, low- or zero-emission fuel cell propulsion systems for automotive applications. The DOE program supports the Partnership for a New Generation of Vehicles (PNGV), a cooperative research and development partnership between the federal government and the U.S. Council for Automotive Research, which consists of Ford, General Motors (GM), and DaimlerChrysler. Since its inception, the Fuel Cells for Transportation Program has supported PNGV through its technology research projects. The Partnership goals are being reevaluated to identify changes that will maximize the potential national petroleum savings benefit of the emerging advanced technologies. When these goal changes have been identified, OTT will adjust the focus of its technology research programs accordingly.

The primary purpose of this report is to document the progress made by the DOE Fuel Cells for Transportation Program during FY 2001 in overcoming the R&D barriers and addressing the tasks identified in the Office of Advanced Automotive Technologies R&D Plan.[1] However, we will also highlight some of the major advances in fuel cell technology made through other private and public initiatives throughout the year.

[1] http://www.tis.anl.gov:8000/db1/cartech/document/DDD/1.pdf.

In October 2000, Ford introduced the world's first production-prototype, direct-hydrogen-powered fuel cell vehicle: the Focus FCV. This car is Ford's second hydrogen-fueled, fuel-cell-powered vehicle. As built today, the Focus FCV has a range of about 100 miles and power that is comparable with that of the standard Focus with an internal combustion engine.

Ford Focus direct hydrogen fuel cell vehicle.

DaimlerChrysler introduced two new methanol-fueled fuel cell cars in the fall of 2000: the NECAR 5 (based on the Mercedes-Benz A Class) and the Jeep® Commander 2. According to DaimlerChrysler, the NECAR 5's fuel cell drive system requires no more space than a conventional drive system, and its energy efficiency is almost twice that of a gasoline engine. The Jeep® Commander 2 is a fuel cell/battery hybrid that uses batteries to (1) provide supplemental energy during acceleration and cold starts and (2) capture energy during regenerative braking.

DaimlerChrysler's NECAR 5 and Jeep Commander 2 methanol-fueled fuel cell vehicle.

General Motors, in collaboration with ExxonMobil, announced the development of a highly efficient gasoline reformer system for fuel cell vehicles. In August 2001, GM introduced a Chevrolet S-10 Fuel Cell Pickup (a concept vehicle) with its Gen III fuel cell engine operating on ultra-low-sulfur gasoline. GM engineers believe that the gasoline fuel processor is a key to the production of fuel cell vehicles in this decade, since consumers would be able to fuel these vehicles in the same way they fuel their present vehicles.

Chevrolet S-10 truck with on-board gasoline reformer.

To accelerate the development of fuel cell vehicles, the California Fuel Cell Partnership (CaFCP) was established in West Sacramento, Calif., in November 2000. For more information on the status and activities of the CaFCP, the reader is referred to the "Fuels for Advanced CIDI Engines and Fuel Cells FY 2001 Annual Report."

The DOE Fuel Cells for Transportation Program is implemented through cost-shared cooperative agreements with automotive suppliers and fuel cell and component developers. Furthermore, DOE national laboratories and universities throughout the United States conduct R&D activities to increase the knowledge base and develop enabling technologies for PEM fuel cells.

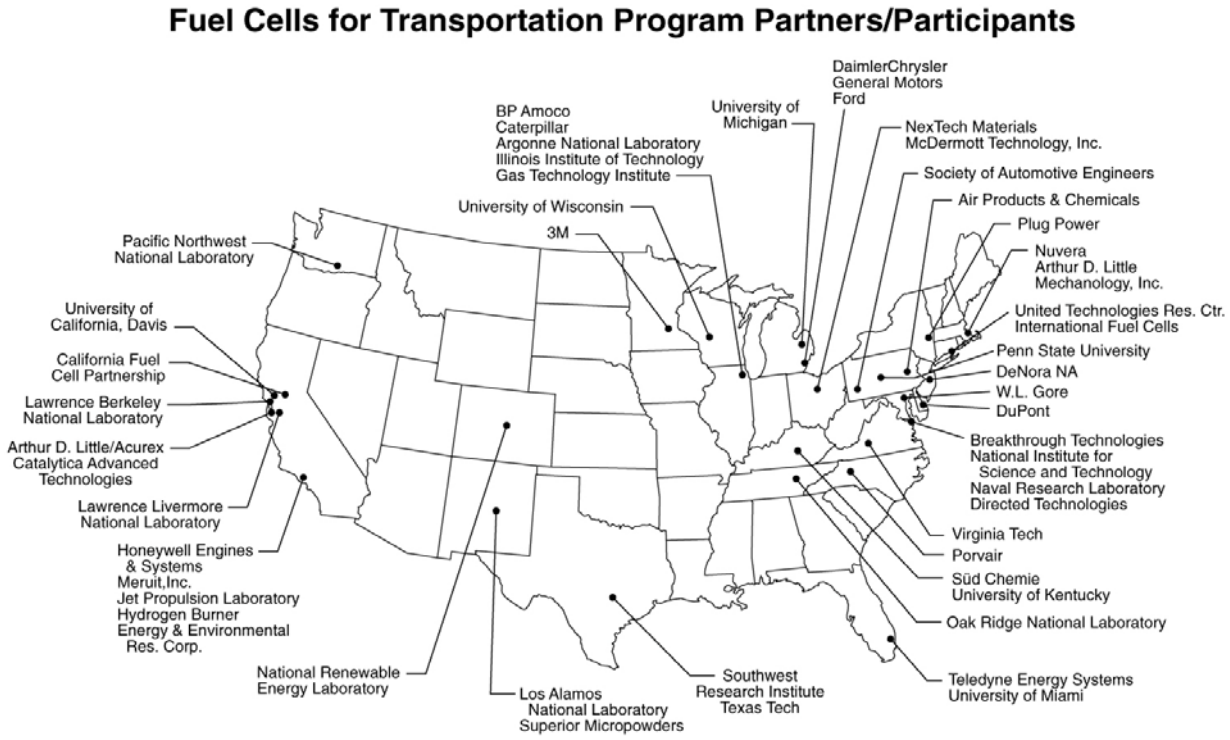

DOE Fuel Cells for Transportation Fuels Strategy

Through the Fuels for Fuel Cells Program, DOE is pursuing a dual pathway to evaluate fuels for fuel cell vehicles. Advanced petroleum-based fuel, which is "gasoline-like," is compatible with the existing refueling infrastructure and will enable the most widespread use of fuel cell vehicles over the next several decades. The program is developing on-board fuel processors to reform gasoline and such alternative fuels as methanol, ethanol, and natural gas to produce the required hydrogen.

In collaboration with the DOE Hydrogen Program, the Fuels for Fuel Cells Program is also developing technologies for a hydrogen-refueling infrastructure that will enable fuel cell vehicles to be powered by hydrogen produced from nonrenewable and renewable resources and stored directly on the vehicle. The two major issues related to these technologies are (1) the economic viability of a new refueling infrastructure as fuel cell vehicles are introduced into the marketplace and (2) an ability to provide sufficient hydrogen storage volume aboard the vehicles.

Technical and Economic Status and Challenges

During FY 2001, the first integrated, automotive-scale, gasoline fuel cell systems were built and tested, enabling us to benchmark the status of the technology and the technical challenges facing automotive fuel cell systems. Before 2001, technical status was projected from component and subsystem performance and not from complete integrated systems. For this reason, 2001 status numbers for systems (see Table 1) may indicate poorer performance when compared with last year (e.g., transient response and start-up time). Our improved understanding of PEM fuel cell systems has also led to revised targets and timing to better reflect the status of the technology, anticipated progress, and future requirements of PNGV fuel cell vehicles.

Technical and economic targets are being developed for direct hydrogen transportation PEM fuel cell systems. Direct hydrogen PEM fuel cell systems are more technically mature and face fewer challenges than systems requiring an on-board fuel processor. Although the demonstrated performance and efficiency of direct hydrogen systems approach the anticipated goals, several issues remain. The primary barriers are lack of a refueling infrastructure, on-board hydrogen storage, cost, durability, size, and weight.

Table 1. 50-kW integrated fuel cell power systems operating on Tier 2 gasoline containing average 30 ppm sulfur.

		Status		
Parameters	Unit	2001	2005	2010
Energy efficiency @ 25% of peak power	%	34	40	45
Energy efficiency @ peak power	%	31	33	35
Power density	W/L	140	250	325
Specific power	W/kg	140	250	325
Cost	$/kW	300	125	45
Transient response (from 10 to 90% power)	s	15	5	1
Cold start-up @ -20°C to maximum power	min	TBD	2	1
Cold start-up @ 20°C to maximum power	min	<10	<1	<0.5
Survivability	°C	TBD	-30	-40
Emissions		<Tier2 Bin5	<Tier2 Bin5	<Tier2 Bin5
Durability	h	1,000 (max)	2,000	5,000

Remaining technical challenges for gasoline-fueled fuel cell power systems include:

- Reducing component and system costs,
  - reducing precious metal requirements
  - developing high-volume manufacturing capability
- Demonstrating component and system durability,
- Reducing system start-up time,
- Developing high-efficiency air management subsystems, and
- Developing a suitable fuel infrastructure (sulfur-free gasoline and hydrogen).

Remaining economic challenges include the capital costs of manufacturing fuel cells, cost of a new fuel infrastructure, and competition from other technologies.

R&D Highlights

Researchers supporting the Fuel Cells for Transportation Program continued to make significant progress in meeting these challenges during FY 2001. Notable advances were achieved in systems development; fuel cell and fuel-processing subsystems technology; air compressor technology; and the development of low-cost, high-volume manufacturing processes for key components. The summaries that follow are selected highlights of the progress made under the program.

IFC Delivers Integrated, Atmospheric-Pressure Fuel Cell Power System. During FY 2001, International Fuel Cells (IFC) successfully tested and delivered a 50-kW (net) gasoline-fueled power plant to DOE for follow-on testing at Argonne National Laboratory (ANL). The system consists of a fully tested 50-kW-equivalent fuel-flexible fuel processing system and a 50-kW PEM stack assembly running at ambient pressure. Using a California Phase II reformulated gasoline fuel, the nominal 50-kW power plant achieved a maximum net output power of 53 kW with a maximum system efficiency of ~35% at a net power output of

~18 kW. At quarter power (12.5 kW), the fuel cell system efficiency was 32%, compared with the 20–25% energy efficiency of a typical internal combustion engine operating at between 20% and 30% of full load. In the second phase of the project, IFC will deliver to DOE an advanced gasoline-fueled 75-kW fuel cell power plant.

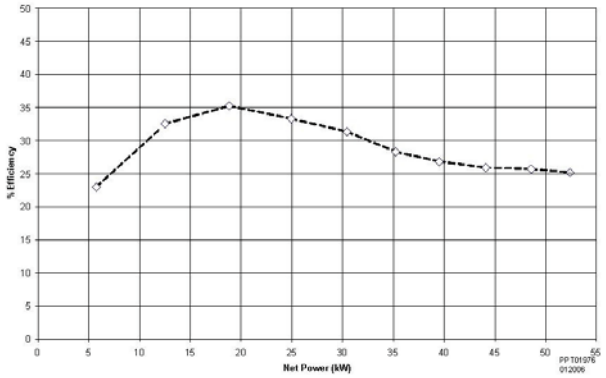

Efficiency of IFC 50-kW gasoline-fueled PEM fuel cell power plant as a function of net power.

ANL Develops Innovative Reforming Catalysts. In a major development this past year, ANL developed and licensed a new class of autothermal reforming (ATR) catalysts modeled after the internal anode materials used in solid oxide fuel cells. Unlike typical industrial reforming and oxidation catalysts, the substrate for the catalysts is an oxide-conducting material. The surface of the substrate is then coated with a metal. The ANL rhodium catalyst has demonstrated very high conversions of iso-octane at temperatures as low as 500°C. The ATR catalyst developed at ANL is commercially available.

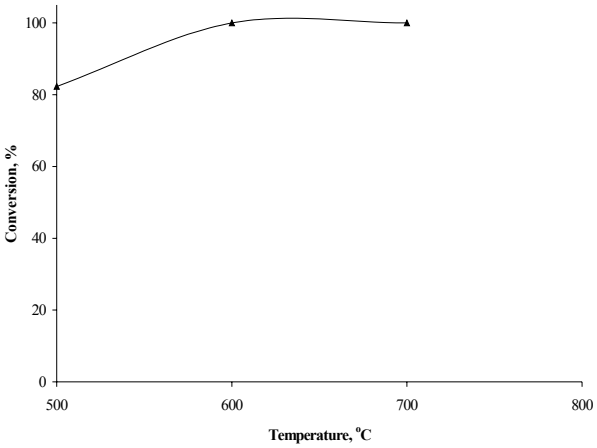

Yield as a function of temperature for iso-octane reforming (0.34 wt% rhodium supported on ANL catalyst).

3M Develops High-Performance MEAs. The membrane electrode assembly (MEA) is the core component of a PEM fuel cell stack. An MEA consists of five basic parts: anode and cathode catalysts, ion-exchange polymer membrane, and anode and cathode gas-diffusion layers. The functions of these basic components are intimately related, and the interfaces formed between them are critical for optimum performance. This 3M project is directed toward demonstrating high-performance, matching PEM fuel cell components that can be manufactured by integrated pilot processes, using a patented nanostructured thin-film catalyst support system, and reducing precious metal loadings. Progress during FY 2001 includes demonstration of improved matching of the electrode backing for improved water management with the nano-structured catalyst-coated membrane (CCM), resulting in a 30% increase in current at 0.75 V on hydrogen. Additional work resulted in significant reduction of anode overpotential by using platinum-alloy electrocatalysts with Pt loadings of 0.1 mg/cm^2. Ongoing work focuses on further improving the MEA for a 10-kW stack. The accompanying figure shows the improvement in pressurized air performance achieved by matching the electrode backings for improved water management with the nanostructured CCM. The same CCM was used to obtain both curves. Only the electrode backings were changed in mid-experiment. Even with humidification conditions more conducive to flooding, the performance with matched components shows much less transport limitation than the nonmatched construction under drier conditions.

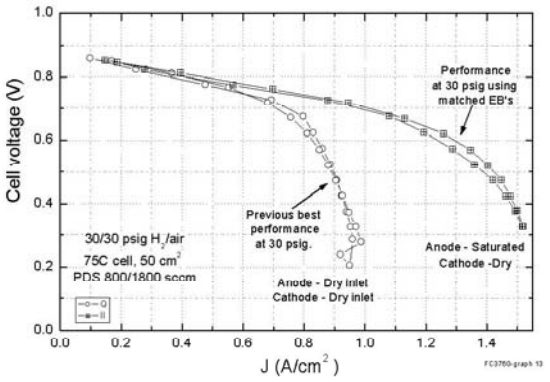

Improvement in 3M cell performance achieved by improved matching of electrode backings (EBs).

SwRI Demonstrates High-Volume Electrode Production. During FY 2001, Southwest Research Institute (SwRI) cooperated with W.L. Gore and Associates, a leading supplier of MEAs for PEM fuel cells, to continue development of a high-volume pilot manufacturing process for electrode material, a crucial (and currently costly) element in the high-volume production of fuel cell MEAs. The key component of this process is a vacuum coating unit capable of producing millions of square feet of high-performance, ultra-low platinum (Pt) -loaded electrodes per year and the potential for MEA production costs below $10/kW. Pilot manufacturing runs have produced electrodes with loadings of 0.1 mg/cm^2 or less by using electrode substrates procured from Gore. MEAs have been tested on reformate (40% H_2, 20% CO_2, 10 ppm CO, balance N_2) in single cells and compare favorably with baseline MEAs with much higher Pt loadings. Work continues to develop the process to achieve target production rates and to evaluate the MEAs in stacks.

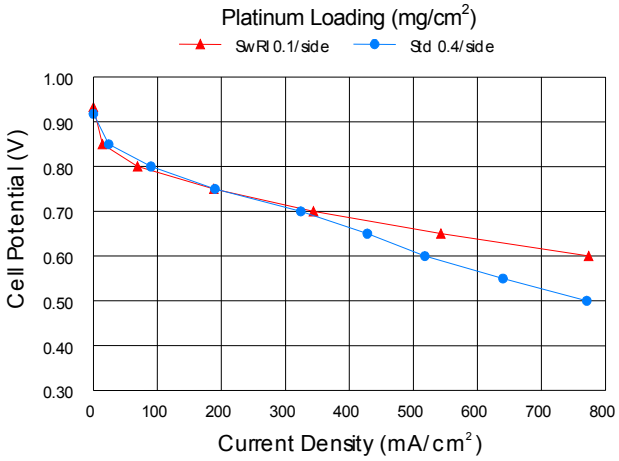

Comparison of baseline and experimental SwRI MEA performance.

ANL Develops Alternative Water-Gas-Shift Catalysts. During 2001, ANL developed a copper/oxide catalyst that has the same activity as commercial copper/zinc oxide low-temperature-shift (LTS) catalyst. The ANL catalyst, however, can operate above 250°C, allowing it to be used in both the LTS and the high-temperature-shift (HTS) stages. The temperature stability of the ANL copper/oxide catalyst allows the LTS stage to run at a higher inlet temperature (e.g., 300°C) than would be possible with copper/zinc oxide (200°C). Thus, the improved kinetics afforded by a higher operating temperature will reduce the size and weight of the LTS stage. The ANL copper/oxide catalyst also has higher activity than the commercial iron-chrome HTS catalyst. Therefore, it can also dramatically reduce the size and weight of the HTS stage. The LTS and HTS catalyst volumes needed for a 50-kW$_e$ reactor were calculated for the ANL copper/oxide catalyst, as well as for the commercial catalysts. The calculated amount of catalysts is that needed to reduce the exit CO concentration to 1% (dry basis) from an inlet reformate gas containing 10% CO. For the commercial HTS and LTS catalysts, a total catalyst volume of 19.2 L is needed. The improvements in the ANL copper/oxide catalyst resulted in a calculated catalyst volume of only 2.4 L, which is an 88% reduction in the total catalyst volume compared with the commercial catalysts. ANL's copper/oxide catalyst also reduces the estimated cost of the WGS catalyst by ~45%, compared with the cost of commercial catalysts. These results demonstrate the potential of the ANL catalyst to meet or exceed DOE's catalyst volume and cost goals for the WGS reactor of < 1 L/kW$_e$ and < $1/kW, respectively.

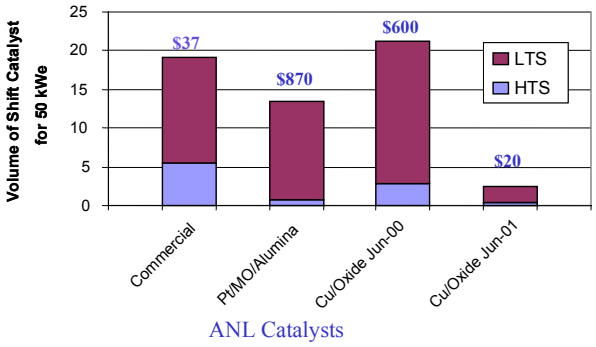

Reduction in shift catalyst volume achieved with ANL Cu/Oxide catalyst (Commercial LTS is Cu/ZnO at 200ºC; commercial HTS is Fe-Cr at 400ºC. ANL Cu/Oxide: LTS at 300ºC; HTS at 400ºC).

PNNL Demonstrates >10-kW Microchannel Steam Reformer. Pacific Northwest National Laboratory (PNNL) has demonstrated a microchannel steam reformer that is sufficient to support a 10-kWe PEM fuel cell. The system consists of four independent reactor cells that operate in parallel and include 25 microchannel heat exchanger units. The apparatus was fabricated from stainless steel in a process that includes photochemical etching of thin metal sheets that are stacked and diffusion-bonded to form a laminated structure with microchannels. In tests of the steam reforming of iso-octane, a trade-off between capacity and conversion effectiveness was found when the reformer was operated over a range of conditions. At a capacity of 11.2 kWe, 99% of the fuel was converted to C1 products (CO, CO_2, and CH_4). At a capacity of 19.3 kWe, the conversion rate fell to 94%. The thermal efficiency of the fuel processor exceeded 90% of the theoretical value over a broad range of operating conditions because of the integration of the steam-reforming reactor with the microchannel-based recuperative heat exchangers, fuel and water vaporizers, preheaters, and condensers. Effort is now under way to integrate microchannel water-gas-shift and CO cleanup reactors with the steam-reforming subsystem to demonstrate a fully integrated fuel processor system.

Productivity (kWe)	11.2	19.3
Fuel Conversion to C1 (%)	98.6	93.6
Estimated SR Efficiency (%)	81	76
Power Density (We/L)	1750	3000
Combustion/Reformate Temperature (^oC)	750/ 722	775/ 734
Combustion Exhaust Temperature (^oC)	43	50
Reformate Exit Temperature (^oC)	129	115
Dry Gas Composition	70.6 % H_2 14.6% CO 13.7% CO_2 0.9% CH_4	69.7 % H_2 16.1% CO 12.3%CO_2 1.3% CH_4

PNNL microchannel steam reformer performance at two load conditions.

DOE Conducts Peer Review of Air System Technology Programs. The performance and overall efficiency of the entire PEM fuel cell system is very dependent on the air management subsystem. Unfortunately, no off-the-shelf compressor/expander/motor (CEM) technologies are available that meet all of the unique air supply requirements of the PEM fuel cell system (e.g., efficiency, performance, cost, size, and weight). Since 1996, when DOE initiated fuel cell compressor/expander R&D, progress in improving the various technologies has been considerable. However, basic deficiencies still remain. In light of this, DOE commissioned the Air System Technology Programs Review Panel on CEM Technologies to review the DOE work in this area and the progress and potential of CEM technology for satisfying the air management requirements of PEM fuel cells for automotive applications. Although DOE sponsored the review, DOE was not involved in the panel's deliberations and played no role in determining the review's outcome. The panel's report provides a review of specific CEM technologies supported by the DOE Fuel Cells for Transportation Program and is based upon the Program Peer Review. The panel assessed the relevance of centrifugal, piston, scroll, twin screw, and intersecting vane compressors/expanders and air-bearing devices. As a result of this Peer Review, DOE downselected compressor/expander projects and will continue to support the development of centrifugal, hybrid scroll, and intersecting vane technologies. Additionally, a new project supporting the air management of ambient-pressure fuel cell systems was initiated.

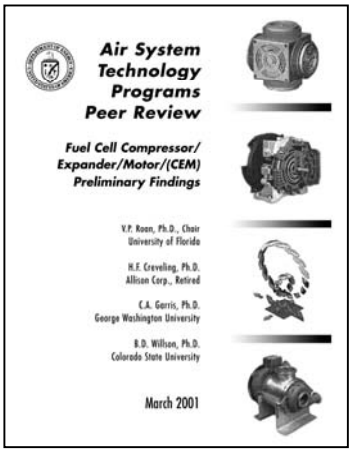

Future Directions

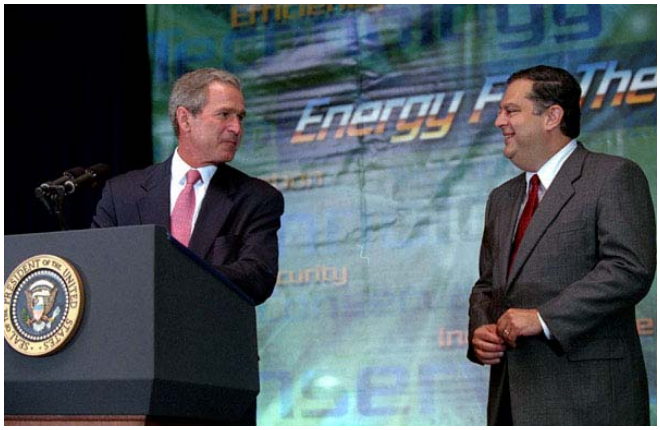

President Bush with Secretary Abraham during award announcement.

During FY 2001, the DOE Fuel Cells for Transportation Program planned and executed an R&D solicitation that resulted in approximately $80 million in new research awards for over 20 projects. On June 28, 2001, President Bush came to DOE and announced the awards: "I'm pleased to announce…grants to encourage academia and the private sector to join with contributions from the [public] sector to accelerate the development of fuel cells, advanced engines, hydrogen technology and efficient appliances…" In addition to R&D associated with materials and components for PEM fuel cell stacks and on-board fuel processors, the awards include increased emphasis on on-board hydrogen storage technologies, which are jointly supported with the DOE's Hydrogen Program. An award was also made for a small stationary PEM fuel cell system that operates on ethanol. With an average industry cost share of 28%, the total R&D value of the new projects is ~$115 million. Approximately 20 organizations, including two universities, received awards for projects that will begin in Fall 2001 and run between two and four years. The new awards were made for projects that addressed the most critical challenges to the commercialization of transportation fuel cell power systems (see Table 2).

Table 2. New R&D projects selected from FY 2001 solicitation.

Project Descriptions	Challenges Addressed	Prime Contractor
Stack Components		
MEAs with High-Temperature Membranes and Higher Activity Cathodes (4 awards)	Cost, Pt Reduction, Manufacturing	3M IFC DeNora/DuPont Superior MicroPowders
Processes for Molding Bipolar Plates (1 award)	Cost, Manufacturing	Porvair
Fuel Processing		
Catalysts/Materials/Components to Reduce Weight and Volume (3 awards)	Start-Up Time, Cost	Nuvera U. Michigan Catalytica
Balance of Plant		
Compressor/Expander, Blowers, Heat Exchangers, Humidifiers (4 awards)	Air Management, Balance of Plant, Size/Cost	IFC Honeywell Arthur D. Little Mechanology
Sensors to Reliably Identify and Quantify Chemical Species (2 awards)	Cost, Durability/Reliability	IFC Honeywell
Hydrogen Enhancement Technologies that are Energy-Efficient (2 awards)	Cost, Durability	UTRC U. Kentucky
Hydrogen Storage		
On-Board Hydrogen Storage (2 awards)	Fuel Infrastructure	UTRC SwRI

Table 2. (Cont.)

Project Descriptions	Challenges Addressed	Prime Contractor
Assessments/Analyses		
Precious Metal Availability and Cost (1 award)	Platinum Cost/Supply	Arthur D. Little
Viability of Fuel Cell Auxiliary Power Units (1 award)	System Cost/Efficiency	Arthur D. Little
Energy, Emissions, and Cost Analyses of Fuels for Fuel Cells (1 award)	Fuel Infrastructure	Arthur D. Little
Fuel Cell Vehicle Codes and Standards and Recommended Practices (1 award)	Fuel Infrastructure	Soc. of Automotive Eng.
Small Stationary PEM Power System Operating on Ethanol (1 award)	Fuel Infrastructure	Caterpillar

New DOE projects de-emphasize system integration and full-scale stack development because industry has the capability to carry these efforts forward. The DOE program will focus on addressing the most critical issues of cost, durability, and performance of materials, components, and enabling technologies. Substantial progress was made during 2001 toward meeting the technical targets for fuel cell systems for light-duty vehicles; however, significant technical and economic challenges remain before fuel cell vehicles will achieve significant market penetration. As we move forward, we will continue to work with our government and industry partners to address these challenges. In addition to the new contracts with industry, the DOE national laboratories will continue to provide valuable support to the Fuel Cells for Transportation Program during FY 2002 (see Table 3). Through these efforts and other related projects, researchers in the Fuel Cells for Transportation Program will continue to improve cost, durability, efficiency, and overall system performance, allowing us to move closer to the commercial availability of fuel cell vehicles.

Table 3. DOE national laboratory R&D in support of fuel cells for transportation program.

Laboratory	R&D Focus
Los Alamos National Laboratory	Improved Cathodes High-Temperature Membranes Durability Studies Fuels Effects
Argonne National Laboratory	Systems Analysis Fast-Start Fuel Processing
Pacific Northwest National Laboratory	Microchannel Fuel Processing
Brookhaven National Laboratory	Low-Pt Electrodes
Lawrence Livermore National Laboratory	Sensors

During the past year, we increased our cooperation with DOE's Hydrogen Program and Fuel Cells for Buildings Program to maximize the existing synergies. In May 2002, the Fuel Cells for Transportation Program and the Hydrogen Program will hold a joint R&D review for the first time. We also increased interactions with the Solid-State Energy Conversion Alliance (SECA), supported through the DOE Office of Fossil Energy, with a focus on fuel cells for auxiliary power to eliminate overnight idling in diesel trucks. The Fuel Cells for Transportation Program will also support R&D associated with fuel cells for portable power. Portable power will likely be the first high-volume market for fuel cells because of their low power

requirements and less-stringent cost target (~$5,000/kW). The manufacturing capability that develops for portable power fuel cells will help accelerate commercialization of fuel cells for transportation.

The remainder of this report presents extended project abstracts that highlight progress achieved during FY 2001 under the Fuel Cells for Transportation Program. The extended abstracts summarize both industry and national laboratory projects, providing the major results of the work being conducted to overcome the technical barriers associated with the development of fuel cell power systems. Each project report identifies the related barriers in the Office of Advanced Automotive Technologies R&D Plan.

Donna Lee Ho Nancy L. Garland Larry Blair JoAnn Milliken Patrick B. Davis

Program Managers
Fuel Cells for Transportation
Office of Advanced Automotive Technologies
Office of Transportation Technologies
Energy Efficiency and Renewable Energy
U.S. Department of Energy

II. FUEL CELL POWER SYSTEM DEVELOPMENT[1]

A. Atmospheric Fuel Cell Power System for Transportation

Murdo J. Smith
International Fuel Cells
195 Governor's Highway
South Windsor, CT 06074
(860) 727-2269, fax: (860) 727-2399, e-mail: smithmu@ifc.utc.com

DOE Program Manager: Patrick Davis
(202) 586-8061, fax: (202) 586-9811, e-mail: patrick.davis@ee.doe.gov

ANL Technical Advisor: Walter Podolski
(630) 252-7558, fax: (630) 972-4430, e-mail: podolski@cmt.anl.gov

Contractor: International Fuel Cells, South Windsor, Connecticut
Contract No. DE-AC02-99EE50567 (1999–2003)

Objective

The objectives of this contract are to deliver to DOE (1) a 50-kW-equivalent gasoline fuel processing system; (2) a fully integrated, gasoline-fueled, 50-kW polymer electrolyte membrane (PEM) power plant; and (3) a fully integrated, gasoline-fueled, 75-kW advanced PEM fuel cell power plant for functional demonstration testing. Although focused on gasoline operation, the fuel processing system will utilize fuel-flexible reforming technology that can be modified to accommodate such fuels as methanol, ethanol, and natural gas. Demonstration testing of each of the units will be performed at IFC. After IFC testing, the PEM power plants will be delivered to Argonne National Laboratory (ANL) for additional operational tests by DOE.

OAAT R&D Plan: Tasks 5, 8, and 11; Barrier J

Approach

- Deliver and test an autothermal fuel processor.
- Deliver and test a 50-kW, ambient-pressure integrated power subsystem.
- Deliver and test a 75-kW, advanced ambient-pressure integrated power subsystem.

Accomplishments

- Delivered and tested a 50-kW-equivalent gasoline fuel processing system.
- Delivered and tested a 50-kW-equivalent PEM cell stack assembly for incorporation into the integrated power plant.
- Delivered and tested a 50-kW integrated power plant configured for system verification testing.
- Delivered the 50-kW integrated power plant to ANL.

[1] The DOE draft technical targets for integrated fuel cell power systems can be found in Table 1, Appendix B. Because the targets in Appendix B were updated after the reports were written, the reports may not reflect the updated targets.

Future Directions

- Support follow-on testing of the 50-kW power plant at ANL.
- Deliver the 75-kW power plant to DOE for follow-on testing at ANL.

Introduction

International Fuel Cells (IFC) is committed to the commercialization of PEM fuel cell power plants for transportation applications. We have in place a program addressing the technology development and verification of each of the necessary components, subsystems, and, ultimately, the fully integrated power plant itself. The focus of IFC's program is an ambient-pressure PEM power plant system operating on gasoline fuel and delivering 75-kW-net dc power to the automotive electrical system.

Project Deliverables

Under the contract, IFC will deliver to DOE a 50-kW-equivalent gasoline fuel processing system, a 50-kW PEM power plant, and a 75-kW advanced PEM power plant.

Results

50-kW Power Plant

A 50-kW power plant was designed, built, and tested. Figure 1 provides a schematic of the gasoline fuel cell power plant. The major subsystems include the fuel processing subsystem, the power subsystem, and the balance-of-plant. The balance-of-plant includes the thermal management subsystem, the air and water subsystems, and the controller and associated electrical equipment.

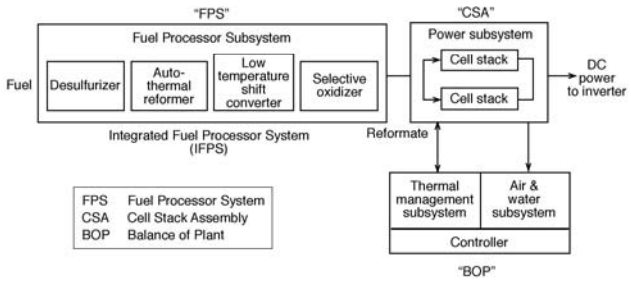

Figure 1. Power plant schematic.

Figures 2 and 3 are photographs of the fully integrated, 50-kW, ambient-pressure, gasoline-fueled power plant showing the locations of major components.

Figure 4 is a photograph of the power subsystem. As shown, it consists of two 25-kW PEM ambient-pressure cell stack assemblies.

The power plant was installed for demonstration testing at IFC's facilities in South Windsor, CT. A California Phase II RFG gasoline fuel was used throughout the test program. Results of the testing include the following:

- Rated power output: 53 kW net
- Efficiency at 5 kW: 22%
- Efficiency at 12.5 kW: 32%

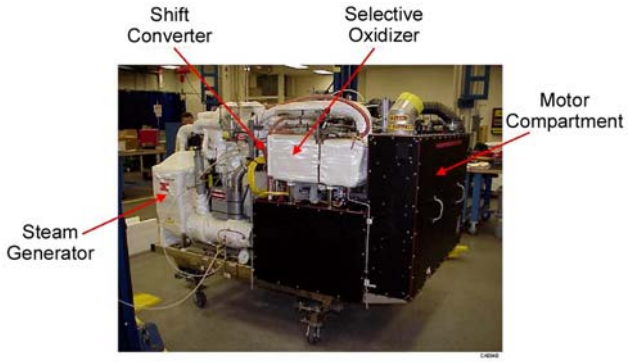

Figure 2. 50-kW gasoline-fueled power plant.

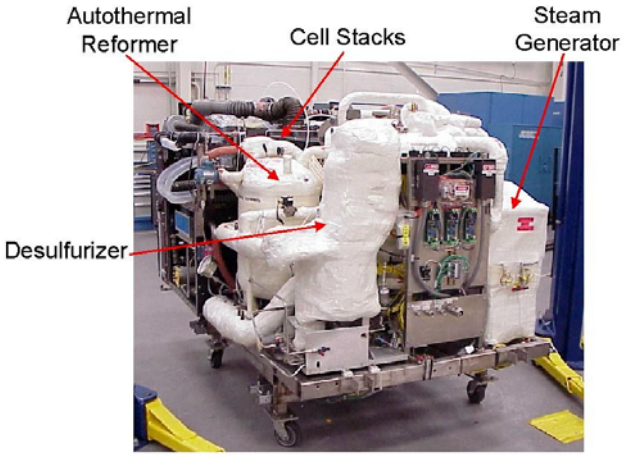

Figure 3. 50-kW gasoline-fueled power plant.

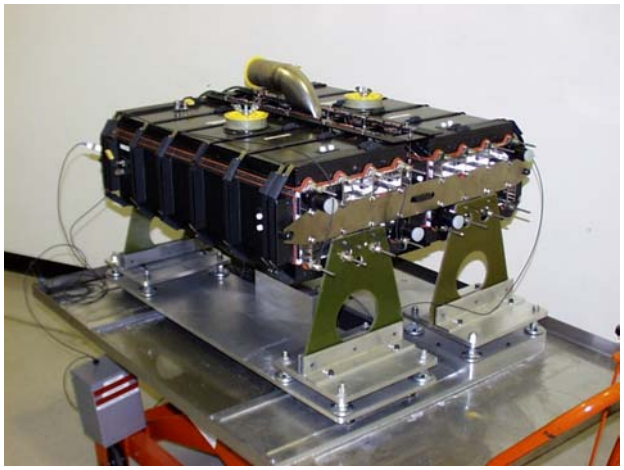

Figure 4. 50-kW power subsystem.

- Specific power: 80 W/kg
- Power density: 70 W/L
- Operating voltage range: 255–420 V

Additional results are shown in Table 1.

Figure 5 shows net power plant output power as a function of fuel flow. Power plant efficiency as a function of power output is shown in Figure 6.

Power plant start-up time was approximately 45 min from ambient temperature to 12.5 kW output power, as shown in Figure 7. Figure 8 shows the 6-s transient time from 12.5 kW to 35 kW.

Table 1. Integrated fuel cell power system performance*.

Characteristic	Units	DOE 2004 Technical Targets	50-kW Actual
Energy Efficiency @ 25% of peak power	%	40	32
Energy Efficiency @ peak power	%	33	25
Power Density	We/L	250	70
Specific Power	We/kg	250	80
Cost	$\$/kW_e$	125	NA+
Transient Response (10–90% power)	s	5	6 s from 25–70% power
Cold Start-Up (-20°C to max power)	min	2	NA+
Cold Start-Up (20°C to 25% of peak power)	min	<1	45
Survivability	°C	-30	NA+
Emissions		<Tier2Bin2	NA+
Durability	h	4000	NA

* Including fuel processor, stack, auxiliaries, and start-up devices — excludes gasoline tank and vehicle traction electronics.
+ NA = Not analyzed or measured.

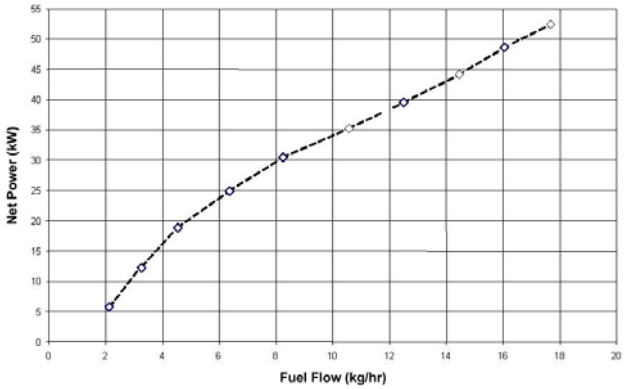

Figure 5. Power plant net output power.

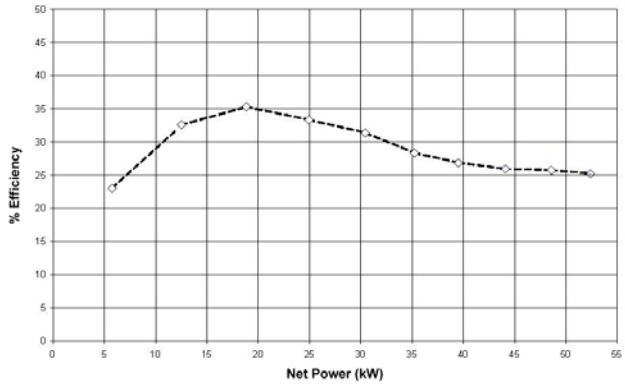

Figure 6. Power plant efficiency.

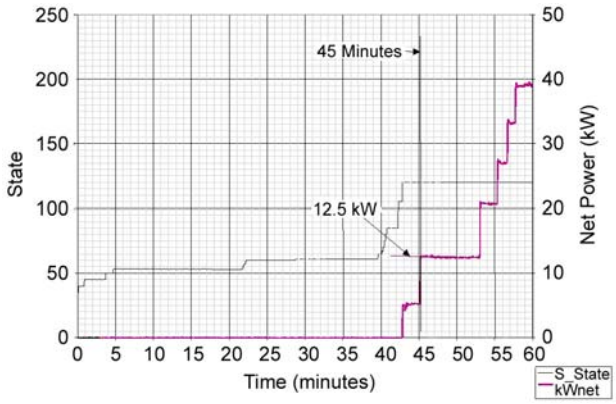

Figure 7. Power plant start-up.

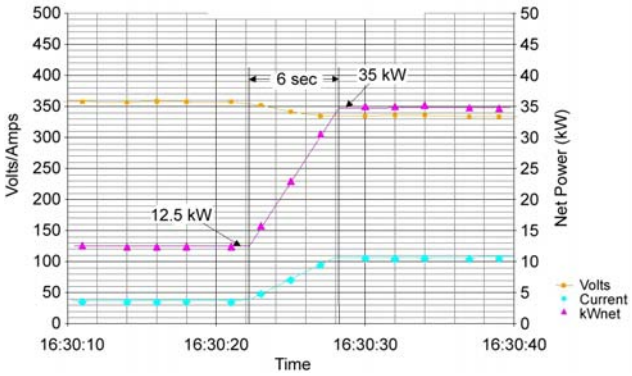

Figure 8. Power plant transient.

75-kW Power Plant

In the second phase of the contract (now initiated), IFC will deliver to DOE an advanced gasoline-fueled 75-kW PEM fuel cell power plant. It is intended that the design of this power plant will address opportunities for distributing components throughout the automobile structure.

Figure 9 provides a comparison between the power subsystem incorporated in the 50-kW power plant and IFC's advanced technology 75-kW power subsystem. As can be seen, the 50-kW subsystem was made up of two 25-kW units. The 75-kW subsystem is made up of a single unit approximately the same size as the 25-kW unit. This subsystem provides more than a twofold increase in power density. Similar advances are being addressed for the fuel processing components.

Figure 9. Advanced 75-kW power subsystem.

Conclusions

IFC is committed to the commercialization of PEM fuel cell power plants for transportation applications. The focus of IFC's program is an ambient-pressure PEM power plant system operating on gasoline fuel. A fully integrated, ambient-pressure, 50-kW PEM power plant was assembled and tested at IFC. The power plant has been delivered to ANL for follow-on testing.

Phase 2 of the plan was begun. Under this phase, IFC will deliver to DOE an advanced 75-kW gasoline-fueled ambient pressure PEM power plant. Power density is expected to be approximately double that of the 50-kW unit.

B. Pressurized Fuel Cell Power System for Transportation

William D. Ernst
Plug Power, Inc.
968 Albany-Shaker Road
Latham, NY 12110
(518) 782-7700, fax: (518) 782-7914, e-mail: William_Ernst@plugpower.com

DOE Program Manager: Donna Lee Ho
(202) 586-8000, fax: (202) 586-9811, e-mail: donna.ho@ee.doe.gov

DOE Program Support: Larry Blair
(202) 586-0626, fax: (202) 586-9811, e-mail: larry.blair@ee.doe.gov

ANL Technical Advisor: Walter Podolski
(630) 252-7558, fax: (630) 972-4430, e-mail: podolski@cmt.anl.gov

DOE Contractor: Plug Power, Inc., Latham, New York 12110
Prime Contract No. DE-FC02-97EE50472, September 30, 1997-December 31, 2001
Major Subcontractor: Nuvera Fuel Cells, Cambridge, Massachusetts 02140

Objectives

- Research and develop a fully integrated fuel cell system that operates on common transportation fuels (gasoline, methanol, ethanol, and natural gas) for automotive applications.
- Deliver a highly integrated, 50-kW_e-net polymer electrolyte membrane (PEM) fuel cell stack with balance of plant components and a 50-kW_e (equivalent) fuel-flexible reformer.
- Provide test data evaluating the system for vehicle propulsion under driving cycle profiles.

OAAT R&D Plan: Tasks 5, 8, and 11; Barriers A-H and J

Approach

Work under this contract has been pursued in four phases:

- Phase I: Define overall system; build and demonstrate a 10-kW_e system.
- Phase II: Develop components for a 50-kW_e system.
- Phase III: Assemble the components into a functionally integrated 50-kW_e brassboard system and test this system.
- Phase IV: Build and test a fully integrated 50-kW_e system for automotive use and test this system in a test stand.

During this report period, DOE and the contractor agreed that Phase IV would be deleted and the contract considered completed at the conclusion of Phase III.

Accomplishments

- Completed the integration of the Nuvera fuel processor subsystem with the Plug Power fuel cell subsystem to create the Phase III brassboard system at Plug Power's Automotive Test Laboratory.
- Performed tests of the integrated brassboard system by using reformate from the fuel processor and an independent air supply.

- Completed tests of the brassboard system by using the Compressor/Motor/Expander Unit (CMEU) in its intended control mode as the air supply for the fuel cell subsystem with reformate from the fuel processor.
- Initiated design of a Phase IV fuel cell subsystem.
- During this report period, DOE and the contractor agreed that Phase IV would be deleted and the contract considered completed at the conclusion of Phase III. Additional work needs to be done to achieve the program goals of 250-W/L power density and 250-W/kg specific power and still meet the overall energy efficiency goal of 40%.

Introduction

The purpose of this DOE-sponsored program has been to develop, demonstrate, and deliver a 50-kW_e (net) integrated fuel cell power system for automotive applications that can use any of the common automotive fuels (i.e., gasoline, methanol, ethanol, or natural gas). The fuel cell subsystem has been developed by Plug Power, Inc., and the fuel processor has been developed by Nuvera Fuel Cells (previously ADL Epyx). The work began in October 1997 and consisted of four phases:

- Phase I — overall system definition, preliminary component development, and demonstration of a 10-kW_e brassboard integrated system;
- Phase II — development of the fuel cell stack, the fuel processor, auxiliary components, control strategy, and hardware for a 50-kW_e system;
- Phase III — assembly and development testing of a 50-kW_e brassboard system by using the Phase II components; and
- Phase IV — fabrication, assembly, and laboratory testing of a 50-kW_e system packaged for automotive installation.

Phase III was concluded with the integrated, combined operation of the fuel cell and fuel processor subsystems on 5 January 2001.

Approach

Plug Power's approach to developing the fuel cell subsystem components has evolved toward working with suppliers that can meet defined requirements, rather than developing all items in-house. During Phase I, membrane electrode assemblies (MEAs) were formulated and fabricated in-house from raw materials; during Phase II, a supplier was identified that made and delivered completed MEAs per Plug Power specifications. Initial Phase I cell plates were fabricated step-by-step at Plug Power; during Phases II and III, suppliers were identified that delivered machined, carbon-composite cell plates per Plug Power's drawings. The material supplier was selected with the intent of progressing to molded plates after development testing. The compressor/motor/expander unit (CMEU) was assembled from a twin-screw compressor and expander from one supplier and a DC motor and controller from a second source, both in accordance with Plug Power's specifications. Beyond the fuel cell stack and the CMEU, the balance of the Phase III fuel cell subsystem has been assembled from commercially available components.

Priorities applied during this work were (1) to achieve functionality and (2) to attain very low emissions and high energy efficiency. Size and/or weight, although recognized as important in the design of the fuel cell stack, were considered to be lower priorities in the design and selection of the balance of plant components and arrangement. A conservative design approach was taken, and additional valves, instrumentation, and filters (beyond what were needed for operation and control) were added in the reactant flow systems to facilitate thorough characterization of the system during testing.

Although the fuel cell and fuel processor subsystems were designed and specified to be functionally integrated, they were physically built as totally separate equipment skids. At the outset of the Phase III brassboard system design, Plug Power and Nuvera jointly formulated interface drawings that formally identified all functional interface points between the two subsystems. At all interface points, the fluid-flow, state-point, electrical, and mechanical form-and-fit parameters were defined and jointly approved. Frequent joint meetings were held to review and update the interface drawings as necessitated by the evolutionary development of component and system designs. Assembly,

development testing, and qualification testing of the two subsystems progressed separately at the Plug Power and Nuvera laboratories. Nuvera's development and evaluation of the fuel processor subsystem during Phases I, II, and III are described in their separate report appended at the end of this report (Appendix A′). When both subsystems were judged to be ready for integration, Nuvera transported the fuel processor skid to Plug Power's laboratory, and final integration connections were made. Joint testing of the Phase III integrated brassboard system was then conducted, and the fuel cell stack was loaded by means of an Aerovironment ABC-150 electronically controlled load bank.

Results

Phase III Fuel Cell Subsystem Brassboard

A 50-kW_e fuel cell subsystem was designed and built as a skid assembly for laboratory testing. The system incorporates the capability of fully automatic, load-following operation under the control of an embedded computer. An integrated but separable PC is also included to provide an operator interface and to enable manual-control intervention when desired. Instrument transducers were installed to enable mass flow and statepoint measurements at key locations in fluid systems. Additional filtering elements were incorporated in the gas flow streams to prevent damage to sensitive flow-measuring elements and contamination of the fuel cells. The fuel cell stack's output voltage, current, and power were measured; also, individual cell voltages were taken for all cells within the fuel cell stack, and electrical power consumption was measured for most auxiliary components.

The measured stack current was input to algorithms in the control software to determine required air flow, which, in turn, set the operating speed for the CMEU. The positive-displacement, twin-screw CMEU compressor determines air flow by speed. Initial testing of the complete fuel cell subsystem revealed that the additional valves and filters inserted in the flow lines raised the pressure drop to a point at which the required CMEU compressor power exceeded the motor's capability. A larger drive motor was obtained to overcome this limitation. The CMEU (with the larger motor) was characterized by testing on a separate test stand before it was incorporated into the subsystem skid. Figure 1 shows representative data from these tests for a given system pressure drop. The fuel processor independently regulates the air flow it needs from the CMEU supply by means of a control valve. Stack operating pressures are established by the back pressure imposed by the stack exhaust passing through the CMEU expander, in conjunction with back pressure control valves used to provide flow balancing adjustments between the two stacks. The design value for stack cathode exhaust is 3.1 atm at system full power and 2.2 atm at one-quarter power.

The fuel cell stack was built as two separate stacks connected in parallel both electrically and with respect to the reactant gas and coolant flow streams. PEM fuel cells having an active area of 320 cm^2 were used; the anode catalyst was a platinum-ruthenium alloy so that the cells can maintain their activity in up to 50 ppm of CO. Figure 2 is a photograph of the fuel cell subsystem skid assembly. Figure 3 presents a flow schematic of the integrated system.

Before the fuel processor skid arrived, the fuel cell stacks and the entire fuel cell subsystem were tested by using simulated reformate as fuel. This gas mixture, with a nominal dry composition of 35% H_2, 44% N_2, 20% CO_2, 1% methane, and 10–50 ppm CO, approximated what Nuvera expected to deliver from the fuel processor. During early tests, operational upsets in the stack humidification system caused the performance of both stacks to be impaired (one so seriously that it was no longer serviceable). In an effort to maintain the program schedule, the remaining stack was divided into two smaller stacks and the test program was continued.

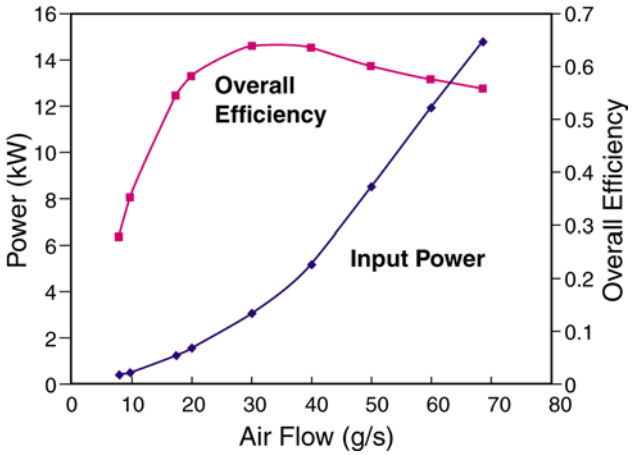

Figure 1. CMEU test data with 13.5-kW motor and 12.5-psi system pressure drop.

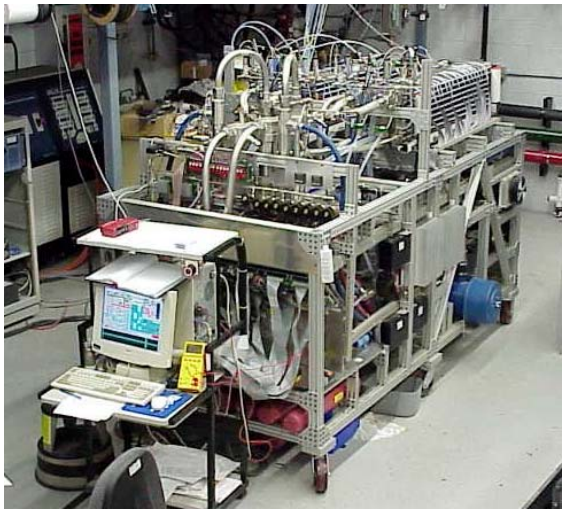

Figure 2. Photo of Phase III brassboard fuel cell subsystem skid.

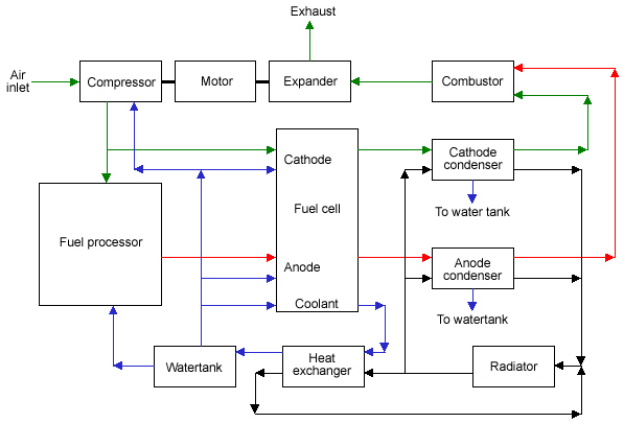

Figure 3. Schematic diagram of Phase III brassboard fuel cell system.

This limited the total power that could be developed to less than the targeted 50 kW_e. Further, the resultant stacks required higher-than-design fuel and air stoichiometry to achieve stable cell voltages.

System Integration

The Nuvera fuel processor skid was integrated with the fuel cell subsystem in January 2001. Some aspects of this integration imposed further constraints on operation of the Phase III integrated brassboard. Because of limited experience in the development of fuel processors with variable inlet air pressure, it was decided that the fuel processor should take its air supply from the laboratory compressed air system at a regulated constant pressure instead of from the CMEU. Also, the tail gas combustor (TGC), a component of the fuel processor, was not connected to the fuel cell stack in accordance with the design intent. After passing through water separators, both stack anode and cathode exhaust gases were to be directed to the TGC, where residual H_2 would be burned, raising the gas temperature before it passed to the CMEU expander. The response time of the TGC discharge temperature control was not believed to be adequate to protect the CMEU expander from over-temperature. The CMEU manufacturer had imposed a limitation of 175°C continuous and 200°C instantaneous on the expander inlet temperature. To accommodate this limitation, the cathode exhaust gas bypassed the TGC and entered the expander directly, at stack outlet temperature. The anode exhaust went to the TGC, which was supplied with air from the laboratory's compressed air system. The hot TGC combustion products were discharged to the atmosphere through a backpressure valve. Using this valve protected the expander from over-temperature, but it also imposed a penalty on the expander because of reduced mass flow and low temperature and enthalpy of the inlet gas. Expander work output was thereby reduced, and motor drive power for the compressor (a system parasitic) was increased.

Phase III Integrated Brassboard Test Results

After completing the integration connections as described above, it was concluded that design operating conditions for the fuel cell stack could most readily be achieved by supplying both the fuel processor and fuel cell subsystems with air from the laboratory compressed air system and not energizing the CMEU. Reactant gas pressures in the stack were established by backpressure valves at the stack exhaust. Figure 4 shows data from this test in polarization-curve format, with measured stack outlet pressures, stoichiometry, and temperature annotated for each test point. At the highest current density, output power from the two parallel stacks was slightly over 35 kW_e. The fuel processor supplied reformate with H_2 concentration very close to the projected level of 40% (dry basis), and CO concentration was generally between 5 and 15 ppm at steady-state conditions. Performance of the fuel processor during these integrated tests is described in greater detail in Nuvera's separate report (Appendix A′). Figure 5 shows the parasitic electric

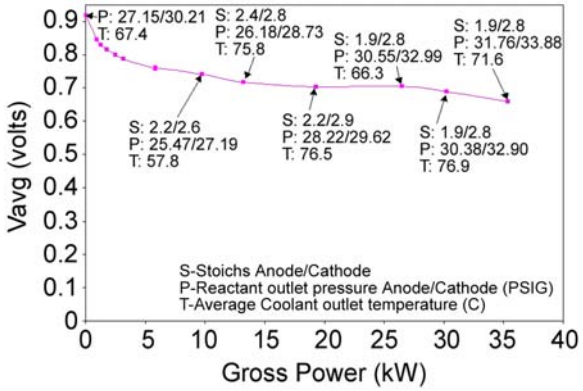

Figure 4. Phase III brassboard test polarization curve (no CMEU)

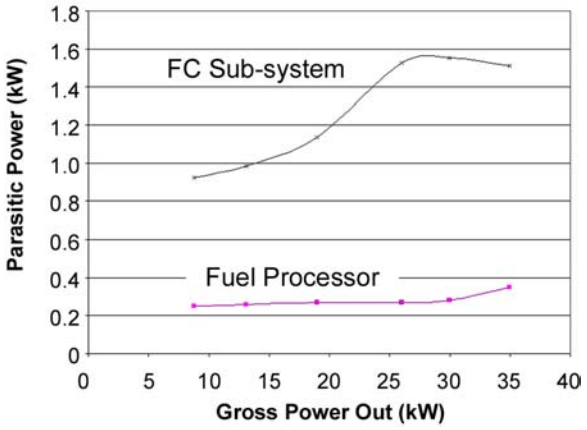

Figure 5. Brassboard subsystem parasitic power demands (no CMEU).

power consumption of the two subsystems as a function of stack gross power output. Fuel processor power demand was relatively low; the major portion of the fuel cell subsystem power consumption was the deionized (DI) water stack coolant pump. Figure 6 shows the efficiency of the stack, subsystems, and overall integrated system as functions of gross power out.

Subsequent tests were run with the CMEU active and supplying cathode air to the fuel cell subsystem; the fuel processor was still supplied with air from the laboratory's compressed air system. Figure 7 presents data in polarization-curve format for these tests. Stack cathode pressure was determined by the CMEU expander backpressure, while anode pressure was set to comparable levels by the backpressure valve at the TGC outlet. Expander backpressure was lower than the design values because of the anode exhaust flow bypassing the expander and the reduced expander inlet

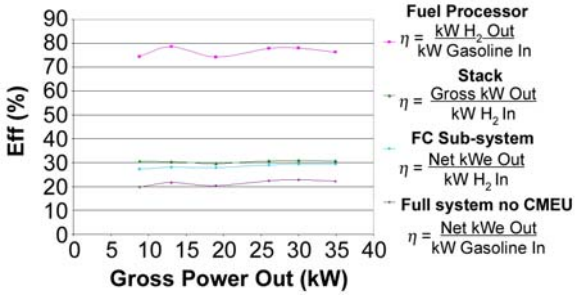

Figure 6. Brassboard system and subsystem efficiencies (no CMEU).

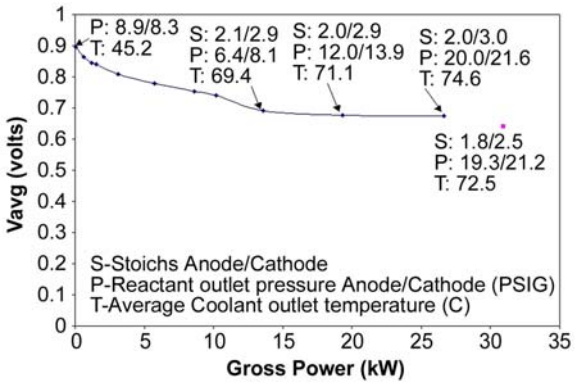

Figure 7. Phase III brassboard test polarization curve (with CMEU).

temperature. The Figure 7 polarization curve is lower than that of Figure 6 because of this lower stack pressure. Maximum stack gross power output was thereby reduced to 30.9 kW_e during this test. Parasitic power consumptions are shown in Figure 8. The CMEU drive motor drew approximately 9.5 kW_e at the maximum power test point because of the reduced power developed by the expander. Figure 9 presents the efficiencies of the stack and subsystems. Comparison of Figures 6 and 9 emphasizes the penalty of excessive parasitic power demand on system efficiency. An additional curve was added to Figure 9, namely the projected overall system efficiency if the pressure drop had been only half the actual value.

Conclusions and Future Work

During Phase I of this program, Plug Power and Nuvera Fuel Cells jointly designed and built a 10-kW_e demonstration fuel cell power system and operated this system on seven different hydrocarbon fuels, including gasoline, methanol, ethanol, and methane. Measured emissions of CO, NO_x, and total

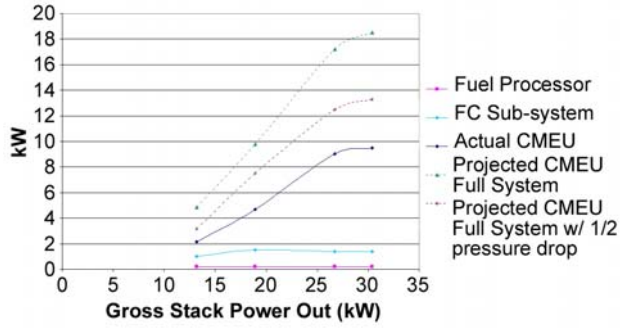

Figure 8. Brassboard subsystem parasitic power demands (with CMEU).

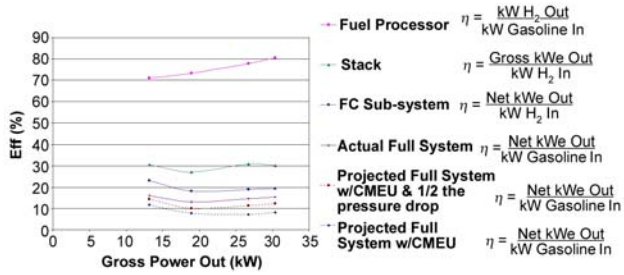

Figure 9. Brassboard system and subsystem efficiencies (with CMEU).

hydrocarbons were all well below 4 mg/kWh over the power range from 4 to 10 kW_e output. Emissions results are discussed in greater detail in Nuvera's separate report (Appendix A).

At the conclusion of Phase III, the contractors completed the design and construction of a 50-kW_e,functionally integrated brassboard fuel cell power system capable of operating on any of the four common automotive fuels. This system was successfully operated on gasoline up to a gross power output of 35 kW_e, which was limited only by the use of one-half the design fuel cell stack size and by operational limitations associated with the TGC/CMEU expander integration. Stack efficiency was below design targets as a result of performance impairment in early testing by operational upsets in the stack humidification system. The fuel processor delivered reformate with the intended H_2 concentration, with CO concentrations generally below 50 ppm and within 5–15 ppm at steady-state conditions.

Twin-screw-type air compressor components give good promise of acceptable performance at reasonable weight and size for air compression and power-recovery expanders in fuel cell systems. To keep the parasitic power demand of the drive motor acceptably low, it is important to minimize pressure drop (by not adding components) throughout the reactant-gas flow systems during design and to provide as high a mass flow and temperature as possible at the expander inlet. The system for maintaining fuel cell membrane humidification and temperature at optimum levels over the entire active area of all cells in the stack must be improved and made more resistant to (or tolerant of) operational upsets.

Substantial additional work is required to achieve the program goals of power density (250 W/L) and specific power (250 W/kg) and yet achieve the overall system efficiency goal of 40%. Test results from Phase III were planned to be used to optimize component selection to be used in Phase IV. The next-generation system should use a single design (one set of schematics) and be built on one compact skid. Stack efficiency can be increased by setting the design operating point at lower current density and higher cell voltage while simultaneously maintaining power density. To achieve a given power level, this requires either new technology to raise the polarization curve or the use of a larger total cell area. Larger total cell area tends toward larger stack size and weight; however, stack power density may increase. Work to improve the stack was begun, including modification of stack humidification to incorporate an enthalpy recovery device. This device recovers the product water vapor from the stack cathode exhaust and transfers both the moisture and its latent energy into the incoming cathode air. Plug Power has used such devices successfully in other applications. In addition, a new cell plate design was completed and successfully tested. This design increased the cell active area by 30%, used a more compact seal design, and demonstrated a 10% improvement in plate area utilization. Other improvements to stack design achieved a 20% improvement in stack power density and a 15-kg reduction in stack weight. The Phase IV work was terminated to conserve program resources for completion of Phase III. The program is now considered complete, and no further work will be done under this contract.

References

1. W.D. Ernst, "Plug Power Fuel Cell Development Program," DOE Automotive Technology Development Customers'

Coordination Meeting, Dearborn, MI, October 27–30, 1997.
2. W. Ernst, J. Law, J. Chen, and W. Acker, "PEM Fuel Cell Power Systems for Automotive Applications," Fuel Cell Seminar, Palm Springs, CA, November 1998.
3. W.D. Ernst, "Reformate-Fueled PEM Fuel Cells," SAE Fuel Cells for Transportation TOPTEC, March 18–19, 1998, Cambridge, MA.

Appendix A′. Pressurized Fuel Cell Power System for Transportation: Fuel Processor Subsystem

William Mitchell, P.E., Srinivasa Prabhu, and Brian Bowers
Nuvera Fuel Cells/Arthur D. Little, Inc., 35 Acorn Park, Cambridge, MA 02140
(617) 498-6149, fax: (617) 498-6655, e-mail: mitchell.w@nuvera.com

---

Objectives

Under our DOE program for advanced fuel processor development, Nuvera Fuel Cells/Arthur D. Little, Inc. (Nuvera), is:

- Developing a fuel reformer capable of processing gasoline and alternative fuels, such as ethanol, and providing reformate for a 50-kW_e fuel cell subsystem.
- Developing and testing an advanced preferential oxidation (PrOx) device based on proprietary catalyst technology, with a major focus on gas purity when reforming gasoline and ethanol.
- Supporting Plug Power in the development of a 50-kW_e integrated fuel cell power system.

OAAT R&D Plan: Tasks 5 and 6; Barriers E, F, and G

Approach

- Phases I and II
  - Initiate an aggressive catalyst and balance-of-plant evaluation and development program with subcontractors and commercial partners.
  - Build and test a brassboard 45-$kW_{thermal}$ multi-fuel reformer (Model A) based on existing reformer designs and other available components as a proof of concept (3-atm pressure).
  - Investigate multiple, steady-state, CO cleanup and anode exhaust combustor options at the 45-$kW_{thermal}$ level.
  - Integrate the Model A fuel processing system with the Plug Power fuel cell subsystem and evaluate overall system performance.
  - Design and build a multi-fuel reformer (Model B) at the 45-$kW_{thermal}$ level to prove advanced reformer design concepts based on experience gained in Phase I.
  - Integrate Model B fuel processing system with the Plug Power fuel cell subsystem and evaluate overall system performance.
- Phase III
  - Assist Plug Power in the development of a test facility for full-scale (50-kW_e) system testing.
  - Continue catalyst and balance-of-plant refinements from Phase I and Phase II.
  - Design and build an advanced fuel processor for a 50-kW_e integrated fuel cell system, on the basis of the outcomes of Phase I and Phase II testing.
  - Test the 50-kW_e fuel processor/PrOx combination at Nuvera/ADL laboratories, including transients.

- Provide integration assistance for testing the 50-kW_e brassboard (Phase III) system demonstration at Plug Power.
- Aid Plug Power in the mechanical design and packaging of the 50-kW_e Phase III system, focusing on system functionality and efficiency of operation.

Accomplishments

- 1998–1999 (Phases I and II)
  - Conducted detailed system modeling studies to investigate the trade-off between different system designs with respect to efficiency, thermal management, water balance, cost, and control complexity.
  - Conducted detailed evaluation of commercially available catalyst technologies to identify their performance in automotive fuel processing application.
  - Established and managed subcontract activity with UOP and Modine manufacturing to evaluate and develop subcomponents for the fuel processing system.
  - Designed and built two generations of reformers at the 45-$kW_{thermal}$ level to evaluate reformer concepts, system integration, and control schemes.
  - Designed and built two generations of carbon monoxide cleanup technologies and integrated them into the fuel processing system.
  - Designed and built two generations of anode exhaust combustor technology and integrated them into the fuel processing systems.
  - Supported integration with Plug Power fuel cell subsystems with each generation of fuel processor and evaluated system level performance issues.
  - Demonstrated the potential for gasoline fuel cell systems emissions to be less than Tier II limits.
- 2000–2001 (Phase III)
  - Designed, built, and integrated a fully automated 190-$kW_{thermal}$ Phase III fuel processor subsystem that exceeded all Phase III targets.
  - Demonstrated fuel processor hydrogen efficiencies in excess of 80% with gasoline.
  - Demonstrated PrOx-exit hydrogen efficiencies in excess of 80% and exit CO concentrations lower than 10 ppm.
  - Integrated the fuel processing subsystem with a Plug Power fuel cell subsystem and demonstrated overall integrated system functionality.
  - Demonstrated low emissions from an integrated fuel cell power system.

Future Directions

- Analyze system data and develop final report for the project.

Introduction

Nuvera Fuel Cells (NFC) is a leading supplier of fuel cell power systems in the stationary and transportation markets. Widespread implementation of fuel cell systems requires significant improvements in many aspects of the technology, including power density, specific power, transient response time, efficiency, and cost. In addition, the ability to operate on a number of hydrocarbon fuels that are available through the existing infrastructure is a key enabler for commercializing fuel cell systems. Nuvera is working with the U.S. Department of Energy to develop efficient, low-emission, multi-fuel processors for transportation applications. The fuels include gasoline, methanol, ethanol, and natural gas.

In this program, Nuvera's focus with Plug Power was on developing reformer subsystems (fuel processor, CO cleanup, and exhaust cleanup) and integrating them with fuel cell subsystems for system-level evaluation of efficiency, water balance, transient response, thermal integration, and parasitic power.

Phases I and II

The objectives of Phases I and II were to evaluate and advance various core technologies that affect the performance of the fuel processing system,

shown schematically in Figure 1. These advances in catalyst, heat exchangers, and various balance-of-plant items were incorporated into reformer system designs and tested at the 45-$kW_{thermal}$ level. The Phase I reformer (Model A) is shown in Figure 2, and the Phase II reformer (Model B) is shown in Figure 3. The performance of the two fuel processors is summarized in Table 1.

The hydrogen efficiencies of the Model B fuel processor with California Phase II gasoline, methanol, and methane are shown in Figure 4. The Phase II Model B reformer was operated successfully to obtain efficiencies in excess of 85% with methanol and 75% with gasoline. This reformer was integrated with a Plug Power fuel cell subsystem, and 10 kW_e of power was demonstrated. In addition, the Model B operated successfully on ethanol and Fischer Tropsch fuel.

In parallel with the fuel processor development, significant advances in the CO cleanup and anode gas combustor technologies were achieved in Phases I and II of the program. Figures 5 and 6 show preferential oxidation (PrOx) CO cleanup reactors

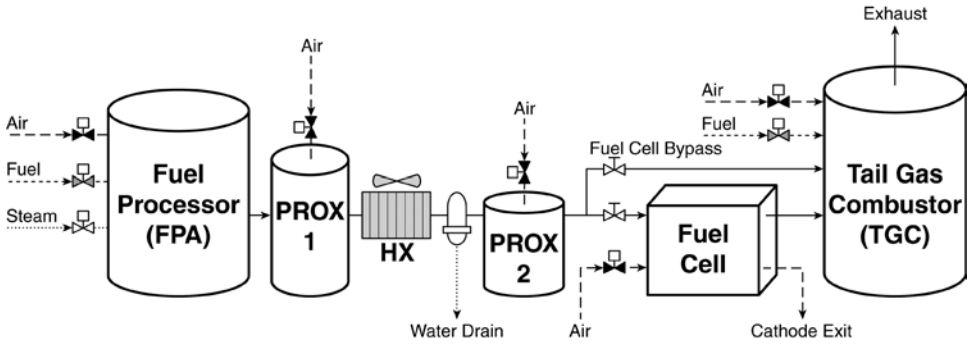

Figure 1. Schematic of the Nuvera fuel processor.

Figure 2. Phase I Model A reformer.

Figure 3. Phase II Model B reformer.

Table 1. Performance of Phase I and Phase II Reformers.

		Phase I	Phase II
Fuel Processor Type		**Model A**	**Model B**
Fuel Processor Fuel Input	(kWth)	45	45
Fuel Processor Hydrogen Efficiency	(%)	57	75
Exit Hydrogen Flow Concentration	(dry vol %)	31	40
Emissions		–	< Tier II

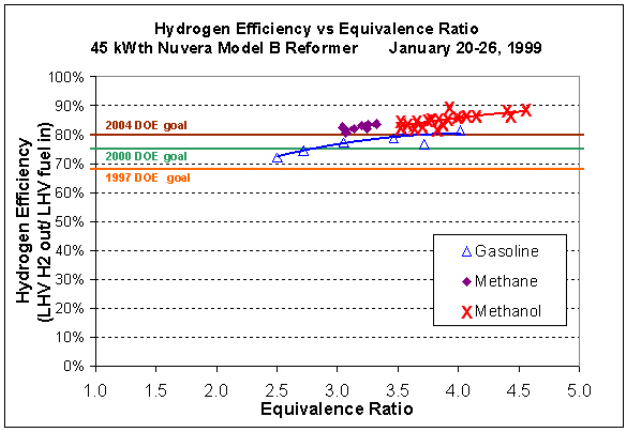

Figure 4. Hydrogen efficiency versus fuel-air equivalence ratio for the phase II 45-kW_{th} model B reformer.

Figure 5. Phase I CO cleanup reactor.

Figure 6. Phase II CO cleanup reactor.

from Phases I and II. Steady-state and transient performance of the Phase II CO cleanup reactor is shown in Figure 7. For Figure 7, the reformer was operated on methanol, and exit CO levels from the fuel processor assembly (FPA) were maintained below 2,000 ppm while CO at the exit of the PrOx was maintained below 10 ppm, even during step transients of 10–45 $kW_{thermal}$ of fuel input. This performance was obtained with high CO selectivity, thus minimizing the loss of hydrogen across the PrOx reactor.

Anode gas combustor technology (also known as a tail gas combustor, or TGC) was also demonstrated during Phases I and II. Figure 8 shows the Phase II TGC used to burn the hydrogen in the fuel cell anode exhaust. Emissions levels were very low (comparable with Tier II and ULEV goals) and are documented in an SAE publication (References 1–2).

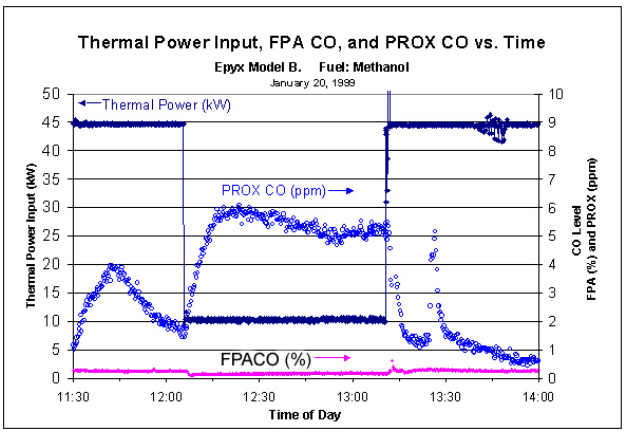

Figure 7. Performance of Phase II CO cleanup reactor (PrOx).

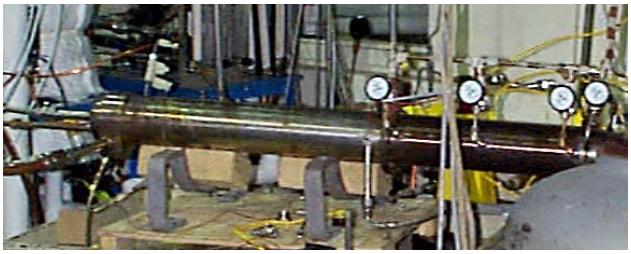

Figure 8. Phase II anode gas combustor (also known as a tail gas combustor, or TGC).

In Phases I and II, all of the major components of the fuel processing subsystem (reformer, CO cleanup, and anode gas combustor) were studied. Significant advances in the design and control of these subsystems were achieved, and this knowledge was incorporated into the design of a 190-$kW_{thermal}$ fuel processing system in Phase III.

Phase III

During Phase III of the program, a fuel processing subsystem was designed and built to produce enough hydrogen for a 50–60-kW_e fuel cell operating at 1.2 times the anode stoichiometric flow rate. The system included an autothermal fuel processor, preferential-oxidation CO cleanup (PrOx), and a tail gas combustor (TGC) for burning anode exhaust and controlling emissions. In addition, a control system was created, including hardware for controlling flows and temperatures via a semi-automated computer interface capable of automatic start-up, process control, and moderate transients.

The performance goals and actual performance for the Nuvera Phase III fuel processor are shown in Table 2. The hydrogen efficiency of the fuel processor is defined as the lower heating value (LHV) of the hydrogen output of the fuel processor divided by the LHV of the fuel input.

A Model B fuel processor capable of a gasoline input of 190 $kW_{thermal}$ was designed and built with a target hydrogen output of 120 $kW_{thermal}$ (based on lower heating values). The actual fuel processor exceeded the target efficiencies, and 136 $kW_{thermal}$ of hydrogen flow was produced with only 164 $kW_{thermal}$ of gasoline input while maintaining CO levels under 50 ppm. Figure 9 shows the hydrogen produced versus the gasoline input and shows that the subsystem was capable of producing the required minimum of 13.6 $kW_{thermal}$ and more than the target maximum of 120 $kW_{thermal}$. The fuel processing subsystem also achieved the goal for hydrogen efficiency (defined above). Figure 10 shows that the subsystem achieved maximum efficiencies of 84% from the fuel processor (exit of low temperature shift) and 82% from the exit of the PrOx, which exceeded the goal of 68%. Figure 10 also shows that the subsystem achieved dry hydrogen concentrations of 45.0% from the fuel processor and 44.7% from the PrOx.

The Phase III subsystem design centered around a Model B reformer (scaled up from the Phase II design), although many other system-level issues were addressed (Reference 3). The Phase III

Table 2. Phase III Fuel Processor Targets vs. Actual Performance.

Parameter	Units	Target	Actual	Target	Actual	Target	Actual
Fuel Processor Fuel Input	(kWth)	175	164	40	40	18	20
Fuel Processor Hydrogen Efficiency	(%)	68	84	68	78	55	69
Exit Hydrogen Flow Concentration	(dry vol. %)	35	45	35	41	28	34
Exit Hydrogen Flow Rate	(kg/h)	3.65	4.11	0.81	0.93	0.30	0.41
Pressure Drop	(psi)	5	3	2	1	1	1
Emissions (see notes in text)		< Tier II	< Tier II	< Tier II	< Tier II	< Tier II	< Tier II
Parasitic Power	(kW)	0.50	0.35	0.20	0.21	0.20	0.21

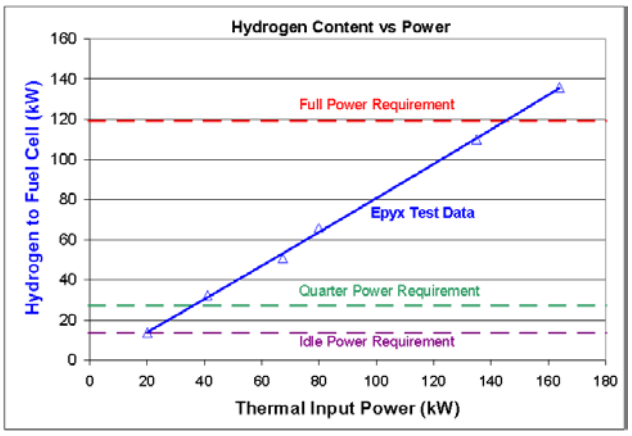

Figure 9. Hydrogen produced versus gasoline input to Phase III fuel processing system.

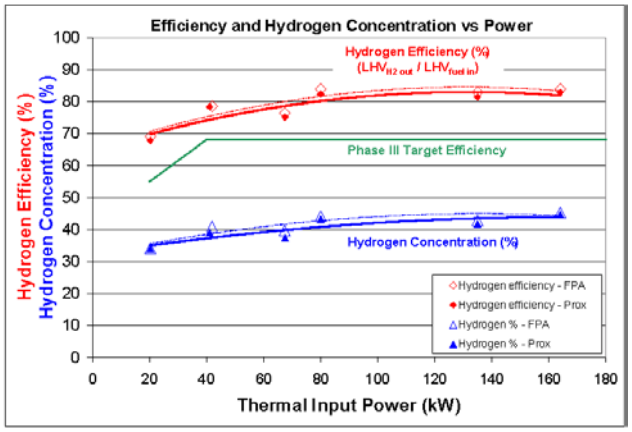

Figure 10. Hydrogen efficiency (LHVH2 out/LHVgasoline in) and dry hydrogen concentration versus gasoline input power (based on LHV) at the exit of the fuel processor and at the exit of the PrOx of the Phase III system.

subsystem included the following improvements from Phase II:

- A low-temperature shift bed separate from the main reformer vessel;
- A new PrOx design that included an integrated heat exchanger for controlling the humidity of the gas going to the fuel cell;
- A water recycle loop that included a reverse-osmosis water cleanup system;
- Low-pressure-drop air flow control to minimize compressor power;
- Major advances in the control system, including computer control of the entire process, automatic start-up, and a system capable of maintaining less than 50 ppm CO during moderate power changes;
- A new Tail Gas Combustor (TGC) design; and
- Advanced thermal management that integrated the heat loads of the fuel processor, PrOx, and TGC.

Figure 11 shows a comparison of the Phase II and Phase III subsystems. Note that the Phase III subsystem shows higher maximum hydrogen efficiencies and hydrogen concentrations due to system improvements and its larger size.

The Phase III fuel processing subsystem was built and tested at Nuvera from August 1999 to February 2000 without the fuel cell subsystem. During this time, the fuel cell was simulated by feeding only a portion of the reformate produced back to the TGC. The subsystem was sent to Plug Power in November 2000, where it was first run without the fuel cell subsystem to verify operation at over 80% efficiency and less than 50 ppm CO. During December 2000 and January 2001, the fuel processing subsystem was integrated with a Plug Power fuel cell subsystem. The fuel processor used laboratory-supplied air, while the fuel cell initially used laboratory air and then used air provided by a compressor/motor/expander unit (CMEU). While running with the fuel cell subsystem, anode exhaust was consumed by the TGC, and the fuel processing subsystem achieved hydrogen efficiencies of up to 80% while maintaining CO levels of under 50 ppm. Although the subsystem was designed to produce enough hydrogen to make 50–60 kW_e of fuel cell

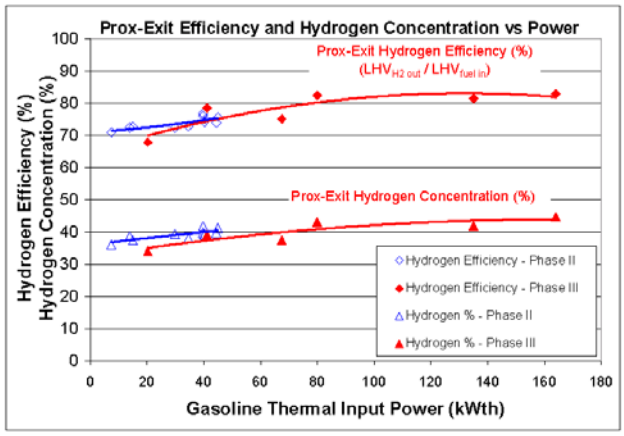

Figure 11. Comparison of Phase II and Phase III hydrogen efficiency and hydrogen concentration.

electricity, smaller fuel cell stacks were used, and 35.5-kW_e gross was achieved with a gasoline input of 148.8 $kW_{thermal}$. Figure 12 shows a comparison of PrOx-exit hydrogen efficiencies at Nuvera and those achieved while running with the fuel cell subsystem at Plug Power.

While running with the fuel cell subsystem at Plug Power, the exhaust from the TGC was monitored for emissions of NO_x, CO, and total hydrocarbons. Since the system did not undergo a true driving cycle, comparisons between the steady-state results and emissions standards give only a rough idea of emissions performance. However, the results showed very low emissions levels. For example, the emissions can be rated by using a specific method to measure the milligrams of emissions per gram of gasoline input. Over the 5–35-kW_e range of gross fuel cell power, the maximum steady-state CO emissions were 0.02 mg/g-fuel, and the maximum steady-state NO_x emissions were 0.04 mg/g-fuel. Converting the federal Tier II/bin 4 emission standards from grams/mile (by assuming 25 mpg and a fuel density of 0.74 g/mL) gives CO limits of 18.77 g/mi and NO_x limits of 0.63 g/mi. So, at steady state, the measured CO and NO_x were well below the equivalent Tier II limit. The steady-state total hydrocarbon emissions were measured as high as 1.1 mg/g-fuel by using a flame ionization detector (which cannot distinguish methane from other hydrocarbons). However, independent analysis on other Nuvera systems has shown the hydrocarbon emissions are more than 90% methane. Therefore, it is believed that less than 0.11 mg/g-fuel of non-methane hydrocarbons were emitted, which is less than the equivalent Tier II bin 4 limit of 0.49 mg/g-fuel. Figures 13, 14, and 15 show plots of the CO, NO_x, and total hydrocarbon emissions.

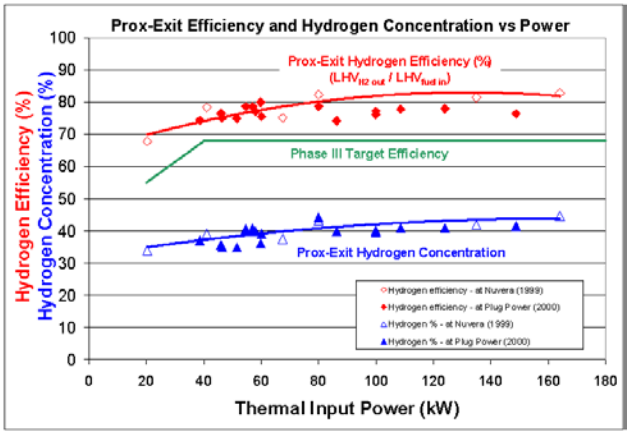

Figure 12. Comparison of Phase III PrOx-Exit hydrogen efficiency at Nuvera without a fuel cell and at Plug Power while integrated with a fuel cell.

Conclusions

A three-phase development program was executed to develop multi-fuel (gasoline, methanol, ethanol, and natural gas) fuel processing technology for fuel cell transportation applications. Multiple generations of reformers, CO cleanup reactors, and anode-gas combustor technologies were developed to advance the state of the art in fuel processing and to identify remaining technical challenges. The major contributions of this work are as follows:

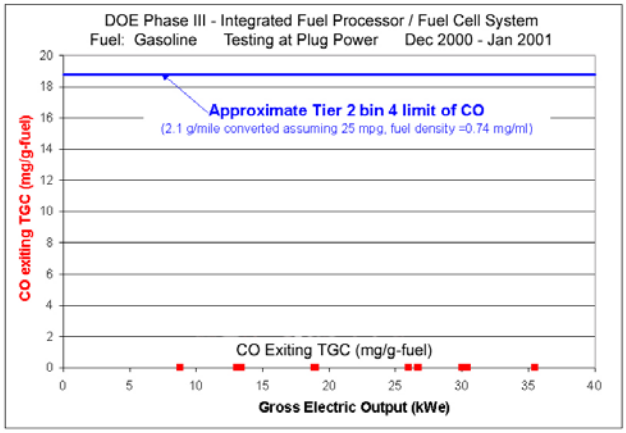

Figure 13. Phase III TGC emissions of CO.

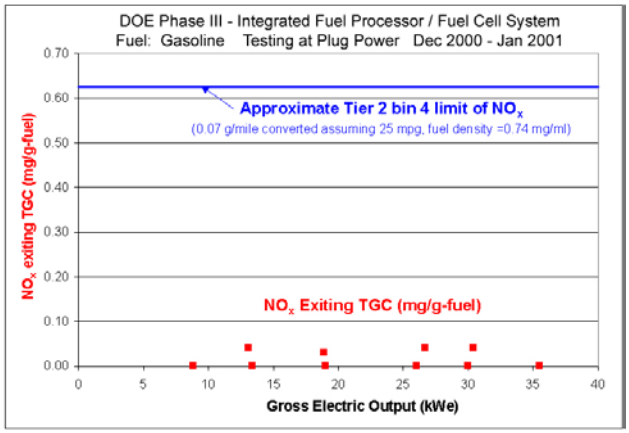

Figure 14. Phase III TGC emissions of NO_x.

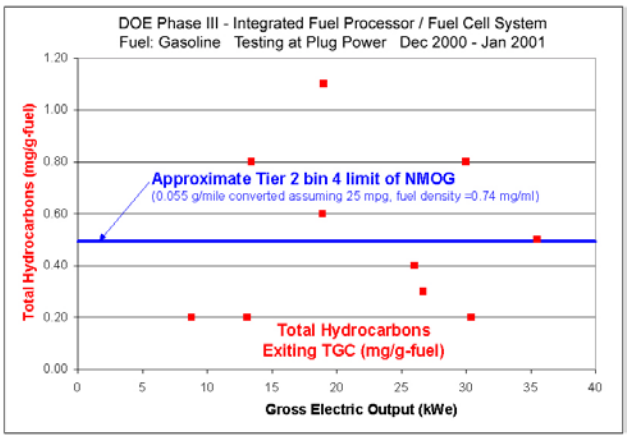

Figure 15. Phase III TGC emissions of total hydrocarbons.

- Demonstrating the viability of reforming hydrocarbon fuels, such as California Phase II gasoline, methanol, ethanol, and natural gas, with efficiencies in line with the DOE/PNGV targets.
- Developing CO cleanup technology capable of maintaining reformate CO concentration levels below 10 ppm under steady-state conditions and under 100 ppm during transients.
- Integration of the reformer, CO cleanup, and anode gas combustor subsystems to maintain high fuel processing system efficiencies.
- Integration of the Nuvera fuel processing subsystems with the Plug Power fuel cell subsystems, demonstrating integrated system functionality, and evaluating system level trade-offs.
- Improving various core technologies, such as catalysts, sulfur traps, heat exchangers, and control hardware, to better integrate these components.

References

1. Bowers, B.J.; Hagan, M.; Rumsey, J.; and Prabhu, S. (2000). Emissions from Fuel Processor/Fuel Cell Power Systems. SAE 2000 Congress. Paper #2000-01-0375.
2. Rumsey, J.; Bowers, B.; Hagan, M.; and Prabhu, S. (2000). Advances in Fuel Processing Systems for Transportation. 2000 Future Car Congress. Paper #00FCC-15.
3. Hagan, M.; Bowers, B.J.; Rumsey, J.; and Prabhu, S. (2000). Automotive Fuel Processing Systems for PEM Fuel Cells. SAE 2000 Congress. Paper #2000-01-0007.

C. Fuel Cell Systems Analysis

Romesh Kumar (primary contact), Rajesh Ahluwalia, E. Danial Doss, Howard Geyer, and Michael Krumpelt
Argonne National Laboratory
9700 South Cass Avenue
Argonne, IL 60439-4837
(630) 252-4342, fax: (630) 252-4176; e-mail: kumar@cmt.anl.gov

DOE Program Manager: JoAnn Milliken
(202) 586-2480, fax: (202) 586-9811, e-mail: JoAnn.Milliken@ee.doe.gov

Objectives

- Identify key fuel-cell-system design parameters and operating efficiencies.
- Assess design, part-load, and dynamic performance.
- Support U.S. Department of Energy (DOE)/Partnership for a New Generation of Vehicles (PNGV) developmental efforts.

OAAT R&D Plan: Task 8; Barrier J

Approach

- Develop, document, and make available an efficient, versatile system design and analysis code.
- Develop models of different fidelity (mechanistic detail).
- Apply models and modeling to issues of current interest as they evolve.

Accomplishments

- Developed detailed component models:
  - transient, multi-nodal radiator model;
  - transient, multi-nodal condenser model with desuperheat section; and
  - kinetic reactor models for the water-gas-shift (WGS) reactors, CO preferential oxidation reactor, and the autothermal reactor (for methane).
- Completed a comprehensive analysis of the effects of operating pressures from 2.0 to 3.2 atm on component sizes and system performance.
- Defined system configurations and component performances to evaluate trade-offs in size, cost, and efficiency.

Future Directions

- Define systems for size, performance, and cost analyses for the following:
  - high ambient temperatures, 49°C (120°F);
  - high power density stack operation, 0.65 to 0.8 V/cell;
  - ambient pressure systems; and
  - high-temperature membrane systems.
- Conduct sensitivity analyses and determine trade-offs (using engineering models for fast transients).
- Explore system configurations for lower-cost, smaller system weights and volumes.

Introduction

While individual developers are addressing improvements in individual components and subsystems in gasoline-fueled, fuel-cell-propulsion systems (e.g., cells, stacks, fuel processors, compressor/expander modules), we are using modeling and analysis to address issues of system integration; thermal management; design point and part-load operation; and component, system, and vehicle-level efficiencies and fuel economies. We develop baseline system definitions for manufacturing cost studies. We provide modeling results and analytical support to DOE program managers, fuel cell developers, the relevant PNGV technical teams, and other researchers in the field.

Approach

For this work, we use the GCtool software package to devise and analyze system configurations and operation. We have developed multi-nodal transient models for cross-flow radiators and condensers (the latter including a desuperheat section, if needed). We have used experimental microreactor data to derive kinetic rate constants for use in models for the WGS, preferential oxidation (PrOx), and autothermal reforming reactors. At the system level, we have analyzed the effects of operating pressure on system sizing and performance.

Results

During FY 2001, our major activities were in the following areas:

1. Reaction kinetics and reactor designs for the WGS and PrOx reactors for CO cleanup from reformate.
2. Detailed, multi-nodal transient models for finned, cross-flow radiators and condensers.
3. Comprehensive analyses of the influence of operating pressure on the sizes of the major components in pressurized fuel cell systems.
4. Effects of the design-point cell voltage on system efficiency and fuel cell stack size.

Reactor Models for the Water-Gas Shift and PrOx Reactors

Using microreactor data on one of the Argonne-developed water-gas shift catalysts, we determined the activation energy, kinetic rate constants, and the parameters for diffusion control of the reaction at the higher temperatures. These kinetic parameters were then used to calculate the conversion of CO to CO_2 as a function of temperature. The fit of the calculated conversions (smooth curve) to the experimentally observed conversions (dots) is shown in Figure 1, which shows that agreement between the two is very good. Thus, these kinetic parameters can be used to examine the effect of varying operating conditions (for example, the H_2O/CO ratio) on the optimum temperature profile in the WGS reactor and the amount of catalyst needed to achieve a given concentration of CO in the WGS outlet. Figure 2 shows the results for H_2O/CO ratios of 1.0, 1.8, and 2.3. For example, at a H_2O/CO ratio of 1.0 in the

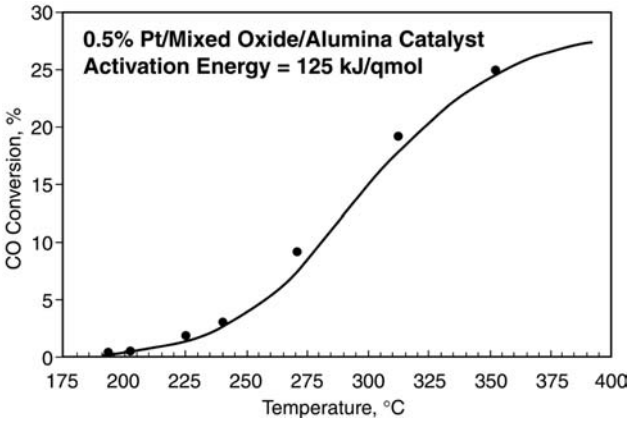

Figure 1. Agreement between the reaction kinetics model and microreactor data in both the kinetically limited low-temperature regime and the diffusion-limited high-temperature regime for one of Argonne's WGS catalysts.

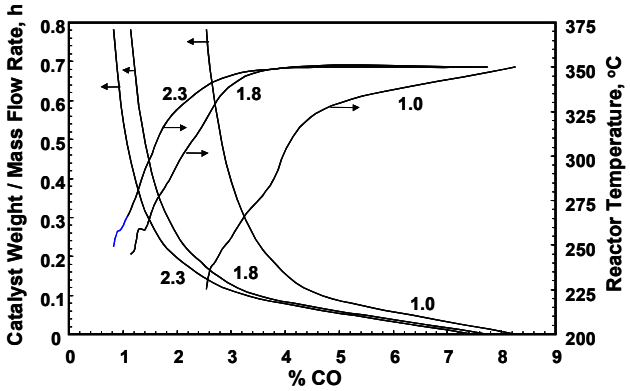

Figure 2. Effect of H_2O/CO ratio on the allowable temperatures and the corresponding required amounts of catalyst to achieve a given CO concentration in the WGS exit gas.

feed to the WGS reactor, the reactor would have to operate at no higher than 250°C to reduce CO to 3% and would require 0.42 kg of catalyst per kg/h of reformate flow. By increasing the H_2O/CO to 1.8, the reactor temperature can be maintained at 340°C and the catalyst mass reduced to 0.12 kg per kg/h of reformate flow to achieve the same 3% CO in the reactor outlet. The temperature could then be successively reduced to ~250°C to lower the CO concentration below 1% in the exiting reformate.

We have also analyzed the relative sizes of the WGS and the PrOx reactors as a function of the level of CO leaving the WGS and entering the PrOx. This analysis was for a pressurized system (3.2 atm) using commercial WGS and PrOx catalysts. The high temperature shift (HTS) reactor using Fe/Cr catalyst was simulated to reduce the CO level from 11 to 3%. The low temperature shift (LTS) reactor further reduced the CO level to various values between 0.3 and 1% through the use of the $Cu/Zn/Al_2O_3$ catalyst. Finally, the PrOx reactor, using Pt on γ-alumina catalyst, reduced the CO level to 50 ppm. As shown in Figure 3, the total amount of the WGS plus PrOx catalysts can be reduced from 133 to 110 kg, if the CO concentration at the inlet to the PrOx reactor is allowed to increase from 0.3 to 1%.

Radiator and Condenser Models

Waste heat rejection and water recovery (for fuel processing and gas humidification) are critical issues in polymer electrolyte fuel cell systems. We have developed detailed multi-nodal models for cross-flow finned radiators and condensers that can be used for transient and steady-state analyses. Figure 4 shows the mass of the radiator and the fin efficiency as a function of fin pitch for one set of conditions for which the heat rejection duty is 58.5 kW (thermal); the radiator mass is at a minimum for a fin pitch of a little less than 0.5 mm. Similarly, Figure 5 shows that the condenser mass is at a minimum, with a fin pitch of between 1.5 and 2 mm. In this simulation, the condenser cooling load was 10.9 kW. For both the radiator and the condenser, the fin efficiency was ~25% at the respective fin pitch leading to minimum weight of the unit.

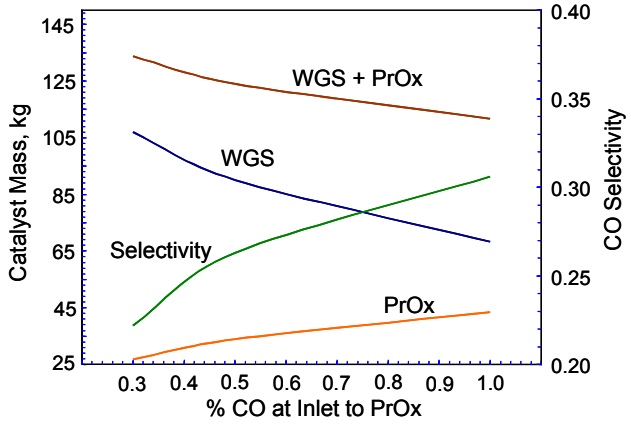

Figure 3. Required amounts of HTS, LTS, and PrOx catalysts as a function of the CO concentration at the exit from the WGS and inlet to the PrOx reactors.

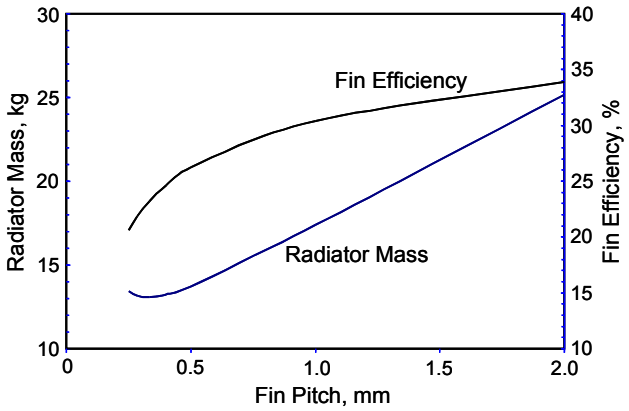

Figure 4. Cross-flow radiator: effect of fin pitch on radiator mass and the resultant fin efficiency.

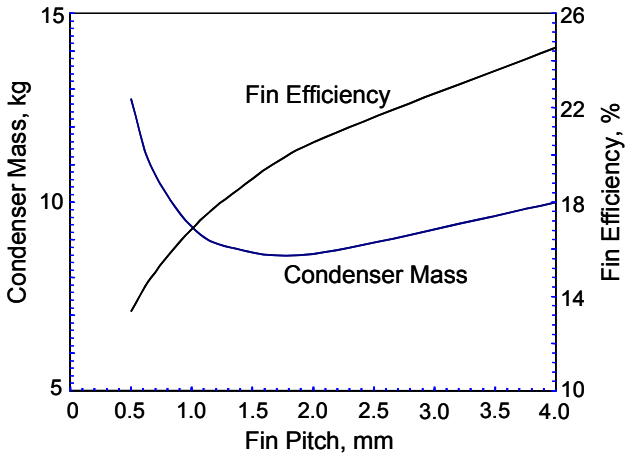

Figure 5. Cross-flow condenser: effect of fin pitch on condenser mass and the corresponding fin efficiency.

Component Sizes versus Operating Pressure

We have examined the influence of system operating pressure (at the rated power point) on the relative sizes of the fuel cell stack, the fuel processor, and the thermal and water management components. The results are summarized in Figure 6. The original DOE guidelines assumed a compressor discharge pressure of 3.2 atm. However, some of the compressor/expander hardware being developed appears more likely to offer somewhat lower discharge pressures. Our analyses indicate that as the operating pressure is reduced from 3.2 to 2.0 atm, the relative increases in size would be ~4% for the fuel cell stack (i.e., active cell area), ~20% for the fuel processor, and ~55% for the radiator and condenser (combined).

Effect of Design-Point Cell Voltage

The fuel cell stack is the most expensive component of the fuel cell system. For a given power rating, it is possible to decrease the amount of active cell area required (and, hence, the cost of the fuel cell stack) by decreasing the cell voltage and increasing the current density at the design operating point. There is, however, a concomitant decrease in system efficiency. These interactions are shown in Figure 7, where the active cell area and the system efficiencies at full load and at 25% of full load are shown as a function of the cell voltage at the rated power point. As the design-point cell voltage is decreased from 0.8 to 0.6 V, the required active fuel cell area decreases from 55 to 14 m^2. The system efficiency also decreases, however, from 41 to 29% at full load and from 45 to 40% at 25% of full load.

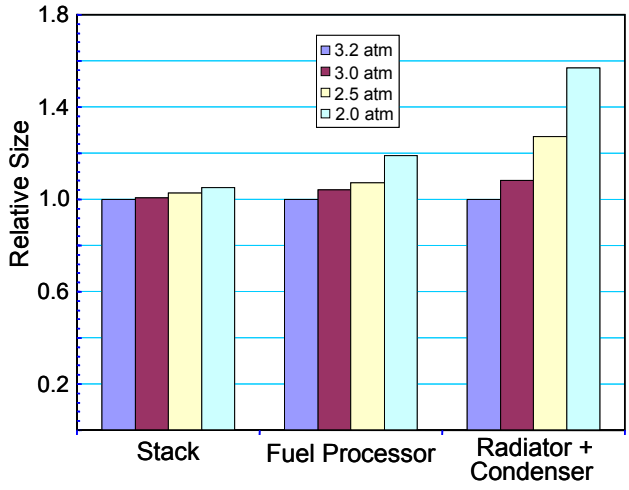

Figure 6. Effect of varying the operating pressure between 2.0 and 3.2 atm on the relative sizes of the fuel cell stack, fuel processor, and the major heat exchangers.

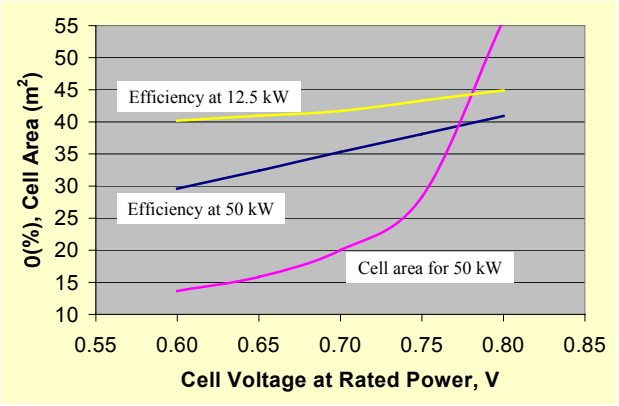

Figure 7. Effect of design-point cell voltage on the required fuel cell stack active area and the overall system efficiency at the rated power and at 25% of the rated power.

Conclusions

- Models for the WGS reactors show the quantitative beneficial effects of excess water for the WGS reaction. Approximately 100% excess water (compared to the amount of carbon monoxide to be converted) can decrease the required mass of WGS catalyst by 70%.
- For a given amount of waste heat to be rejected and water to be recovered, optimum radiator and condenser designs can be developed. An important design parameter is the fin pitch, which may be less than 0.5 mm for the radiator and 1.5–2 mm for the condenser, for each unit to be of minimum mass.
- Lowering the design-point operating pressure from 3.2 to 2.0 atm is expected to increase the required active area of the fuel cell stack by less than 5%, but it will increase the fuel processor size by 20% and the radiator plus condenser size by almost 55% to maintain the same system performance (efficiency).
- The active area of the fuel cell (and cost) can be reduced by a factor of ~4 by decreasing the design-point cell voltage from 0.8 to 0.6 V. However, the corresponding system efficiency at full load would decrease from over 40% to less than 30%, on the basis of gasoline's lower

heating value. The efficiency decrease is proportionately less at one-fourth of the rated power, from 45 to 40%.

FY 2001 Publications/Presentations

- R.K. Ahluwalia, H.K. Geyer, E.D. Doss, and R. Kumar, "System Level Perspective On Fuel Cell Air Management," Fuel Cell Air Management Workshop, Argonne National Laboratory, October 10–11, 2000, Argonne, IL.
- E.D. Doss, R. Kumar, R. Ahluwalia, and M. Krumpelt, "Gasoline PEM Fuel Cell System's Issues: System Pressure, Reforming Temperature, And Cell Voltage," IEA PEFC Annex XI Meeting, November 3–4, 2000, Portland, OR.
- R. Kumar, S. Ahmed, M. Krumpelt, and X. Wang, "Promise and Problems of Solid Oxide Fuel Cells for Transportation," International Symposium on Fuel Cells for Vehicles, November 20–22, 2000, Nagoya, Japan.
- R. Kumar, "Systems Analysis: Effect of Operating Pressure, Cell Voltage," NAS/NRC Peer Review of PNGV Progress, USCAR, December 7–8, 2000, Southfield, MI.
- R. Kumar, R. Ahluwalia, E. Doss, H. Geyer, and M. Krumpelt, "Automotive Fuel Cell Systems Modeling and Analysis," 2001 Annual National Laboratory R&D Meeting, DOE Fuel Cells for Transportation Program, June 6–8, 2001, Oak Ridge, TN.
- R. Kumar, "Comparative Analysis of the Polymer Electrolyte and Solid Oxide Fuel Cells for Transportation Applications," IQPC conference on Fuel Cells for Transportation, Developing a Commercially Viable Fuel Cell Product and Hydrogen Infrastructure, July 16–17, 2001, Chicago, IL.

D. Fuel Cell Vehicle Systems Analysis*

Keith Wipke and Tony Markel
National Renewable Energy Laboratory (NREL)
1617 Cole Blvd.
Golden, CO 80401
(303) 275-4451, fax: (303) 275-4415; e-mail: keith_wipke@nrel.gov

Keith Hardy, Aymeric Rousseau, Rajesh Ahluwalia, and Howard Geyer
Argonne National Laboratory
9700 S. Cass. Ave., Bldg. 362
Argonne, IL 60439-4815
(630) 252-3088, fax: (630) 252-3443; e-mail: khardy@anl.gov

DOE Program Manager: JoAnn Milliken
(202) 586-2480, fax: (202) 586-9811, e-mail: JoAnn.Milliken@ee.doe.gov

DOE Program Manager: Robert Kost
(202) 586-2334, fax: (202) 586-6109, e-mail: robert.kost@hq.doe.gov

---

Objectives

- Develop and validate models and simulation programs to predict fuel economy and emissions and aid in setting performance targets for electric and hybrid vehicles.
- Conduct R&D on vehicle propulsion subsystem and ancillary subsystem technologies for advanced light-duty passenger vehicles, including fuel cell vehicles (FCVs).
- Validate the achievement of Office of Advanced Automotive Technologies (OAAT) targets for fuel cells and other technologies at the component, subsystem, and vehicle levels.

OAAT R&D Plan: Section 3.1 Vehicle Systems Program, Tasks 1, 2, 3A, and 4

Approach

- Guide and support the application and development of advanced vehicle systems models for FCVs, including ADVISOR and PSAT.
- Collect experimental data for advanced technology propulsion subsystem components, including fuel cells, to support modeling efforts and validate hardware systems.
- Link analysis tools to provide a digital functional vehicle for exploring and transferring new technologies and design processes to industry.

Accomplishments

- Major ADVISOR and PSAT model development highlights for FY 2001:
  - ADVISOR and PSAT hybrid models benchmarked against production hybrids by using Insight and Prius vehicle test data collected at national laboratories;
  - Four-wheel-drive functionality for both conventional and hybrid configurations added to PSAT;
  - Adaptive control strategy for parallel hybrids included in ADVISOR 3.0;
  - ADVISOR and PSAT enhanced with interactive interface features for detailed design exploration;

* This project was funded by the Vehicle Systems Program of OAAT.

  - PSAT model library expanded with data and models from FutureTruck competition;
  - MEEM engine model integrated into PSAT to provide emissions predictions based on extensive vehicle testing database; and
  - ADVISOR and PSAT data libraries expanded with new national laboratory test data including new motors, batteries, and engines.
- Third major iteration of the OAAT R&D plan technical targets analysis completed and presented to the fuel cell tech team to highlight impacts of revised technical targets at the vehicle system level.
- Results of fuel cell vs. battery size trade-off study published by Virginia Polytechnic Institute and State University and National Renewable Energy Laboratory (NREL) at SAE 2001 Congress.
- Plan developed for simplified engineering model of fuel cell system based on GCtool for use in vehicle systems models.

Future Directions

- Collect vehicle and subsystem data from technology development partners for development and validation of new and existing fuel cell systems models.
- Develop control strategies for fuel cell hybrid electric vehicles.
- Work with industry to apply the digital functional vehicle, multi-disciplinary analysis process to the optimization of fuel cell hybrid electric vehicle systems.
- Complete transient fuel cell engineering model based on GCtool for use in vehicle systems models.
- Compare design alternatives and operating characteristics of both neat fuel cell and fuel cell hybrid vehicles.

Introduction

The Vehicle Systems Program within OAAT of the U.S. Department of Energy (DOE) has supported the development of vehicle and subsystem computer models to provide research and development program guidance for promising future research directions and to evaluate applications of existing advanced technologies. The existing models, ADVISOR (Advanced Vehicle Simulator) and PSAT (PNGV Systems Analysis Toolkit), are currently developed and supported by the staff of NREL and Argonne National Laboratory (ANL). These models share a common development platform in the Matlab/Simulink programming environment and have a similar look and feel to their graphical user interfaces. The underlying fundamentals of the models differ in that ADVISOR performs a backward-facing calculation, while PSAT applies a forward-facing modeling approach. As a result, each model has specific roles within the Vehicle Systems Program. ADVISOR is used mainly for target setting, systems analysis, and optimization, while PSAT is used mainly to evaluate detailed vehicle and component control strategies and to support hardware-in-the-loop component testing and validation.

Results

Technical Target Analysis Summary

The objective of the technical target analysis effort is to periodically review the subsystem technical targets defined in the OAAT R&D Plan for consistency and to confirm that these targets will satisfy the vehicle level technical targets. In the past, the results from this effort have led to revision of the subsystem technical targets to ensure that the vehicle level goals are achieved. Between each iteration of the review, the level of uncertainty in the analysis results has been decreased substantially through the improvement of the models and methods and the inclusion of data for state-of-the-art components. The review process helps guide future R&D emphasis and leads to greater credibility for the overall Plan.

The most recent round of analysis focused on three vehicle configurations: internal-combustion-engine (ICE) -powered parallel hybrid, gasoline reformed fuel cell hybrid, and hydrogen fuel cell hybrid. The results for the current status and the year 2004 were generated. Within the model, vehicles are constructed on the basis of existing baseline

component data. The component characteristics are then scaled and adjusted to represent the target characteristics. For example, the baseline engine data have a peak efficiency of 41%, while the efficiency target is 45%. Therefore, the fuel use map for this engine is scaled by 41/45. Table 1 summarizes the baseline components used in this analysis.

The technical target analysis was performed by using ADVISOR. The analysis assumes that the vehicle must satisfy all PNGV vehicle performance targets, including:

- 0–60 mph in 12.0 s
- 40–60 mph in 5.3 s
- 0–85 mph in 23.4 s
- 6.5% grade at 55 mph for 20 min.

The component sizes (both power and energy) are scaled such that the minimum component size is used that will allow the vehicle to satisfy these constraints.

Figure 1 provides the predicted composite fuel economy for vehicles, on the basis of the technical targets. Composite fuel economy is calculated by the following equation:

$$\text{Combined FE} = \Big/\left(\frac{0.55}{cold-FTP}+\frac{0.45}{hot-HWY}\right)$$

Cold-FTP represents the fuel economy from an SOC-balanced FTP-75 cycle from ambient conditions; hot-HWY represents the fuel economy of an SOC-balanced Highway Fuel Economy Test cycle from fully warmed conditions. This figure shows that, on the basis of the current state-of-the-art technologies, it is unlikely that the PNGV vehicle fuel economy target is feasible. However, if all of the technical targets are achieved by 2004, the results show that all three configurations are likely to meet or exceed the vehicle fuel economy target (dotted line).

Table 1. Technical target analysis baseline components.

Component	Description
Fuel Converter (ICE)	1.7-L 60-kW Mercedes diesel engine
Fuel Converter (Gasoline Fuel Cell)	50-kW reformed fuel cell system (based on ANL model results)
Fuel Converter (Hydrogen Fuel Cell)	IFC 50-kW fuel cell system
Traction Motor	VPT 83-kW AC Induction
Energy Storage System	Saft 6-Ah Li-ion batteries

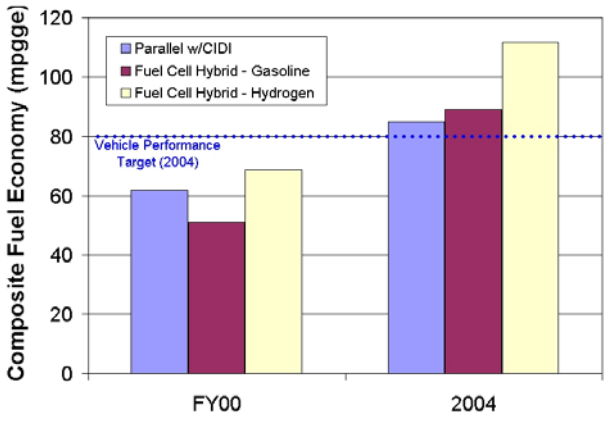

Figure 1. Technical target analysis composite fuel economy.

In Figure 2, a breakdown of the vehicle mass is presented by subsystem. The subsystem masses are the result of the necessary component size to satisfy the performance goals and the power and energy density targets outlined in the Plan. This shows that the current technical targets would provide a vehicle with a total mass within 100 kg of the target of 2,000 lb (889 kg) in all three cases.

A goal detailed in the Plan states that the advanced vehicles should be cost competitive with comparable conventional vehicles. Figure 3 provides an estimate of the powertrain system manufacturing cost on the basis of the resulting component characteristics and the subsystem cost targets detailed in the Plan. It is clear that the advanced

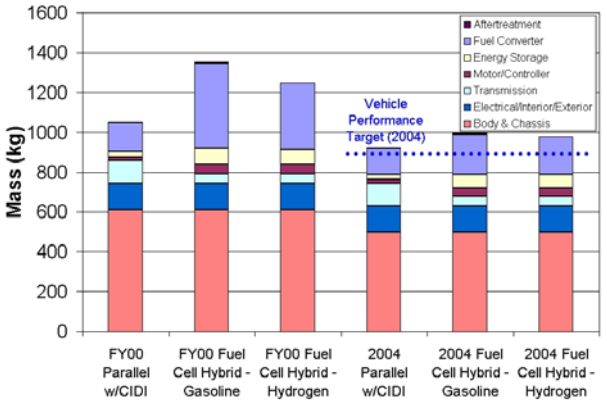

Figure 2. Technical target analysis vehicle system mass breakdown.

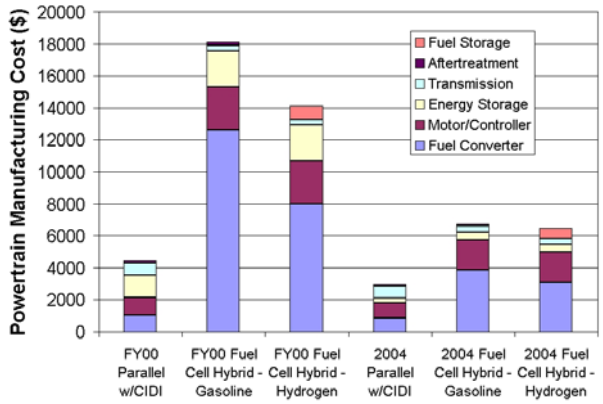

Figure 3. Technical Target Analysis Powertrain System Cost Breakdown.

technologies are extremely expensive today, but if the technical targets are achieved, significant progress will be made in reducing powertrain costs by 2004.

Fuel Cell Hybrid Sport Utility Vehicle (SUV) Optimization Study

Since 1999, NREL has been working with Virginia Polytechnic Institute and State University to collect data and improve fuel cell vehicle models on the basis of the results of student-built competition vehicles. At the 2001 SAE Congress, Virginia Polytechnic Institute and State University presented the results of a fuel cell versus battery size trade-off study for several classes of vehicles. The PNGV Technical Teams in earlier meetings specifically highlighted the sizing analysis as an area of interest. These results showed that, regardless of vehicle class, a fuel cell to total vehicle power (fuel cell + battery) of ~85% was desirable on the basis of fuel economy results.

As follow-on to this parametric study, various types of optimization algorithms were applied to a similar fuel cell hybrid SUV design problem. The problem assumptions were modified slightly to allow more design flexibility and to improve the inter-relationships between the design parameters and their effects on the vehicle system.

The study objective was to maximize city/highway composite fuel economy via the modification of four component size characteristics (fuel cell power, battery power, battery capacity, and motor power) and four energy management strategy parameters while enforcing seven constraints related to vehicle performance.

Five different optimization algorithms were applied to the same design problem. Three of these algorithms (VisualDOC DGO, VisualDOC RSA, and ISIGHT DONLP) apply gradient-based search methods in different ways. Two of the algorithms (DIRECT and ISIGHT GA) apply non-gradient-based search methods. These labels are used to identify the various datasets in Figure 4.

From Figure 4, we see that many of the algorithms found locally optimal solutions but stopped before finding what is believed to be the global optimum for this problem. The local versus global characteristics of the DIRECT algorithm are clear in Figure 4, as it quickly found a good local area to search within, while many more global evaluations were necessary to achieve significant additional gains. By starting ISIGHT DONLP (gradient-based) at the best point found by DIRECT, it quickly converged to a solution that was only fractionally better.

Given the number of function evaluations completed, we can have good confidence that the best point found is likely to be the global optimum. This design achieved a composite fuel economy of 56.6 mpgge and consisted of a 64-kW (net) fuel cell system, a 124-kW traction motor, and a 105-kW battery pack packaged in a mid-size SUV (i.e., Jeep Cherokee).

Fuel Cell System Engineering Model Development

Engineers at ANL have been developing and applying fuel cell systems models for many years. This effort has been focused on a software package

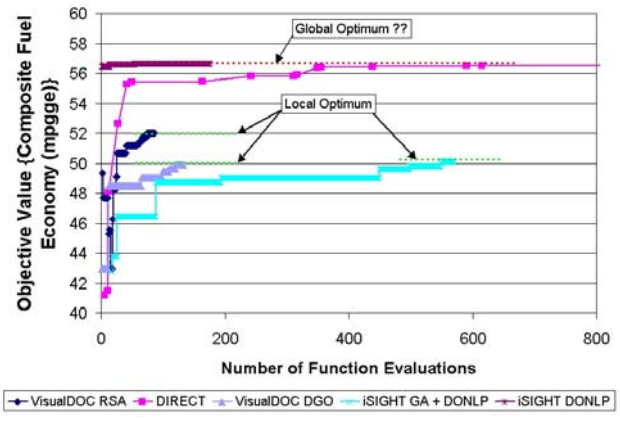

Figure 4. Multi-Algorithm Exploration of Fuel Cell Hybrid SUV Design Space.

called GCtool. It has an extensive level of detail with models for many energy conversion devices used in fuel cell systems. The models within GCtool, however, are too detailed and too slow to be used directly with vehicle simulation codes. As a result, ANL has started to develop engineering models of fuel cell (FC) systems and components using GCtool architecture and to link them to PSAT. The engineering models solve the governing conservation equations for energy, mass, species, and momentum but with the source terms interpolated from the performance maps. The maps can be constructed from the fundamental models in GCtool or from the experimental data taken at ANL's Fuel Cell Test Facility. The models are transient, can be multinodal, and may directly interact with other components. To date, models have been formulated for the autothermal reformer, water gas shift reactors, preferential oxidation reactor, and the polymer electrolyte fuel cell stack.

To automate linkage with PSAT, a translator has been written to produce a MATLAB/Simulink executable from the GCtool driver. The executable link then becomes a member of the drivetrain library in PSAT. Figure 5 shows the overall strategy of constructing the FC system configuration by using the GCtool platform and exporting an executable program to PSAT. The linked GCtool (ENG) – PSAT code provides a capability for analyzing transient fuel cell system responses during drive cycle simulations of hybrid vehicles. In the coming year, the code will also be used to evaluate control strategies for fuel cell hybrid vehicles in detail.

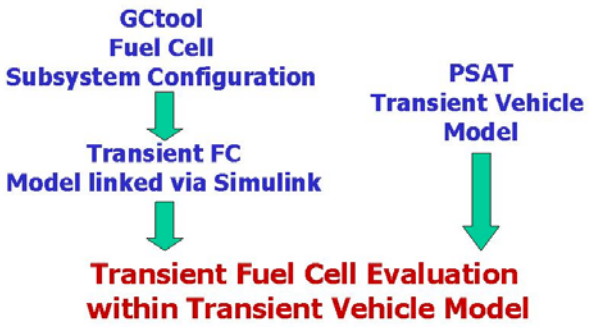

Figure 5. Linkage of the transient FC system model with PSAT.

Conclusions

The development of vehicle systems models and the application of these models to systems design have contributed to the fuel cell program efforts during the past year through the direct support of the Vehicle Systems Program. This support has resulted in improved models and expanded data libraries and has influenced analysis conclusions. On the basis of the select results presented here, the following conclusions can be offered:

- A third major iteration of the review of the OAAT R&D Plan technical targets analysis was completed and results were provided. The results showed that, if all current proposed targets were satisfied with hardware, it is likely that the targeted PNGV vehicle fuel economy could be achieved with an internal combustion engine (ICE) -powered parallel hybrid, a gasoline reformed fuel cell hybrid, or a hydrogen fuel cell hybrid vehicle. The analysis also supported the conclusion that greater emphasis may need to be placed on subsystem cost and mass reductions.
- The optimization of a hydrogen-fueled fuel-cell-powered hybrid SUV was completed as a follow-on study to the fuel cell vs. battery size trade-off study completed earlier in the year by Virginia Polytechnic Institute and State University and NREL. This most recent study suggested that the design space for this problem is highly populated with locally optimal solutions. However, through a combination of optimization algorithms, we can confidently say that the best design for the current assumptions would operate with a thermostatic control strategy with some power following behavior and would consist of a 64-kW (net) fuel cell system, a 124-kW traction motor, and a 105-kW battery pack. This vehicle achieved a city/highway composite fuel economy of 56.6 mpgge.
- A process to build a link to take advantage of the complexity and advanced functionality of GCtool through the use of engineering fuel cell models has been detailed. This model development/integration plan, when completed, will provide users of vehicle systems models with the capability to model fuel cell systems at greater levels of detail, including transient

behavior, and quantify the impacts of such design details on the vehicle system.

Publications

- An, F., and A. Rousseau. 2001. "Integration of a Modal Energy and Emission Model into the PNGV Vehicle Simulation Model: PSAT," SAE World Conference, Detroit, March 5–8.
- Atwood, P., S. Gurski, D.J. Nelson, and K.B. Wipke. 2001. "Degree of Hybridization Modeling of a Fuel Cell Hybrid Electric Sport Utility Vehicle," SAE Publication 2001-01-0236, Proceedings of SAE Congress 2001, Detroit, Michigan, Jan.
- Markel, Tony. 2001. "Hybrid Vehicle Systems Optimization using ADVISOR and iSIGHT," presented at the iSIGHT User's Conference. Southfield, Michigan, May.
- Rousseau, A., et al. 2001. "Honda Insight Validation Using PSAT," FTT Conference, Costa-Mesa, August 22–24.
- Rousseau, A., et al. 2001. "The New PNGV System Analysis Toolkit PSAT V4.1 — Evolution and Improvements," FTT Conference, Costa-Mesa, August 22–24.
- Rousseau, A., and R. Larsen. 2001. "Validation of a Hybrid Modeling Software (PSAT) Using its Extension for Prototyping (PSAT-PRO)," GPC Conference, Detroit, June 5–7.
- Rousseau, A., and P. Pasquier. 2001. "Validation Process of a System Analysis Model: PSAT," SAE paper 01-P183, SAE World Conference, Detroit, March 5–8.

E. Cost Analyses of Fuel Cell Stacks/Systems

Eric J. Carlson (primary contact) and Dr. Johannes H.J. Thijssen
Arthur D. Little, Inc.
Acorn Park
Cambridge, MA 02140-2390
(617) 498-5903, fax: (617) 498-7012, e-mail: carlson.e@adlittle.com

DOE Program Manager: Nancy L. Garland
(202) 586-5673, fax: (202) 586-9811, e-mail: nancy.garland@ee.doe.gov

DOE Program Support: Larry S. Blair
(202) 586-0626, fax: (202) 586-9811, e-mail: larry.blair@ee.doe.gov

ANL Technical Advisor: Robert D. Sutton
(630) 252-4321, fax: (630) 252-4176, e-mail: sutton@cmt.anl.gov

Contractor: Arthur D. Little, Inc., Cambridge, Massachusetts
Prime Contract No. DE-FC02-99EE50587, May 1999–March 2004

Objective

To develop an independent cost model for polymer electrolyte membrane (PEM) fuel cell (FC) systems for transportation applications and to assess cost reduction strategies for year 2000–2004 development programs.

OAAT R&D Plan: Task 8; Barrier J

Approach

- Develop a baseline system configuration and cost estimate based on best-available and projected technology and manufacturing practices and assess the impact of potential technology developments on system cost reduction during the first two years.
- Annually update the baseline cost model and system scenarios based on assessments of developments in PEMFC system technologies and manufacturing processes during the subsequent four years.

Accomplishments

- Presented baseline system configuration and cost model to fuel cell component and system developers for feedback and discussion.
- Modified baseline cost model and system configuration as a result of developer feedback and comments from Partnership for a New Generation of Vehicles (PNGV) Technical Committee.
- Assessed most important cost drivers and integrated impact of variation in model input parameters via a sensitivity and Monte Carlo analysis.
- Assessed impact of several system configuration scenarios on system cost and performance. For example, we considered the case where the fuel cell stack was designed to operate near its high power point at rated power rather than 0.8 V. Assessed the impact of hybridization on system cost ($/kW) and weight where the rated output of the fuel cell ranged from 25 to 100 kW.

Future Directions

- Develop projections of future system performance and cost on the basis of continued industry feedback, alternative system scenarios, and projected technology developments.

Introduction

In 1999, a baseline cost estimate for a 50-kW PEM fuel cell system for passenger vehicles was developed on the basis of technology available in the year 2000, but a high-production-volume scenario (i.e., 500,000 units per year) was used. The allocation of components within the major subsystems is shown in Table 1. In year 2000, we solicited feedback from system and component developers on the system configuration, design and performance parameters, and manufacturing process and costing assumptions. We also assessed the impact of several different system design scenarios.

Approach

We approached component and system developers for feedback by using the baseline system configuration and cost estimate as a basis of discussion. Developer sites were visited for face-to-face discussions, which were followed up by subsequent exchanges of information that could be used in a public report. As a result of these discussions, the following revisions to the baseline model were made: (1) increased the cost basis of the electrolyte membrane from \$50 to \$100/m^2 to better account for the cost contribution of the membrane in the near future, (2) increased the platinum cost from \$13.50 to \$15.00 per gram (London Metal Exchange) and included a cost for conversion of platinum metal to a distributed catalyst material on carbon, (3) added a window frame around the membrane electrode assembly (MEA) and an integral gasket, and (4) decreased yields in the fuel cell stack processes, such as MEA manufacture.

In addition to the incorporation of developer comments into the updated cost projection, the PNGV Technical Team and the DOE Fuel Cell Team suggested system scenarios that were configured, and their cost was estimated. We modified the system design parameters and manufacturing assumptions to assess the impact of these changes on the overall system cost and weight. Specifically, we assessed the impact of designing the system for a stack sized near its high power operating point (e.g., 0.65 V), rather than at 0.8 V. The impact of the system power rating (kW) on the dollar/kilowatt cost of the system was estimated for use in consideration of the benefits of system hybridization.

Table 1. Allocation of components between subsystems.

Fuel Processor Subsystem		Fuel Cell Subsystem	Balance of Plant
Reformate Generator • Autothermal Reformer (ATR) • High-Temperature Shift (HTS) • Sulfur Removal • Low-Temperature Shift (LTS) • Steam Generator • Air Preheater • Steam Superheater • Reformate Humidifer	**Fuel Supply** • Fuel Pump • Fuel Vaporizer	• Fuel Cell Stack (Unit Cells) • Stack Hardware • Fuel Cell Heat Exchanger • Compressor/Expander • Anode Tailgas Burner	• Start-up Battery • System Controller • System Packaging • Electrical • Safety
Reformate Conditioner • NH_3 Removal • PrOx • Anode Gas Cooler • Economizers (2) • Anode Inlet Knockout Drum	**Water Supply** • Water Separators (2) • Heat Exchanger • Steam Drum • Process Water Reservoir		
• Sensors and Control Valves for each section			

Results

Revisions to the baseline model increased the overall system cost for the year 2000 by 10% to $16,200 (or 324 $/kW). As shown in Table 2, the changes in the fuel cell stack material costs (i.e., the electrolyte and catalyst costs) had the largest impact on the system cost. Our discussions with developers did not give us reason to increase the performance of the stack (e.g., the power density) or to lower the catalyst loading. Other comments led us to lower cell fabrication process yield numbers and to add more features to the MEA seal design. The other changes to the fuel processor and assembly process had minor impact on the overall system cost.

Feedback from the PNGV Technical Team for fuel cells led us to design the system for heat rejection at an ambient temperature of 120°F rather than 95°F as in our original system configuration. This increased the size of the fuel cell radiator but had negligible impact on parasitic fan power because the fan design was revised from 2- to 0.5-in. water column pressure drop. Gross stack power remained at 56 kW and the system efficiency at 37%.

The PNGV Technical Team had also indicated that practical designs would size the fuel cell stack at or near its high power point to reduce the size of the stack and to lower the system cost because of reduced platinum and other MEA materials in the stack. Table 3 shows the impact on the subsystem costs. Overall, the system cost was reduced by 20% because of the significantly lower stack cost; however, system efficiency also decreased by 20% — from 37% to 29%. Increases in power density through reduction in the stack weight were negated by increases in the fuel processor and the fuel cell heat exchanger weight as a result of the lower efficiency of the fuel cell stack, as shown in Figure 1.

Table 2. Revisions to the 2000 baseline cost estimate.

Factory Cost Estimate*				
Subsystem	**2000 Baseline ($/kW)**	**2001 Baseline ($/kW)**	**% Change**	**Driver**
Fuel Cell	177	221	+25	Electrode and membrane material cost basis revised resulting in net increase
Fuel Processor	86	76	-12	Catalyst bed calculation basis revised
BOP	10	10	0	No changes to 2000 Baseline
System Assembly	21	17	-19	Reduction in assumed welding times
Total	294	324	+10	Overall increase due to fuel cell subsystem cost increase

Table 3. Impact of operating the fuel cell at its high power point on overall system cost (factory cost).

Subsystem	2001 Baseline ($/kW)	High Power ($/kW)	% Change
Fuel Cell	221	143	-35
Fuel Processor	76	85	12
BOP	10	11	10
System Assembly	17	20	17
Total	324	259	-20

Hybrid fuel cell designs have been proposed to improve transient performance and to reduce the size and cost of the fuel cell system. The cost of fuel cell systems of 25-kW and 100-kW rated power were estimated by using the same model but modified to scale certain components by size and to leave others, such as the controller, fixed. The estimated hybrid cost does not include the cost of the battery and associated power electronics. At 25 kW, the cost per kilowatt increased to approximately $425/kW and decreased to $275/kW at 100 kW because of the increasing or decreasing contribution of the fixed cost components, as shown in Figure 2.

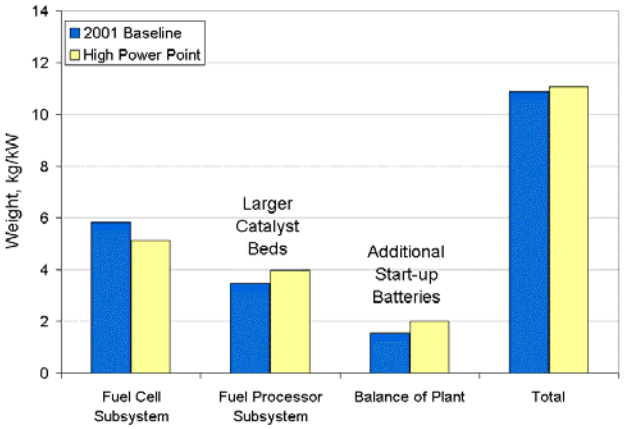

Figure 1. Impact of high power design point on fuel stack and fuel cell subsystem weight.

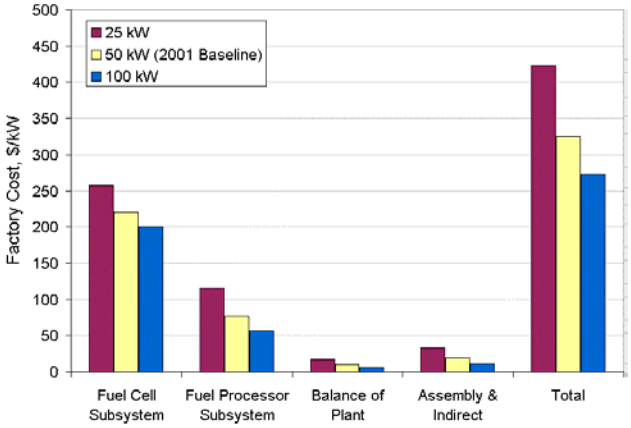

Figure 2. Impact of system rated power on system cost ($/kW).

Conclusions

In our discussions with developers, we did not find performance or design factors that would lead to reduced cost. On the contrary, system cost increased. The fuel cell subsystem, driven by the stack costs, continued to dominate system cost largely driven by the MEA materials (i.e., platinum and membrane).

Not surprisingly, the sensitivity analysis showed that parameters related to the size of the stack (power density), platinum loading, and MEA material costs (i.e., membrane price and cost of platinum) were the dominant cost contributors.

As expected, operating the fuel cell stack near the maximum power point decreased the size and cost of the stack. However, the benefit of lower stack cost was offset by decreased system efficiency and increases in fuel processor and heat exchanger weight due to the lower fuel cell efficiency. On balance, the high-power stack design (0.65 V) was not attractive because of the reduced system efficiency and negligible weight benefit.

If the size of a fuel cell system can be reduced through hybridization with batteries, the cost benefits of a lower power stack will be tempered by increased power cost ($/kW). Our estimates would be further increased by the cost of the battery, regenerative braking system, and power electronics. However, for larger fuel cell systems (greater than 50 kW), the power costs on a dollar/kilowatt basis will decrease.

F. DFMA Cost Estimates of Fuel-Cell/Reformer Systems at Low/Medium/High Production Rates

Brian D. James (primary contact), C.E. (Sandy) Thomas, Jonathan Ho, and Frank D. Lomax, Jr.
Directed Technologies, Inc.
3601 Wilson Blvd., Suite 650
Arlington, VA 22201
(703) 243-3383, fax: (703) 243-2724, e-mail: Brian_James@DirectedTechnologies.com

DOE Program Manager: Nancy L. Garland
(202) 586-5673, fax: (202) 586-9811, e-mail: nancy.garland@ee.doe.gov

ANL Program Manager: Walter Podolski
(630) 252-7558, fax: (630) 972-4430, e-mail: podolski@cmt.anl.gov

ANL Contractor: Directed Technologies, Inc., Arlington, Virginia
Prime Contract No. 993002401, December 1999–December 2003

Objectives

- Develop a realistic and internally consistent detailed design for an automotive gasoline fuel processor and PEM fuel cell system by using current-year technology.
- Apply Design for Manufacturing and Assembly (DFMA) design and costing techniques to achieve realistic cost estimates at low, medium, and high annual production rates.

OAAT R&D Plan: Task 8; Barrier J

Approach

- Develop a detailed design of a baseline 50-kW_{net} automotive gasoline fuel processor and fuel cell system upon which mass production cost estimates may be based.
- Apply DFMA techniques to assess the manufacturing methods and costs (material, manufacturing, and assembly) associated with complete system production at annual production rates of 500, 10,000, 30,000, and 500,000 units.
- Update the cost estimates annually.
- Conduct a series of in-depth trade studies on selected issues to assess pathways to lower cost systems.

Accomplishments

- Completed detailed baseline design and thermodynamic modeling.
- Completed preliminary detailed cost estimates of the fuel cell stacks and reactor integrated assembly.
- Completed less-detailed cost estimates of all remaining system components.

Future Directions

- Continue exploring alternative manufacturing and design improvements of entire system to lower cost.
- Prepare a cost estimate of the entire reformer/fuel cell system wherein the fuel cell operates at 0.6 V/cell rather than the baseline 0.7 V/cell.

- Prepare a cost estimate of a direct hydrogen fuel cell system for comparison with the cost of a reformate fuel cell system.
- Conduct more detailed cost estimates of peripheral systems.
- Begin in-depth trade-off studies (as detailed below) after finalization of detailed cost estimates at all production volumes.

Introduction

Directed Technologies Inc. (DTI) is under contract with Argonne National Laboratory (ANL) to conduct DFMA-style cost estimates of a complete onboard gasoline reformer and fuel cell system at several system annual production volumes. DFMA, Design for Manufacturing and Assembly, is a rigorous design/redesign and cost estimation methodology, the goal of which is to identify the lowest cost system design and manufacturing methods.

Approach

The approach to this project follows the four tasks contained in the contract statement of work. In Task 1, a baseline system architecture is defined for the entire reformer/fuel cell system. This task consists of (1) identifying the basic layout of the system; nominal operating temperatures, pressures, and flow rates; and materials and methods of construction and (2) defining a baseline bill of materials. In Task 2, DFMA techniques are applied to estimate the material, manufacturing, and assembly costs and to suggest alternative design choices and material and manufacturing choices that may lead to lower total cost. The techniques are inherently iterative, and thus the process is not completed until the costs of all rational design choices have been estimated and compared to determine the lowest-cost pathway. Task 3 consists of annual updates to the system cost estimate to reflect changing technology. Task 4 consists of a variety of specific trade-off studies designed to elaborate basic system architecture or operating modes. These studies include analysis of ambient versus pressurized operation, analysis of high-temperature operation, analysis of fuel sulfur level tolerance, comparison of steam versus autothermal methanol reformation, evaluation of a Direct Methanol Fuel Cell system, evaluation of a Solid Oxide Fuel Cell system, and an analysis of hydrogen purification methods.

Scope of Project

Table 1 and Figure 1 detail the main components and subsystems included in the cost analysis. In summary, all elements of the power system necessary to convert gasoline into hydrogen and then into electrical power are included in the system. The cost estimate includes the fuel supply and delivery system, the gasoline autothermal reformer to create a hydrogen-rich fuel stream, a Preferential Oxidation (PrOx) gas cleanup unit to reduce the fuel stream's CO content to below 20 ppm, a polymer electrolyte membrane (PEM) fuel cell stack system operating on the reformate gas and air, and the control/electrical/safety systems for all of the above. Items specifically not included in the cost are the Traction Inverter Module, the main automotive traction electric motor, and any peak-power or load-leveling battery subsystems.

Four annual production rates have been selected for cost estimation: 500, 10,000, 30,000, and 500,000 units per year. Obviously, the lower production rates are meant to allow cost estimates of reformer/fuel cell systems during the early phases of fuel cell vehicle (FCV) introduction, and the high production rates are for cost estimates of mature FCV production. While it will naturally take several years to ramp up to the high production rates (and to ramp up demand), all cost estimates are made for the same technology level (i.e., improvement in catalyst activity or fuel cell performance is not assumed for the higher production rates). However, manufacturing methods and material selections do vary between production levels.

Results

Reformer Baseline Definition

The reformer system is based on an autothermal reformer (ATR) and a preferential oxidation unit running on reformulated California gasoline to achieve a low-sulfur (< 1 ppm), low-carbon monoxide (less than 20 ppm), hydrogen-rich

Table 1. Summary of main system components.

Integrated ATR Assembly
Autothermal reactor
Low- and high-temp. water gas shift
Sulfur removal
Water boiler
Reformate Loop
PrOx unit
Air control solenoid
Catalytic burner
Condenser
Fuel Loop
Fuel tank assembly
High-pressure fuel pump
High-pressure fuel injector
Fuel Cell Stacks
MEA and bipolar plates
Endplates and brackets
Air Loop
Air compressor/expander
Air mass flow sensors
Air throttle body
Air humidifier
Water loop
Water pump and reservoir
Knock-out drum, condensers
High-pressure rail system
Water deionization filter
Coolant Loop
Pump, motor, and controller
Radiator assembly
Thermostat and by-pass valve
Controls
Electronic engine controller
CO sensors
Miscellaneous/Balance of Plant
Start-up battery
Electrical
System mounting
Misc.

reformate stream suitable for use by a PEM fuel cell. Figure 2 shows a drawing of the integrated ATR assembly as an aid to understanding its operation and construction.

The fuel enters the ATR and is mixed with steam before flowing over the ATR catalyst bed. The ATR bed is broken into two zones. The first zone consists of ATR catalyst washcoated on a zirconia foam support, and the second zone consists of ATR catalyst washcoated on a zirconia toughened mullite extrudate support. For both zones, the catalyst is modeled as 0.4% Pt on alumina and assumes the ATR activity values demonstrated by Argonne National Laboratory with its proprietary catalyst compositions.

The reformate gas next flows past a water spray quench and into a high-temperature water-gas-shift (HTS) zone. The HTS catalyst system is modeled as a 0.14% Pt/mixed oxide catalyst on 600 cells per inch (cpi) cordierite monolith. The catalyst layer is assumed to be 40-μm thick and applied via washcoating of γ-Al_2O_3, followed by catalyst application by the incipient wetness technique or other applicable routes. Five ring-shaped slices of HTS catalyst are used to complete the annulus around the ATR zone.

The reformate gas next flows into a finned plate heat exchanger to simultaneously raise steam for the ATR zone and reduce the reformate temperature exiting the HTS zone. This flattened-tube heat exchanger has two passes to approximate an isothermal reformate gas temperature distribution entering the sulfur removal bed.

The sulfur removal bed also consists of two beds. The first bed is modeled as a 600-cpi cordierite monolith washcoated with a 100-μm layer of zinc oxide. Because channeling has been experimentally observed at ANL, wherein some sulfur molecules can pass through the laminar monolith without contacting the ZnO absorbent, a second zone of ZnO-coated foam is included to ensure 100% of design sulfur capture. The beds are sized for 100,000-mi vehicle life, assuming the US06 drive cycle and 30-ppm S gasoline.

The reformate next flows into the low-temperature water gas shift (LTS) bed, which consists of a single zone of Cu oxide catalyst on a 600-cpi cordierite monolith. The catalyst activity is based on the work of ANL for air-tolerant shift catalysts. The reformate next flows into a second finned plate heat exchanger to further drop the temperature in preparation for the preferential oxidation (PrOx) reactor.

Fuel Cell Baseline Definition

The fuel cell subsystem is based on four stacks producing a total of 55 kW gross and 50 kW net at 0.7 V/cell and 400 mA/cm^2 to achieve a power density of 280 mW/cm^2. Further details of the stack system are shown in Table 2.

The reformate fuel cell design assumes a low current density (400 mA/cm^2) and high cell voltage

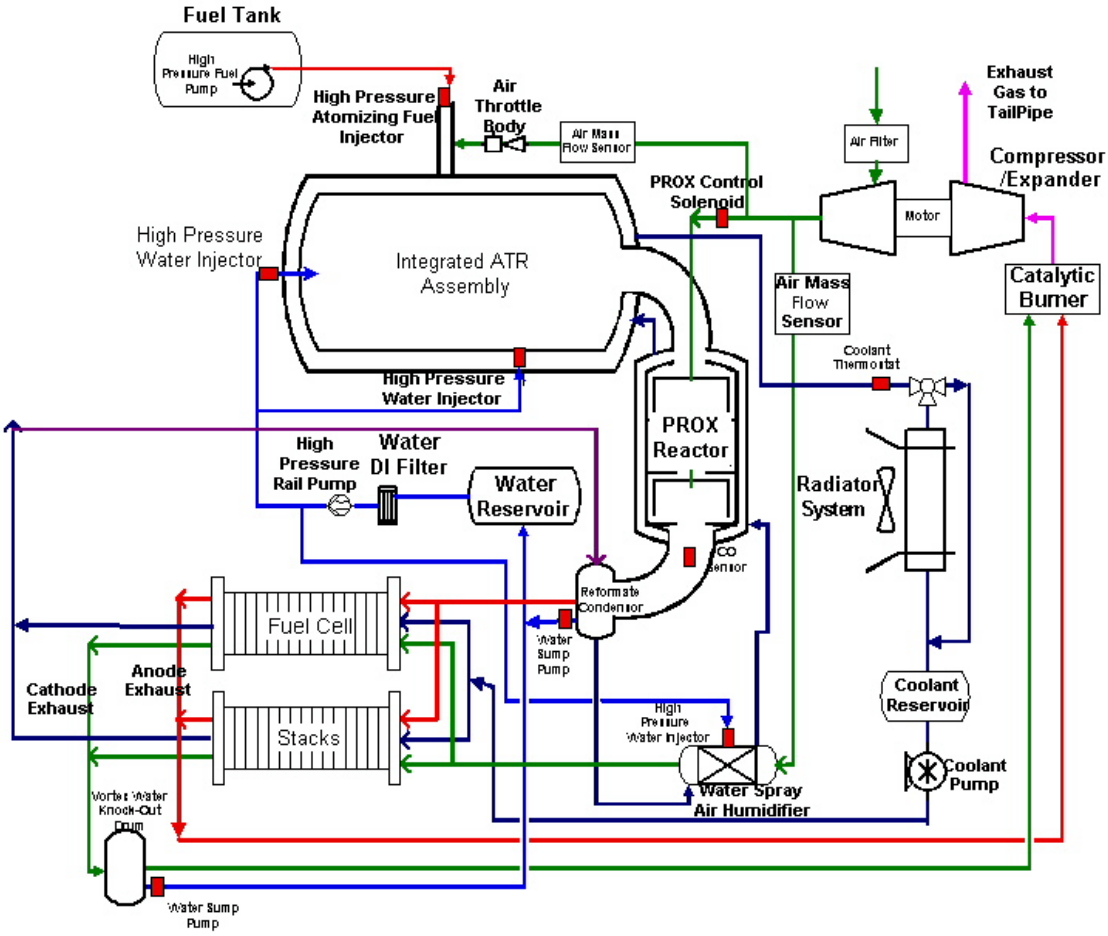

Figure 1. Gasoline reformer and fuel cell system schematic.

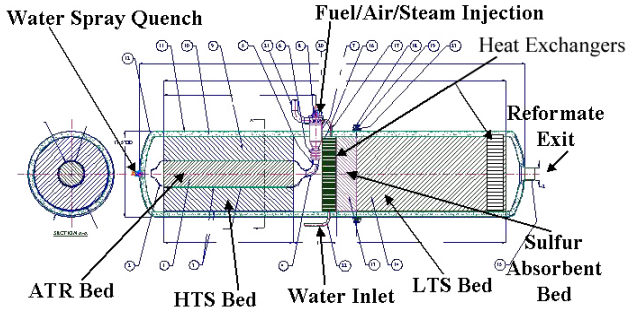

Figure 2. Basic configuration of the integrated ATR assembly.

(0.7 V/cell) to achieve high system efficiency. However, this design leads to a very low power density (280 mW/cm^2), which is approximately four times lower than the 1-W/cm^2 power density possible with current membrane electrode assemblies (MEAs) operating on pure hydrogen. As a result, the fuel cell stack is approximately four times larger and four times more expensive than an equally powerful fuel cell operating on pure hydrogen.

Multiple approaches to cell fabrication were considered, but the cost estimates are based on injection molding of 60% polypropylene/40% carbon black parts. Current collectors are aluminum blankings, insulators are injection molded, and endplates are machined or die-cast. The MEA is fabricated by hot pressing the membrane and carbon paper gas diffusion layer (GDL) into an injection-molded manifolding frame.

The membrane costs are based on Gore-type composite membranes (ionomer-impregnated expanded poly-tetra-fluro-ethylene [PTFE]) fabricated via roll-to-roll processing. Care was taken to obtain realistic capital equipment costs for the membrane fabrication conditions dictated in Gore patent literature. For low-volume production, the roll-to-roll process approach was retained, but

Table 2. Fuel cell stack system parameters.

Peak Power Conditions	Value
Gross Power (kW)	55
Net Power (kW)	50
Cell Voltage (V)	0.7
Current Density (mW/cm^2)	400
Nom. Operating Pressure (atm)	2.2
Power Density (mW/cm^2)	280
Number of Strands (lines in parallel)	1
Number of stacks per strand (stacks in series)	4
Number of cells per stack	110
Total number of cells	440
Total active membrane area (m^2)	19.64
Active area per cell (cm^2)	446.4
Peak voltage (V) (at 0.92 V/cell)	405
Min voltage (V) (at peak power)	308
Max current (A) (at peak power)	178.6
Catalyst Loading	
Cathode	0.3 mg/cm^2 Pt
Anode	0.4 mg/cm^2 Pt 0.2 mg/cm^2 Ru

equipment was reused to minimize capital cost and increase utilization fraction. (That is, the membrane roll was passed several times through one machine rather than building one continuous roll-to-roll machine.)

Preliminary Cost Estimates

Preliminary cost estimates for a fuel cell stack system at several annual production rates appear in Table 3. These estimates are for the four stacks alone (summing to 55 kW gross power output) and do not include ancillary components. The cost estimates include a 10% cost markup provision, as is standard automotive cost estimate practice. Additionally, the estimates are preliminary and may be reduced as alternative manufacturing methods are identified.

MEA cost is observed to dominate overall stack cost, primarily because of catalyst cost and ionomer material cost. Fuel cell catalyst cost is carried at a constant value based on bulk Pt at $662/troy ounce and bulk Ru at $155/troy ounce and represents 28–56% of total stack cost, depending on manufacturing rate. Catalyst preparation costs have not been estimated separately. The membrane cost is primarily high because of the current very high cost of the base protonically conductive ionomer.

Table 3. Fuel cell stack (55 kW gross power) cost estimates.

Cost Item	System Annual Production Rate			
	500	10,000	30,000	500,000
Bipolar Plates				
Cathode Plate	$505	$412	$405	$405
Anode Plate	$505	$412	$405	$405
MEA				
Membrane — Materials and Fabrication	$8,117	$2,024	$1,913	$1,282
Catalyst — Preparation and Application	$4,304	$4,304	$4,304	$4,304
Gas Diffusion Layer — Material and Fabrication	$1,143	$945	$895	$746
MEA Gasket — Material and Fabrication	$67	$50	$47	$47
MEA Hot pressing	$307	$281	$281	$280
Current Collectors	$62	$24	$22	$22
Insulators	$45	$7	$6	$5
Endplates	$286	$90	$71	$66
Tie-Rods	$36	$32	$30	$22
Stack Assembly	$124	$56	$55	$54
Stack Inspection/Leak Check	$30	$20	$20	$20
10% Cost Provision	$1,726	$962	$939	$851
Total Stack Cost	$17,258	$9,618	$9,394	$8,509

Ionomer material cost represents 15–26% of total stack cost, depending on manufacturing rate. Additionally, membrane cost is exacerbated by the high cost of low-production-rate roll-to-roll membrane fabrication. Clearly, both future cost studies and R&D efforts should be focused on reducing catalyst and ionomer costs.

Preliminary ATR cost estimates at several annual production rates appear in Table 4. The cost estimates are for the integrated reactor alone and do not include the substantial additional subsystems necessary for a functioning system. The catalytic beds and sulfur absorbent bed are observed to have

Table 4. Integrated ATR assembly cost estimates.

Cost Item	Annual Production Rate			
	500	10,000	30,000	500,000
Reactor Vessel & Insulation ($)	599	344	295	217
ATR Catalyst ($)	360	217	192	174
HTS Catalyst ($)	130	90	76	72
Sulfur Bed ($)	356	231	188	174
Water Vaporizer and HX ($)	1,253	558	374	317
LTS Catalyst ($)	379	249	202	191
Miscellaneous ($)	26	20	16	15
Assembly ($)	106	58	51	42
10% Cost Provision ($)	321	177	139	120
Total	$3,531	$1,945	$1,532	$1,322

approximately the same cost at each of the production levels. This similarity is primarily due to the comparatively high cost of the substrates and washcoating used to some extent in each of the beds, not because the beds contain equally expensive catalyst. A rolled metal monolith will be investigated as a lower cost option to the cordierite. The water vaporizer and heat exchanger are also expensive elements in the overall ATR, and future effort should be made to minimize their costs.

Conclusions

In summary, cost differences between the production rates are a result of differences in markup rates, bulk material prices, tooling amortization, and manufacturing/assembly procedures. The manufacturing approach remains substantially the same (from 500 to 500,000 units per year) because of the large number of repeat parts in the fuel cell and the economical use of stampings, catalyst support extrusions of low frontal area, and tubular shapes. Stamping generally transitions from individual die processes (<30,000 per year) to progressive dies (500,000 per year). Fuel cell endplates are machined at 500 units per year and die-cast at higher production volumes. Several boiler and heat exchanger manufacturing methods were examined to reduce low-production-rate costs, but the high-production method of a custom bending machine proved to be the lowest cost for all production rates considered. Fuel cell stack assembly is completely manual at 500 units per year, transitions to automated assembly of the repeat parts and manual final assembly at 10,000 and 30,000 units per year, and becomes fully automated assembly at 500,000 units per year. Full manual assembly (at custom workstations) is assumed for the integrated ATR assembly and final system assembly.

Table 5 contains summary cost estimates of the total 50-kW_{net} reactor system. These cost estimates are preliminary; the ATR integrated assembly and the fuel cell stacks have received much more detailed analysis than the other components. Overall, the system cost varies from \$550/kW_{net} at 500 units per year to \$262/kW_{net} at 500,000 units per year. This compares with the year 2004 DOE cost goal of \$125/kW_{net} and the year 2008 DOE goal of \$45/kW_{net}.

Table 5. Total power system cost estimate.

	System Annual Production Rate			
Cost Item	**500**	**10,000**	**30,000**	**500,000**
Fuel Cell Stack ($)	17,258	9,618	9,394	8,509
Air Loop ($)	1,160	821	734	529
Water Loop ($)	1,106	832	757	605
Coolant Loop ($)	620	486	450	386
ATR ($)	3,531	1,945	1,532	1,322
Reformate Loop ($)	1,172	838	739	658
Fuel Loop ($)	879	616	573	466
Controls ($)	719	501	442	316
Misc./BOP ($)	320	240	220	150
System Assembly ($)	723	487	442	157
Total Cost	$27,489	$16,384	$15,282	$13,099
Total Cost/kW_{net}	$550	$328	$306	$262

Notes:
- Based on a 50-kW_{net} system.
- All costs are preliminary as DFMA optimization had not yet been completed.
- ATR and fuel cell stack examined in more detail than other system components.
- All costs include 10% cost contingency and markup to reflect profit, G&A.

III. FUEL PROCESSING SUBSYSTEM[1]

A. Next-Millennium Fuel Processor™ for Transportation Fuel Cell Power System

Prashant S. Chintawar (primary contact), William Mitchell (PI), Srinivasa Prabhu, Robert Rounds, Frank Qi, James Cross, and Jong Hong
Nuvera Fuel Cells, Inc.
35 Acorn Park
Cambridge, MA 02140
(617) 498-6577, fax: (617) 498-6655, e-mail: chintawar.p@nuvera.com

DOE Program Manager: Patrick B. Davis
(202) 586-8061, fax: (202) 586-9811, e-mail: patrick.davis@ee.doe.gov

ANL Technical Advisor: Walter Podolski
(630) 252-5964, fax: (630) 972-4430, e-mail: podolski@cmt.anl.gov

Contractor: Nuvera Fuel Cells, Inc., Cambridge, Massachusetts
Prime Contract No. DE-FC02-99EE50580, June 1999–January 2003
Subcontractors/Partners: Corning, Inc., SubChemie, Inc., NexTech Materials, Ltd., and STC Catalysts, Inc.

Objectives

On the basis of our current in-depth understanding of fuel processing and fuel cell systems, we are carrying out a three-part program that will yield a fully optimized fuel processor for transportation applications. Two generations of ≥50-kW_e transportation multi-fuel processors will be developed and tested with fuel cells.

OAAT R&D Plan: Task 6; Barriers E, F, G, and H

Approach

- Perform automotive system analysis and identify strategies to meet Partnership for a New Generation of Vehicles (PNGV) targets.
- Evaluate the control strategies on a 10-kW_e fully automated system.
- Set targets (weight, volume, performance, efficiency) for key technologies and components on the basis of the results of the system analysis.
- Develop advanced catalyst, substrate, desulfurization, and heat exchanger technologies by working closely with Nuvera's partners.
- Develop conceptual design of fuel processor based on new technologies and draft control and fuel cell integration strategies.
- Design, fabricate, and test fuel processor on all fuels and investigate efficiency, emissions, steady-state and transient performance, and reformate purity.

---

[1] The DOE draft technical targets for fuel-flexible fuel processors can be found in Table 2a, 2b, and 2c, Appendix B. Because the targets in Appendix B were updated after the reports were written, the reports may not reflect the updated targets.

- Integrate fuel processor and fuel cell, investigate the performance of the power system, and identify system-level integration issues (Phase I).
- On the basis of Phase I results, continue technology development and refinement for Phase II.
- Test fuel processor, integrate power system, and obtain test data (Phase III). The Phase III system is expected to meet PNGV targets.

Accomplishments

- SFAA 1A
  - Developed control system and strategies for integrated fuel cell power system.
  - Designed and built fuel cell test cart for laboratory integration.
- SFAA 1L
  - Analyzed and quantified trace components, such as ammonia, aromatics, and oxygenates, in reformate by using advanced analytical tools.
  - Investigated trace components minimization and/or elimination strategies by manipulating fuel processor operation.
  - Tested several cleanup media for trace components.
  - Searched and selected high-temperature metals suitable for fuel processor application.
- SFAA 1J
  - Completed the conceptual design for the Phase I multi-fuel processor.
  - Completed extensive bench-scale tests of the subcomponents contained in the fuel processor.
  - Designed, built, and tested a 90-kW_e natural gas (NG) fuel processor based on STAR (Substrate-based Transportation Application Autothermal Reformer) technology, which exhibited power density of >625 W/L and efficiency exceeding 80%.
  - Completed integration of entire STAR fuel cell and fuel process piping and instrumentation diagram (P&ID).
  - Completed schematic layout of the STAR fuel cell system.
  - Determined key interconnection points between fuel cell and processor systems.

Future Directions

- SFAA 1A
  - Integrate 15-kW_e fuel processing system with the fuel cell stack in September 2001.
  - Conduct detailed system trade-off and control strategy evaluation with the integrated system.
  - Use 15-kW_e fuel cell power system to validate system models at Argonne National Laboratory.
- SFAA 1L
  - Set up test facility to investigate advanced material degradation.
  - Test selected high-temperature material in the real environment.
  - Investigate accelerated catalyst degradation.
  - Develop endurance test plan for integrated fuel processor systems.
  - Test integrated fuel processor endurance.
- SFAA 1J
  - Complete design and test STAR fuel processor.
  - Integrate STAR fuel processor and gasoline-reformate-tolerant polymer electrolyte membrane fuel cell (PEMFC) stack and demonstrate ≥50-kW_e fuel cell power.
  - Perform emission characterization of STAR fuel cell power system.
  - Conduct detailed system trade-off and control strategy evaluation.
  - On the basis of STAR results, formulate and implement R&D strategies for Phase II of the program.

Introduction

Nuvera Fuel Cells, Inc. (Nuvera), is a leading developer and supplier of fuel cells, fuel processors, and integrated power systems in the stationary and transportation markets. Widespread implementation of fuel cell systems for transportation markets requires significant improvements in many aspects of the technology, including power density, specific power, response, efficiency, and cost. In addition, the ability to operate on a number of hydrocarbon fuels that are available through the existing infrastructure is a key enabler for commercializing fuel cell power systems.

We are working with U.S. Department of Energy staff to develop efficient, low-emission, multi-fuel processors for transportation applications. The fuels include gasoline, methanol, ethanol, and natural gas. In this program, the challenges identified in our previous work are being addressed through an intensive technology development effort. On the basis of our current in-depth understanding of fuel processing and fuel cell systems, we are conducting a three-part program that will yield a fully optimized fuel processor for transportation applications. Two generations of ≥50-kW_e transportation multi-fuel processors will be developed and tested with fuel cells.

In part one of the program (SFAA 1A), we will integrate existing fuel processing hardware into a 10-kW_e multi-fuel power system to identify key system-level trade-offs in the design of a fuel processing subsystem and to allow validation of computer models developed both internally and by Argonne National Laboratory.

In part two of the program (SFAA 1L), we will use existing integrated and modular fuel processors to perform endurance testing that will identify and address material and catalyst degradation mechanisms. The output of this part of the program will feed directly into the final fuel processor design in the third part of the program.

In part three of the program (SFAA 1J or STAR), we will execute the STAR (Substrate-based Transportation Application Autothermal Reformer) program, which will yield an integrated ≥50-kW_e fuel cell power system (FCPS). The major element of STAR is an in-depth core technology development program that has been constructed to identify high-activity, low-cost, transportation-specific catalysts. To enhance power density and specific power, as well as to reduce start-up time, we will develop and design compact adsorbents, catalysts, and heat exchangers. These novel media, which have been found to be an order of magnitude superior to the conventional syngas catalysts, are based on transportation-specific substrates (such as monoliths). To address the issue of system durability, we are developing fuel purification (sulfur removal) and reformate cleanup technologies. The new catalysts and supports will be integrated into a fuel processor package specifically suited to the optimized catalyst suite. The output of this program will be a fully integrated fuel processing subsystem that meets or exceeds 2004 PNGV targets.

Results

We have extensive experience in the design and control of gasoline-powered fuel cell systems. Over the past year, we have addressed significant issues in the automation of the control system for both the fuel processor and fuel cell subsystems. Currently, Nuvera Fuel Cells Europe, SrL, is designing and testing a 20-kW_e, gasoline-reformate-capable, fuel cell stack that will be delivered to Nuvera Fuel Cells, Inc., in July for integration into the fuel cell power system. Figure 1 shows the fuel processor and fuel cell test carts, and Figure 2 shows the fuel processor performance.

Figure 3 shows how operating conditions affect the formation of a common contaminant, and Figure 4 shows the performance of different adsorbents for selectively adsorbing this trace species.

At the onset of the SFAA program, we performed automotive system analyses and set performance and cost targets for key components, such as catalysts, heat exchangers, adsorbents, desulfurizer media, and sensors. We had reported advanced component technology in the last progress report. We had also identified system-level strategies for weight and volume reduction of fuel cell power system.

This year's focus has been to integrate these components in a compact fuel processor that meets not only the PNGV targets, but also has the shape factor and packaging for automotive application. Our first attempt at such a design was a 90-kW_e NG fuel processor of 143-L volume that was built last year and is now being tested. We have collected

Figure 1. Nuvera's integrated fuel processor (left) and fuel cell test station (right).

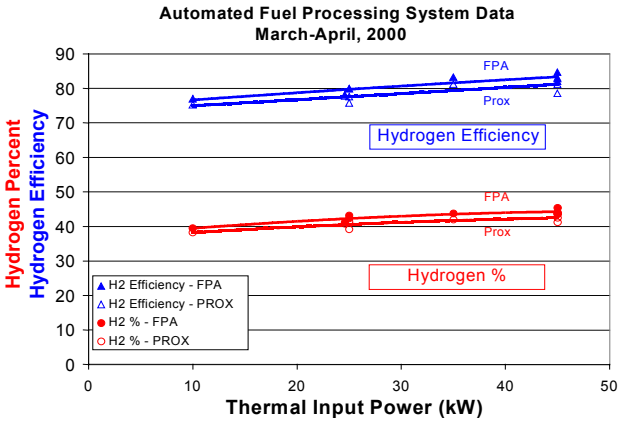

Figure 2. Fuel processor performance.

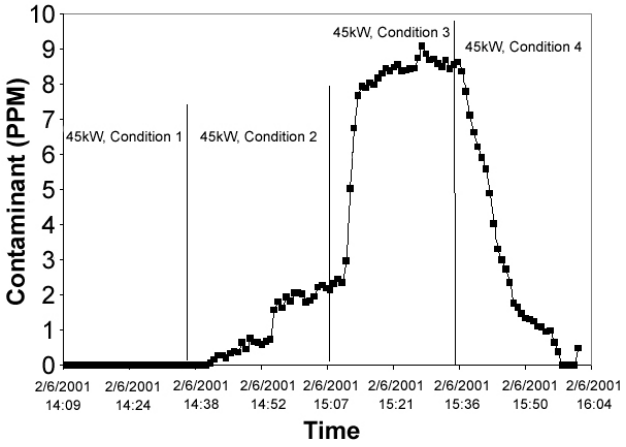

Figure 3. Effect of operating conditions on contaminant concentration.

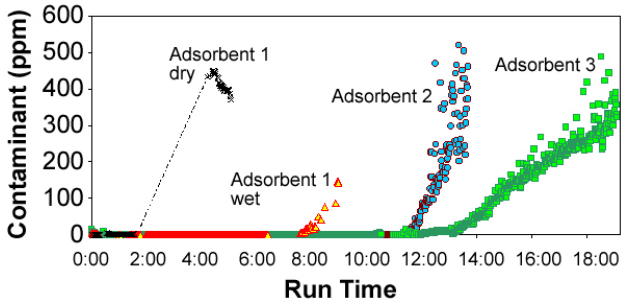

Figure 4. Comparison of different adsorbents for the removal of potential fuel cell contaminant from reformate.

preliminary data on this fuel processor. The data shown in Figure 5 indicate efficiency exceeding 80% over a wide operating regime.

On the basis of the results of the NG fuel processor, Nuvera kicked-off design efforts for a multi-fuel processor STAR this year. The conceptual design is ~70 L in volume. The STAR fuel processor will also contain a compact (<2 L) and highly efficient (>95% removal) external desulfurizer. Our computational fluid dynamics (CFD) and theoretical analyses suggest full power hydrogen efficiency of >80% on California Phase II gasoline. Note that the extensive use of structured catalysts suggests that this new generation of fuel processor can be mounted vertically or horizontally.

The conceptual design for the Phase I multi-fuel processor has been completed and is shown in Figure 6. This multi-fuel processor vessel is 70 L in displaced volume and contains all of the necessary reactors to produce fuel-cell-quality reformate. The adsorbents, compact heat exchangers, and intricate

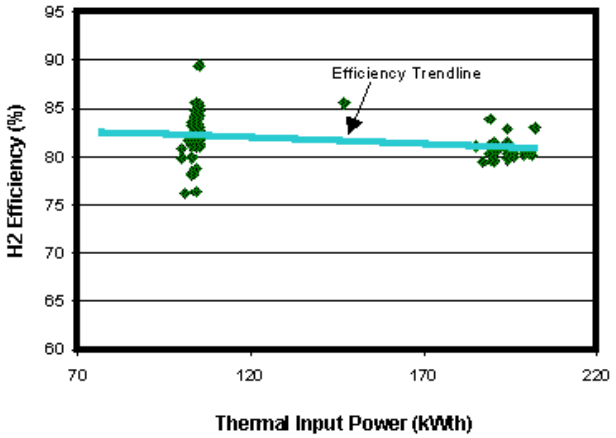

Figure 5. Nuvera 90-kW_e NG fuel processor test data — H_2 efficiency vs. output power.

Figure 6. STAR multi-fuel processor – conceptual design.

design not only exceeds the program goals for specific power, but it also is easy to package in a vehicle. We are in the process of completing the detailed mechanical design and building the first prototype for the Phase I program, which will be tested in fall 2001.

Extensive bench-scale tests of the subcomponents contained in the fuel processor have been completed. The high specific power of the fuel processor requires high-performance catalysts, mechanical devices. All crucial pieces of equipment have been tested separately and/or modeled by using computer simulation to improve the design. We have modeling capability using CFD, FEA, Hysis Process, and internally developed computer simulation to complement experimental testing and engineering calculations. Steady-state and transient testing of key fuel processor components indicates that the fuel processor will be able to meet the PNGV durability target.

Conclusions

- The concentration of trace components in reformate can be dramatically reduced by changing operating conditions.
- Trace components can be completely and economically removed.
- By using advanced media for catalysts, adsorbents, heat exchangers, and novel design concepts, it is possible to reduce the weight, volume, and start-up time of a multi-fuel processor and meet several PNGV targets.
- By using advanced sulfur removal technology, it is possible to effectively use gasoline as a fuel for automotive fuel cell power systems.

B. Multi-Fuel Processor for Fuel Cell Electric Vehicle Applications

Tom Flynn
McDermott Technology, Inc.
1562 Beeson Street
Alliance, OH 44601-2196
(330) 829-7622, fax: (330) 829-7283, e-mail: tom.j.flynn@mcdermott.com

Brian Engleman (subcontractor)
Catalytica Energy Systems, Inc.
430 Ferguson Drive
Mountain View, CA 94043-5272
(650) 940-6391, fax: (650) 960-0127, e-mail: bde@catalyticaenergy.com

DOE Program Manager: Nancy L. Garland
(202) 586-5673, fax: (202) 586-9811, e-mail: nancy.garland@ee.doe.gov

ANL Technical Advisor: Walter Podolski
(630) 252-7558, fax: (630) 972-4430, e-mail: podolski@cmt.anl.gov

Contractor: McDermott Technology, Inc., Alliance, Ohio
Prime Contract No. DE-FC02-99EE50586, June 1999–September 2002
Subcontractor: NexTech Materials

Objectives

- Design, build, and demonstrate a fully integrated, 50-kW_e, catalytic autothermal fuel processor system. The fuel processor will produce a hydrogen-rich gas for direct use in polymer electrolyte membrane (PEM) fuel cell systems for electric vehicle applications.

OAAT R&D Plan: Task 5; Barriers E, F, G, and H

Approach

- Develop preliminary design of 50-kW_e fuel processor system and performance goals for individual components.
- Evaluate alternative approaches for the major catalytic components (e.g., desulfurizer, reformer, shift reactor, and selective oxidation reactor).
- Conduct subsystem testing of major components by using best catalyst approach.
- Develop final design of overall system and design specifications for individual components.
- Assemble 50-kW_e fuel processor system.
- Perform demonstration testing on gasoline and methanol.
- Ship fuel processor system to Argonne National Laboratory.

Accomplishments

- Finalized process flow models for a catalytic autothermal reformer (ATR) for three load cases: 50 kW_e, 30 kW_e and 12.5 kW_e.
- Conducted peer review of preliminary design of fuel processor system.
- Developed dynamic model simulation.

- Finalized catalyst selection for each catalytic reactor.
- Conducted kinetic studies of the NexTech Cooperative Automotive Research for Advanced Technologies (CARAT) Program medium-temperature-shift (MTS) catalyst.
- Developed pelletization process for Pt/ceria MTS catalyst (NexTech).
- Permitted Los Alamos National Laboratory and Battelle/Pacific Northwest National Laboratory to supply selective oxidation reactor and steam generator (microchannel heat exchangers), respectively.

Future Directions

- Perform peer review of final design.
- Complete fabrication and assembly of fuel processor system.
- Conduct performance tests of fuel processor system.
- Ship fuel processor system to Argonne National Laboratory for further evaluation and testing.

Deliverables

- 50-kW fully integrated fuel processor.

Introduction

Development of a compact, efficient, and low-cost processor for converting carbon-based fuels to hydrogen is an important aspect of the successful implementation of fuel cells for transportation applications. A catalyst-based reforming approach for fuel processing can provide fast start-up and transient response, high efficiency, and compactness. When coupled with a liquid-fuel desulfurizer, the multifuel processor under development by McDermott Technology, Inc./ Catalytica Energy Systems (MTI/CESI), Inc., promises to approach the Partnership for a New Generation Vehicle (PNGV) targets.

Approach

The fuel processor will consist of a liquid-phase desulfurizer, a catalytic reformer, two stages of water-gas-shift reaction, a selective oxidizing unit, and ancillary components (including pumps, compressor/expander, heat exchangers, and controls). A general arrangement concept drawing of the fuel processor system is shown in Figure 1. The design has been described previously [1]. The program consists of five major tasks: Preliminary Design, Catalyst Development, Subsystem Testing, Final Design, and Prototype Assembly and Demonstration.

The liquid fuel desulfurizer reduces sulfur in gasoline to less than 3 ppm. The reformer unit,

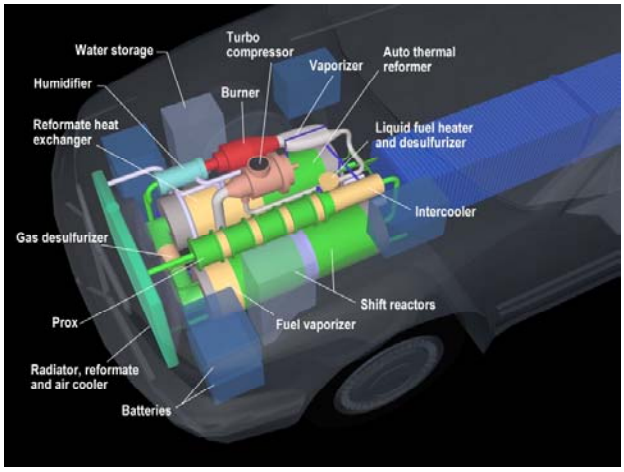

Figure 1. General arrangement drawing.

operating at an average temperature of 800°C, produces a hydrogen-rich gas from the fuel feed. Two approaches were evaluated during the program: a packed bed consisting of a single catalyst and a plate-based catalyst system. A bifunctional ATR catalyst that was developed by CESI was selected for use over the plate-based design. A shift reactor consisting of two stages of a medium-temperature-shift catalyst developed by NexTech Materials, Ltd., reduces the CO concentration in the reformate gas to approximately 2000 ppm. Final reduction of CO in the reformer gas is achieved in a selective oxidation reactor.

MTI developed the overall system design, including heat integration, mechanical design,

ancillary equipment, and instrumentation/controls. Catalytica Energy Systems developed the catalytic components, including a state-of-the-art autothermal reforming catalyst. NexTech, as a subcontractor on the project, contributed its expertise and technology in the area of shift catalysts.

Results

During this reporting period, a peer review of the preliminary design was completed. Subsystem characterization tests were conducted on the pelletized shift catalyst from NexTech Materials. The final design was completed, including final process simulation model runs, for three design load cases. The general arrangement drawings for the system, as well as the assembly drawing for the U-tube reactor, were completed.

Steady-state ASPEN process simulation models were generated for the catalyst-bed reformer concept. Three design loads were used to develop the design of the system. The maximum efficiency design point is 25% load (12.5 kW_e). The thermal integration is optimized around 60% load (30 kW_e). The maximum continuous rating design point is 50 kW_e. The performance specifications for the autothermal reformer catalyst concept system are summarized in Table 1. The predicted fuel processor efficiency is 80.58% at 25% load, assuming 70% hydrogen utilization in the fuel cell and 50% efficiency for the fuel cell. Actual performance data for the fuel pump, humidifier, compressor/expander, and fuel cell were incorporated into the simulation model.

Size and weight predictions are summarized in Table 2 and compared with PNGV targets. The system power density and specific power are 283 W/L and 165 W/kg, respectively. The size and weight are actual size and weight using commercially available components or developmental components for control and thermal management. The compressor/expander and start-up burner are excluded from the totals. A humidifier is included in the fuel processor scope as part of the water management system.

The catalyst scheme is summarized in Table 3. We have opted to use two medium-temperature-shift beds operating in series rather than separate high-temperature-shift (HTS) and low-temperature-shift (LTS) catalyst beds. The NexTech catalyst is a

Table 1. Predicted performance for autothermal fuel processor system.

		Predicted Performance		
Characteristic	**Units**	**Nominal**	**Design**	**Maximum**
Load	kW_e (net)	12.5	30	50
Reformer S/C Ratio		2.00	2.00	2.00
Total S/C Ratio		2.58	2.89	3.31
Total A/F Ratio (includes Selox)		13.4	14.5	16.1
Reformer Stoichiometry		0.23	0.25	0.28
Fuel Equivalence Ratio		4.31	3.98	3.58
Fuel Value of Gasoline, LHV	kW	35.1	92.7	167.2
Fuel Value of H_2 to Fuel Cell, LHV	kW	31.2	80.4	141.0
Electrical Output, gross	kW_e	13.97	35.81	62.86
Electrical Output, net	kW_e	12.74	30.68	50.38
Carbon Conversion	%	99.82	99.45	99.76
Cold Gas Efficiency (LHV)	%	88.92	86.74	84.37
Fuel Processor Efficiency	%	80.58	82.42	81.99
Overall System Efficiency (LHV)	%	32.84	31.43	29.26
Compressor Efficiency	%	67.0	74.4	73.0
Expander Efficiency	%	75.7	81.8	85.0
Expander Output	kW_e	0.4	2.3	4.0
Parasitic Loads	kW_e	1.6	7.5	16.5
Radiator Heat Rejection	kW	13.8	34.6	63.5
Fuel Cell Operating Temperature	°C	60	60	60
Fuel Cell Voltage (Assumed)	V	0.7	0.7	0.7
Fuel Cell H_2 Utilization	%	80.11	79.83	79.86
Fuel Cell O_2 Utilization	%	50.07	49.90	49.91
Fuel Cell Efficiency, LHV	%	44.78	44.54	44.58
Selox O_2/CO Ratio		0.98	0.98	0.98
Selox Selectivity		0.51	0.51	0.51
Selox CO Conversion	%	99.78	99.66	99.47
System Pressure Drop	KPa	6.74	15.75	38.69

Table 2. Summary of sizes and weights of components and overall system.

Subsystem Totals	Size (L)	Weight (kg)
Reformate Generator	128.00	280.25
Steam Generator	6.50	7.70
Reformate Conditioner	45.00	30.00
Fuel Supply	11.28	22.63
Water Supply	18.80	40.70
Controls & Piping (1/10 demonstration unit)	19.48	15.15
Overall Total	222.38	380.63
Power, kW_e (Gross)	62.86	62.86
Power Density/Specific Power (W/L, W/kg)	283	165
DOE PNGV 2004 Target (W/L, W/kg)	700	700
DOE PNGV 2008 Target (W/L, W/kg)	800	800

medium-temperature shift catalyst and, as such, is not intended to operate in the same temperature range as LTS, so direct comparison is not possible.

However, the NexTech catalyst possesses some important properties that warrant continued consideration for the prototype design [2]. The NexTech catalyst remains active in the oxidized or reduced state. It is less sensitive to condensed moisture. Noble metal washcoating on a monolith catalyst substrate is proven technology. Since the lower limit for its operating temperature is higher than that for conventional base-metal shift catalysts, the minimum achievable CO concentration, which is limited by thermal equilibrium, is higher than that for conventional base-metal shift catalysts. As a result, the selective oxidation reactor must be designed to handle a higher inlet CO concentration.

MTI continued to work with Pacific Northwest National Laboratory to design a steam generator based on its microchannel heat exchanger technology. Los Alamos National Laboratory will supply a selective oxidation reactor suitable for demonstration with monolith catalysts.

Catalytica Energy Systems performed extended evaluation tests of the NexTech Materials platinum/ceria medium-temperature-shift catalyst to quantify activity versus time at different temperatures. The results allowed MTI to determine the required size of the shift catalyst beds. An Arrhenius plot of the activity data acquired at 250, 300, 350, and 400°C (as seen in Figure 2) exhibits very good linearity (correlation coefficient of 0.98). This feature, along with the computed activation energy of 69.9 kJ/mole, indicates an absence of

Table 3. Catalyst scheme.

	Catalyst Beds				Cleanup Beds	
Parameter	**ATR**	**HTS/MTS**	**LTS**	**PrOx**	**Sulfur Removal**	**NH_3 Removal**
Temperature (°C)	807	399	263	94	322	None
Catalyst	Rh	Pt	Cu/ZnO	Pt	ZnO	None
Support	Zirconia	Ceria/Zirconia	ZnO/Al_2O_3	Alumina	None	None
GSHV (L/h)	9,165	13,833	13,623	25,000	134,405	None
Bed Volume (L)	10.0	10.0	11.2	7.4	1.0	None
Bed Weight (kg)	14.4	15.0	15.0	2.23	1.4	None

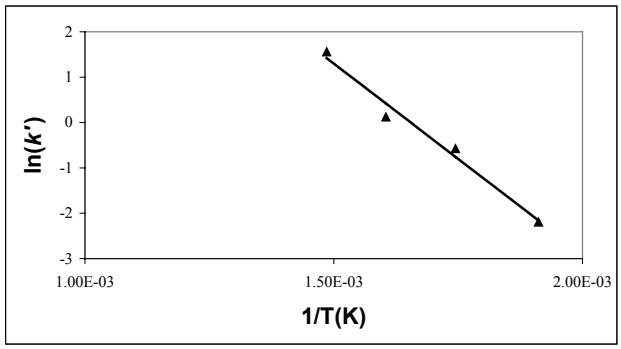

Figure 2. Arrhenius plot for the NexTech-III WGS catalyst.

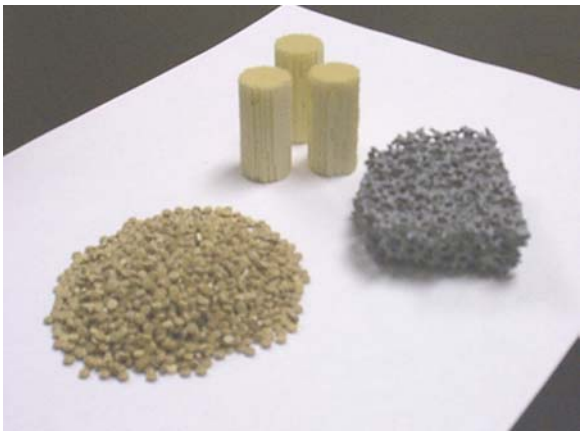

Figure 3. Packaging methods for NexTech materials Pt/ceria medium-temperature shift catalyst.

diffusional limitations (under these conditions) for the 0.42–0.50-mm catalyst pellets (Figure 2). Figure 3 illustrates the different Pt/ceria packaging methods that NexTech Materials is pursuing, including pelletizing, washcoating on honeycomb monoliths, and infiltration of ceramic foams.

Conclusions

A catalytic autothermal fuel processor based on bifunctional catalysts continues to show progress toward meeting the PNGV targets. The weight target continues to be more challenging than the size target.

References/Publications

1. T.J. Flynn, R.M. Privette, M.A. Perna, K.E Kneidel, D.L. King, and M. Cooper, "Compact Fuel Processor for Fuel Cell-Powered Vehicles," International Congress and Exposition, Detroit, MI, March 1–4, 1999, SP-1425, pp. 47–53.
2. Scott L. Swartz, "Nanoscale Water-Gas-Shift Catalysts," Snapshots of CARAT Projects, Phase 2, published by Argonne National Laboratory, Transportation Technology R&D Center, March 2000, pp. 11–12.

C. Integrated Fuel Processor Development

S. Ahmed (primary contact), C. Pereira, S.H.D. Lee, and M. Krumpelt
Argonne National Laboratory
9700 S. Cass Ave.
Argonne, IL 60439
(630) 252-4553, fax: (630) 972-4553, e-mail: ahmed@cmt.anl.gov

DOE Program Manager: JoAnn Milliken
(202) 586-2480, fax: (202) 586-9811, e-mail: joann.milliken@ee.doe.gov

---

Objectives

- Determine the design and operating conditions of an integrated fuel processor that can meet Partnership for a New Generation of Vehicles (PNGV) targets.
  - Identify preferable operating conditions for different catalysts and fuels.
  - Study the effects of component integration and identify methods that improve performance of the total fuel processor.

OAAT R&D Plan: Task 3; Barriers E, F, G, and H

Approach

- Study fuel processing steps individually in microreactors to determine suitable catalysts, their kinetic parameters, and desirable operating conditions.
- Verify component performance in the integrated reactor, validate reactor model, and identify concepts that improve fuel processor performance.

Accomplishments

- Demonstrated a concept for integrating the preferential oxidation unit.
- Demonstrated the integrated fuel processor:
  - With microchannel monoliths in the reformer.
  - At 78% efficiency at 4.7 kW_e, produced 44% hydrogen in reformate from hydrocarbon fuels.
  - Pressure drop through the device was recorded at less than 1 psig up to 6 kW_e.
- Adjusted temperature profiles in the shift reactor zone of the integrated unit to reduce CO level to ~1% (dry) in the reformate gas.
- Iniated negotiations to license technology to a commercial developer.

Future Directions

- Integrate the preferential oxidation unit such that the reformate gas contains less than 50 ppm carbon monoxide.
- Demonstrate operation of the unit at 10 kW_e with transportation fuels.
- Demonstrate ≥ 80% efficiency with hydrocarbon fuels.
- Identify constraints (e.g., thermal mass, start-up protocol) that limit rapid start and design/demonstrate hardware to enable rapid start.

Introduction

The objective of this work is to determine the fuel processor layout, design, and operating parameters such that it can meet PNGV's (Partnership for a New Generation of Vehicles) targets (for efficiency, size, weight, cost, response, etc.) for the automotive fuel cell system.

Approach

To achieve this objective, the fuel processor is being studied at two levels. First, a microreactor process train has been established with a series of reactors set up to represent the various unit processes. Each microreactor is enclosed in an electric furnace for accurate temperature control. The feed stream to each unit can be a simulated reformate gas metered in from a cylinder or from the previous unit process in the fuel processing train. The feed and product streams can be sampled and analyzed by using an on-line GC/MS system or with infrared analyzers. At the second level, an integrated fuel processor has been developed at Argonne National Laboratory (ANL) to study the effects of component integration and identify methods that improve performance of the total fuel processor.

Results

Figure 1 shows a picture of the integrated fuel processor developed at Argonne National Laboratory (ANL). Operating on ambient feeds, the unit includes the reformer, a sulfur trap, and the water gas shift reactor. With its 10-cm. diameter and 41-cm. length, the fuel processor has a total volume of 13 L. The reforming section uses a combination of micro-channel monoliths and pellets, comprising a volume of 1.4 L. It has been operated at up to 6 kW_e with gasoline.

ANL's current integrated fuel processor produces reformate gas exiting the water gas shift reactor. Figure 2 shows the temperature profile within the shift reactor. The reformate, containing 8% (dry) CO, entered the reactor at 400°C and exited at 150°C containing 1.1% CO.

To further reduce the level of CO to less than 50 ppm, a preferential oxidation (PrOx) unit is necessary. The next-generation integrated unit will include the preferential oxidation process that is being developed in collaboration with Los Alamos National Laboratory.

Figure 1. Picture of the engineering-scale integrated fuel processor.

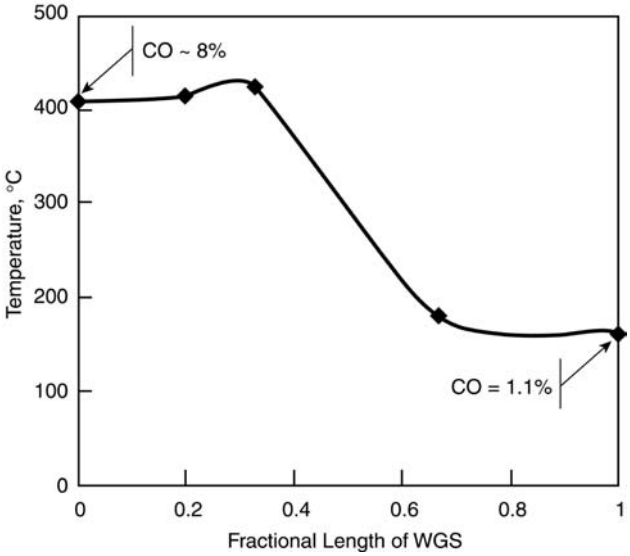

Figure 2. Temperature profile in the water gas shift reactor.

Preliminary studies have been conducted to test some options for the PrOx. Applying one such option in the microreactor process train (operating as a differential reactor), it was possible to reduce the CO level by 6% and the CH_4 level by 7%, with no significant change in hydrogen concentration. Extending that study by retrofitting the integrated

unit, the CO concentration was reduced by 40%, which was accompanied by 5% reduction in hydrogen concentration. The results are shown in Figure 3. Mass balance analysis revealed that 30% of the injected oxygen reacted with carbon monoxide. It is anticipated that higher selectivities can be achieved in a reactor designed for this operation.

Figure 4 shows the historical progress of ANL's fuel processor development work with respect to some performance parameters. The current fuel processor has been demonstrated at 78% efficiency [defined as the lower heating value (LHV) of the hydrogen produced as a percentage of the LHV of the fuel feed] with hydrocarbon fuels at 4.7 kW_e.

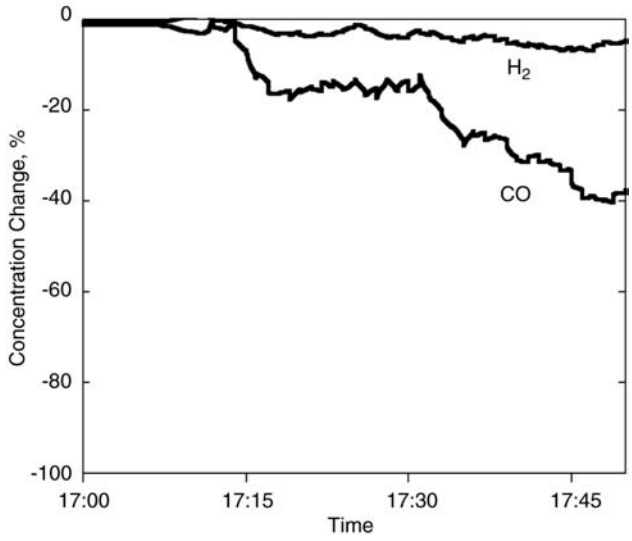

Figure 3. Reduction in CO and CH_4 resulting from air injection into the retrofitted ANL fuel processor.

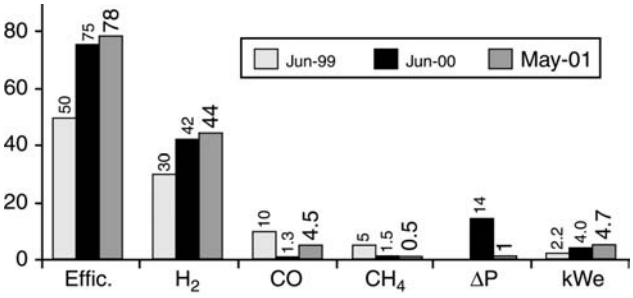

Figure 4. Historical performance of ANL's integrated fuel processor.

Since it operates with ambient feeds, the efficiency value includes the energy required to vaporize the water. The product gas contained 44% hydrogen. Although the CO level for this particular run was at 4.5%, other experiments have produced ~1% CO. The methane content in the reformate was less than 0.5%, showing improvements that reflect directly on the efficiency.

Conclusions

ANL is developing fuel processor technology for fuel cell systems in light-duty fuel cell vehicles. This project studies the components in microreactors and subsequently investigates the options for integrating them into a single assembly.

Current efforts are directed at integrating the preferential oxidation unit and improving the thermal characteristics of the different components such that the fuel processor can meet the U.S. Department of Energy's (DOE's) performance (e.g., efficiency, CO level, etc.) and hardware (e.g., power density, specific power, etc.) goals. Preliminary experiments suggest that the PrOx unit can be integrated effectively into ANL's engineering hardware (~10 kW_e).

Publications

- S. Ahmed and M. Krumpelt, "Hydrogen from Hydrocarbon Fuels for Fuel Cells," International Journal of Hydrogen Energy, 24(4), pp. 291–301, April 2001.
- R. Kumar, S. Ahmed, M. Krumpelt, and X. Wang, "Promise and Problems of Solid Oxide Fuel Cells for Transportation," Proceedings of the International Symposium on Fuel Cells for Vehicles, Nagoya, Japan, November 2000.
- S. Lee, C. Pereira, S. Ahmed, and M. Krumpelt, "Fuel Flexible Fuel Processor for Reforming Hydrocarbon Fuels," AIChE 2000 Annual Meeting, Los Angeles, CA, November 2000.
- S. Ahmed, D. Applegate, J.M. Bae, B. Bergin, D. Myers, C. Pereira, L. Ruscic, and M. Krumpelt, "Fuel Processor Development at Argonne National Laboratory," Army Research Office Workshop, Romulus, MI, June 2000.

Patents Issued

1. S. Ahmed, R. Kumar, and M. Krumpelt, "Methanol Partial Oxidation Reformer," U.S. Pat. 6,244,367, June 12, 2001.
2. S. Ahmed, R. Doshi, R, Kumar and M. Krumpelt, "Partial Oxidation Catalyst," U.S. Pat. 6,110,861, August 29, 2000.

D. Microchannel Fuel Processor Development

Greg A. Whyatt, Ward E. TeGrotenhuis, Robert S. Wegeng, David L. King, Victoria S. Stenkamp, Kriston P. Brooks, James M. Davis, John G.H. Geeting, and Larry R. Pederson (primary contact)
Pacific Northwest National Laboratory
P.O. Box 999
Richland, WA 99352
(509) 375-2731, fax: (509) 375-2167, e-mail: larry.pederson@pnl.gov

DOE Program Manager: JoAnn Milliken
(202) 586-2480, fax: (202) 586-9811, e-mail: JoAnn.Milliken@ee.doe.gov

---

Objectives

- Develop a compact, energy-efficient, integrated fuel processing system for the onboard automotive reforming of hydrocarbon fuels based on microchannel technology.
- Develop highly effective recuperative heat exchangers, fuel and water vaporizers, and vapor-liquid separators that are broadly applicable to fuel processing and fuel cell systems.

OAAT R&D Plan: Task 3; Barriers F, G, and H

Approach

- Emphasize endothermic steam reformation to best take advantage of unique heat and mass transfer advantages available in engineered microstructures.
- Achieve high energy efficiency through integration of a steam-reforming reactor with microchannel recuperative heat exchangers, fuel and water vaporizers, condensers, and separators.
- Utilize microchannel architectures to provide the precise control of temperature that is important for water-gas-shift (WGS) and preferential oxidation reactors and integrate microchannel architectures with the steam-reforming subsystem.
- Utilize steam reforming, WGS, and preferential oxidation/methanation catalyst formulations developed elsewhere by participants of the DOE Fuel Cells for Transportation Program and commercial suppliers to produce optimized engineered catalyst structures.

Accomplishments

- Steam reformation of isooctane was demonstrated at >10 kW_e, >99% conversion, and at >90% of theoretical efficiency in an integrated microchannel reactor. The integrated microchannel steam reformer consisted of 4 parallel process trains and 25 heat exchangers (vaporizers, recuperators, preheaters, and condensers). The steam-reforming system achieved a power density of 2,000 We/L at 99% fuel conversion (excluding water gas shift and CO cleanup).
- A modular 200-W_e steam-reforming subsystem has been developed, which provides flexibility in performance and lifetime testing.
- A compact microchannel water vaporizer has been developed that successfully vaporizes water at a rate in excess of 2 g/s with a gas-side pressure drop of less than 6.2 mbar (2.5 in. water). Low pressure drop is a critical requirement for polymer electrolyte membrane (PEM) fuel cell systems operating at ambient pressures.
- A single-channel condenser/vapor-liquid separator has been demonstrated, which provided complete separation of water liquid and vapor and a pressure drop of less than 10 mbar (4 in. water). Results obtained from this apparatus enabled the design of compact multichannel devices aimed at recovering water from reformate, anode, and cathode streams.

- Prototype microchannel reactors for WGS and CO cleanup have been fabricated and testing has been initiated.

Future Directions

- Demonstrate WGS and preferential oxidation in microchannel reactors and integrate those stages with the steam-reforming subsection.
- Evaluate long-term performance of reactors, heat exchangers, and catalysts.
- Modify reactor designs to facilitate rapid start-up and improved transient response.
- Increase emphasis on the reformation of transportation fuels.
- Investigate design modifications to lower manufacturing costs and improve productivity.

Introduction

Advantages in heat and mass transfer offered by engineered microchannels are being utilized in the development of a compact, integrated, energy-efficient hydrocarbon fuel processing system based on steam reformation. Consisting of reactors, recuperative heat exchangers, fuel and water vaporizers, combustors, and separators, the fuel processing system achieves high efficiency through meticulous heat management. Steam reforming is endothermic and can therefore make effective use of heat from the catalyzed combustion of unutilized hydrogen and methane in the fuel cell anode exhaust. The hydrogen content in the reformate stream is higher than that obtained from partial oxidation or autothermal reforming because the reformate is not diluted with nitrogen from air. High reformate pressures can be generated by pumping fuel and water in liquid form without the need to compress air to the reaction pressure.

Approach

A microchannel steam-reforming subsystem was designed and constructed that was sufficient to support a 10-kW_e PEM fuel cell. This experimental system consists of four parallel reactors, various high- and low-temperature recuperators, and fuel and water vaporizers, all of which are shown in Figure 1. Altogether, there are 25 microchannel heat exchanger units within this system. The apparatus was fabricated from 316L stainless steel in a process that includes photochemical etching of thin metal sheets that are stacked and diffusion-bonded to form a laminated structure with microchannels (Matson et al. 2000).

The reactor section consists of four independent reactor cells operating in parallel. Each cell has a dedicated water and fuel vaporizer, as well as a reformate recuperator. Since each cell is independent, the processing rates of each cell can be varied independently. On the combustion gas side, air flows through the four reactor cells in series and then through four high-temperature recuperator/vaporizers in parallel. While the combustor provides most of the necessary heat, additional fuel is burned after each pass through a reaction cell to restore the desired temperature before returning to the reactor.

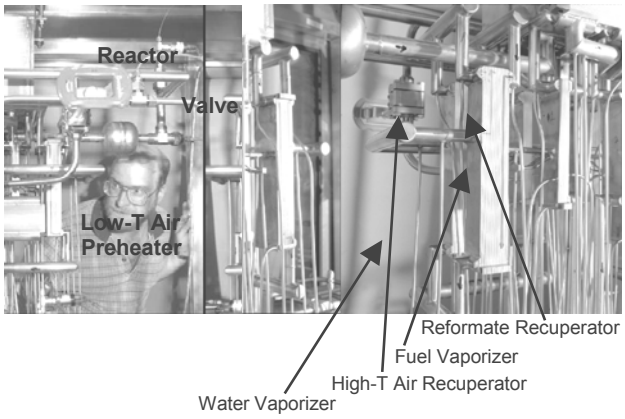

Figure 1. 10-kW_e steam-reforming subsystem. Subsystem includes a four-cell reactor shown at the top integrated with high- and low-temperature recuperative heat exchangers, fuel and water vaporizers, combustors, and preheaters.

Controls required to operate the system include metering pumps for each fuel and water inlet, a controller to maintain the desired flow rate on the combustion side, and four temperature controllers tied to combustion gas flow controllers that are used to control combustion temperatures at the primary combustor and at each of the three secondary combustion points. In addition, there is a manual

valve that allows incoming air to be diverted around the high-temperature recuperator if more heat is needed in the vaporizer. This valve is used to operate the combustor at higher capacities when a proportional increase in combustion air flow is not available.

Multichannel architecture has also been utilized in the development of a water vaporizer designed so that the pressure drop on the gas side is extremely low (less than 2.5 in. water, or 6.2 mbar). A microchannel condenser/vapor-liquid separator has also been demonstrated, the purpose of which is to recover moisture from the reformate and fuel cell streams.

Results

Steam-Reforming Subsection

A trade-off between capacity and conversion effectiveness was found when the steam reformer was operated over a range of conditions. This trade-off is apparent in the summary of operational results for two discrete operating points given in Table 1. At a productivity of 11.2 kW_e, 99% of the fuel was converted to C1 products, whereas, at a productivity of 19.3 kW_e, the conversion rate fell to 94%. Combustion gases were well recuperated, exiting at 50°C or less from an operating temperature of 750–775°C. The reformate was also well recuperated. Reformer efficiency is also a function of operating conditions. Efficiency values given in Table 1 are calculated as 0.95*(LHV H_2 and CO in product)/[lower heating value (LHV) C_8H_{18} feed + (fuel burned – anode gas)]. The term 0.95 is included as an approximate factor to account for the costs of cathode air compression attributable to the reformer. The LHV of CO is included as a product since the WGS reactor has not yet been integrated with the reformer. The "fuel burned" term includes the total fuel actually burned to operate the system, which includes vaporization and preheat of water and fuel reactants. The anode gas term subtracted from the fuel burned takes into account that a fraction of the fuel required to operate the system may be obtained by catalytically combusting the fuel cell anode exhaust gas. To calculate the anode gas composition, PEM fuel cell hydrogen utilization is assumed to be 85% and includes any methane slip from the fuel processor.

Table 1. Steam reformer system performance at two conditions.

Parameter	Value	
Productivity[(a)] (kW_e)	11.2	19.3
Fuel Conversion to C1 (%)	98.6	93.6
Estimated SR Efficiency (%)	81	76
Power Density (W_e/L)	1750	3000
Combustion/Reformate Temperature (°C)	750/ 722	775/ 734
Combustion Exhaust Temperature (°C)	43	50
Reformate Exit Temperature (°C)	129	115
Dry Gas Composition	70.6% H_2 14.6% CO 13.7% CO_2 0.9% CH_4	69.7% H_2 16.1% CO 12.3% CO_2 1.3% CH_4

[a] Calculated potential power output from a PEM fuel cell is based on assuming 90% CO conversion and 100% selectivity to CO_2 in a downstream water-gas shift reactor and a fuel cell with 44% efficiency and 85% H_2 utilization.

The efficiency of the fuel processor unit is given in Figure 2 over a range of operating conditions. Theoretical efficiency referred to in Figure 2 corresponds to complete conversion of the fuel to an equilibrium mix of C1 compounds at the reaction temperature, zero heat loss, recovery of heat from the reformate stream sufficient to bring it to the

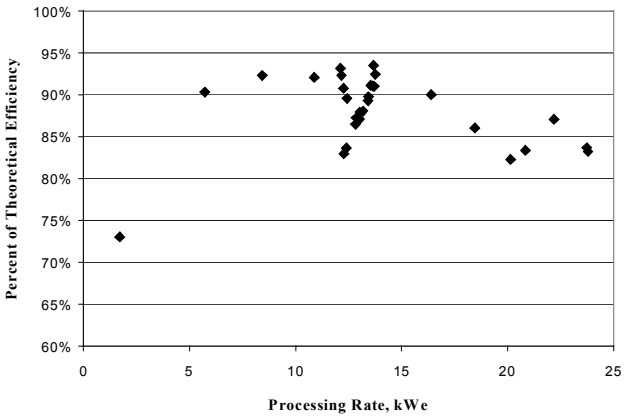

Figure 2. Fraction of theoretical efficiency achieved at various temperatures and fuel-processing rates. Test conditions shown are limited to a 3:1 steam-to-carbon ratio and reformate exit temperatures between 650 and 750°C. Theoretical efficiency is defined as complete conversion of fuel to an equilibrium mixture of single carbon compounds at the reaction temperature, zero heat loss, recovery of heat from the reformate stream to bring it to the dewpoint, and complete utilization of the LHV of the fuel combusted for heat.

dewpoint, and complete utilization of the lower heating value of the fuel combusted for heat. Efficiencies exceeding 90% of the theoretical value were achieved over a fairly wide range of operating conditions.

Fuel conversion increased with increased operating temperature, following an approximate Arrhenius relationship. The extent of fuel conversion as a function of isooctane feed rate at various operating temperatures is shown in Figure 3, along with calculated curves based on an Arrhenius relationship. Data plotted are restricted to a 3:1 steam-to-carbon ratio and reaction pressures near ambient. Studies are under way to establish the temperature range over which the Arrhenius relation holds and to establish conditions where heat and mass transport become limiting. Increasing productivity by increasing the reformer operating temperature is an approach for reducing the size of the reformer system.

The efficient operation of the steam-reforming system depends on the performance of a number of microchannel heat exchangers. The heat exchanger network was intended to be sized to operate at a processing rate of up to ~20 kW_e such that the heat exchangers would not limit system operation. Heat exchanger volumes and observed heat transfer duties for two different operating conditions are summarized in Table 2. The reactor system contains four of each heat exchanger, except that there is only one low-temperature preheater. The volume is taken as the volume of the diffusion bonded stack, which includes the volume of internal flow distribution headers. Duties reflect those of a single exchanger. For all units but the low-temperature air preheater, the total system duty can be determined by multiplying by four. Air flow available to the system was limited and was only increased by 12% in going from the 11.2-kW_e condition to the 19.3-kW_e condition. A control valve intentionally bypassed incoming air around the high-temperature air recuperator to reduce its duty and increase heat available in the vaporizer section.

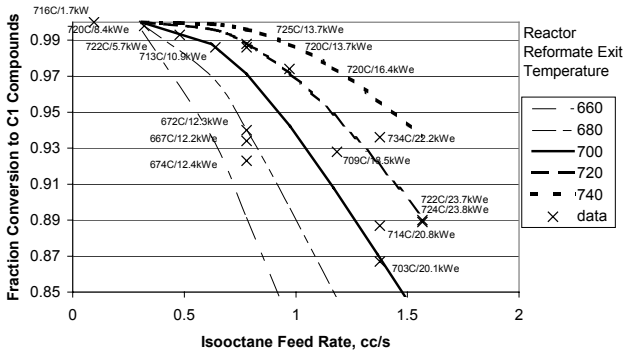

Figure 3. Relationship between fuel reformation rates and conversion at various temperatures. Lines show model predictions for conversion, while actual operating points are labeled with reformate outlet temperatures and productivity. The data are restricted to a 3:1 steam-to-carbon ratio and reaction pressure near ambient.

Table 2. Heat exchanger duties for conditions reported in Table 1.

Exchanger	Bonded Stack	Heat Exchanger Duty		Bonded Stack Heat Transfer Density	
	cm^3	13.7-kW_e Reformate	22.2-kW_e Reformate	13.7-kW_e Reformate	22.2-kW_e Reformate
		W	W	W/cm^3	W/cm^3
Reformate Recuperator	41.3	705	1,087	17	26
High-T Air Preheater	74	1,517	1,119[(a)]	21	15[(a)]
Low-T Air Preheater	726	1,228	1,346	1.7	1.9
Fuel Vaporizer	10.3	55	98.5	5	10
Water Vaporizer	125	1,346	2,344	11	19

[a] At the higher processing rate, incoming air is diverted around the high-temperature air preheater to reduce its duty and provide additional heat to the water vaporizer.

Steam reformer performance indicators compared with 2004 Partnership for a New Generation of Vehicles (PNGV) targets are summarized in Table 3. A capacity of >10 kW_e was achieved at or better than the PNGV 2004 target of 99% conversion of isooctane. Steam reformer system efficiency exceeded PNGV targets and is the result of extensive thermal integration. The power density for the steam reformer subsystem also exceeded PNGV targets, although the specific power targets were not yet met. Warm transient response, which is currently limited by the response of liquid pumps, is expected to be close to targets. Research and development efforts during the coming year will include long-term durability testing, modifications to improve start-up characteristics and improve specific power, and integration of WGS and CO cleanup reactors with the steam-reforming subsystem.

Table 3. Performance compared with 2004 PNGV targets.

Performance Criteria	Current Performance	2004 PNGV Target	Explanation
Capacity (kW_e)	>10	50	At >99% conversion of isooctane
SR energy efficiency (%)	81	78	Depends on extent of thermal integration
Durability (h)	>100	4,000	Long-term testing not yet conducted
Power density (W/L), Specific power (W/kg)	2,000, 350	700, 700	Reflect steam-reforming subsystem only
Transient response (s)	15–20	5	Response currently limited by liquid pumps
Start-up to full power, 20°C (min)	15	<1	Will improve with reactor productivity enhancements
Steady-state CO content in reformate	15%	10 ppm	WGS, CO cleanup not yet integrated with SR

Microchannel Reactors for WGS and CO Cleanup

Work was initiated to develop compact microchannel reactors for WGS and CO cleanup. Prototype reactors were designed and fabricated that are integrated with microchannel heat exchangers to provide the precise temperature control that is important for these two classes of reactions. Catalysts for this work have been obtained from commercial and other developers and converted to an appropriate engineered form for use in microchannel reactors.

Low-Pressure-Drop Water Vaporizer

A water vaporizer exhibiting extremely low gas-side pressure drops has been developed, as shown in Figure 4. The active volume of the heat exchanger panel measures $5.0 \times 3.6 \times 0.5$ in. ($12.7 \times 9.1 \times 1.27$ cm). A plot of the performance observed when generating 50-psig steam is shown in Figure 5. Exchanger duty refers to the measured steam side duty, while effectiveness is the observed steam-side duty relative to the maximum duty that could theoretically be obtained. The heat transfer intensity in the active region (excludes headers) when vaporizing at 2.2 cm^3/s is 40 W/cm^3.

The pressure drop on the gas side has been minimized by making the flow distance very short and by providing a large cross-sectional area for gas flow. Low pressure drop is especially important in fuel cell systems that are operated at pressures very

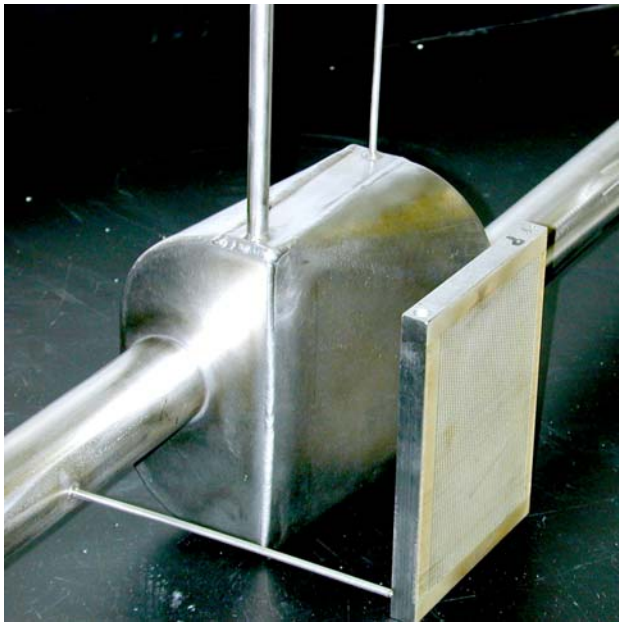

Figure 4. Low-pressure-drop vaporizer. The bonded panel is shown next to finished heat exchanger. Water enters the small vertical tube while steam exits the larger vertical tube. Combustion gas flows in the larger horizontal tubes. Heat exchange occurs as the hot gas passes through the large face of the 1.25-cm-thick panel.

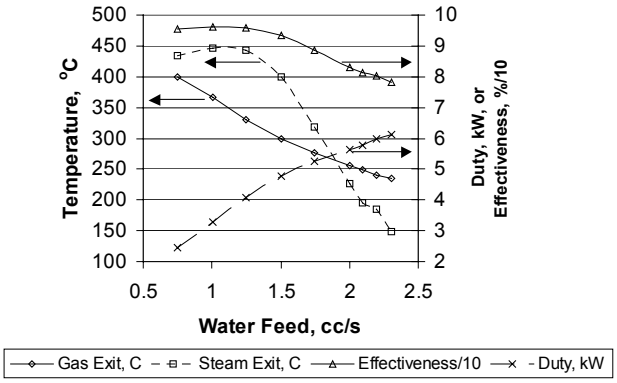

Figure 5. Performance of a low-pressure-drop microchannel water vaporizer versus liquid water inlet rate. Combustion gas flows were 965 standard liters per minute with an inlet temperature of 500–510°C; steam was generated at 50 psig. The gas-side pressure drop was less than 6.2 mbar (2.5 in. water). Percent effectiveness values have been divided by 10.

close to ambient. Multiple vaporizers are fabricated in a single diffusion-bonded stack and are separated by using wire electric discharge machining methods. The units are designed to vaporize 2 g of water per second, which is approximately that needed for a 10-kW_e steam-reforming reactor at a 3:1 steam-to-carbon ratio.

Condenser/Vapor-Liquid Separator

Water is required by all fuel processors for steam reforming and WGS reactions, and it is required for PEM fuel cells to prevent membrane drying. Recovery of water from the reformate, anode, and cathode waste gas streams would help to reduce the need for a large water inventory. Partial condensation requires the separation of the condensate from the noncondensibles, which can be performed either within a condensing heat exchanger or subsequently in a gas/liquid separator.

A single-channel condenser has been developed that provides complete separation of liquid water from the vapor. Performance features include extremely high heat fluxes – up to 55,000 W/m^2, overall heat transfer coefficients of 200–1,000 W/m^2 K, and mean Nusselt numbers of 8–41. Performance results from tests of the single-channel device enabled the design of a multichannel cathode gas condenser that is substantially more compact than that designed by using conventional technology. The unit is designed to recover approximately 70% of the available moisture in the cathode waste stream when cooled from 80 ^oC to 60^oC and at a pressure drop of less than 10 mbar.

Conclusions/Future Work

Steam reformation of liquid hydrocarbon fuels in a compact microchannel reactor has been demonstrated at greater than 10 kW_e and greater than 90% of theoretical efficiency. High efficiency is the result of integrating the steam-reforming reactor with a series of microchannel-based recuperative heat exchangers, fuel and water vaporizers, preheaters, and condensers. A compact water vaporizer has been developed that vaporizes in excess of 2 g water per second with a gas-side pressure drop of less than 6.2 mbar and an effectiveness of greater than 80% while achieving high heat transfer intensity (~40 W/cm^3). A microchannel condenser/vapor-liquid separator has been developed that provides complete separation of liquid water from a gas stream at similarly high effectiveness and low pressure drop. This device is intended for use in recovering moisture from the reformate, as well as from cathode and anode fuel cell streams.

Through the integration of the steam-reforming subsystem with WGS and CO cleanup stages, a critical goal has recently been identified. Promising catalyst compositions developed elsewhere are being converted to an appropriate engineered form and tested in single and multichannel reactors. Advantages in temperature control offered by microchannel architecture should lead to very compact CO cleanup systems.

Lifetime, start-up, and transient response performance will receive increased emphasis. Modular 200-W_e microchannel reactors have been developed that offer considerable flexibility to support catalyst lifetime, fuel-flexibility performance, and sulfur-tolerance testing. Start-up and transient response performance will be enhanced by further improvements in reactor productivity per unit volume and mass.

Reference

- Matson, D.W., P.M. Martin, D.C. Stewart, A.Y. Tonkovich, M. White, J.L. Zilka, and G.L. Roberts, 2000. *Fabrication of Microchannel Chemical Reactors Using a Lamination Process.* Microreaction Technology: Industrial Prospects. IMRET 3: Proceedings of the 3rd International Conference on Microreaction Technology, W. Ehrfeld, ed. Springer-Verlag.

FY 2001 Publications/Presentations

- Wegeng, R.S., L.R. Pederson, W.E. Tegrotenhuis, and G.A. Whyatt, 2001. *Compact Fuel Processors for Fuel Cell Powered Automobiles Based on Microchannel Technology,* Fuel Cells Bulletin No. 28, January, ISSN 1464-2859, © 2001 Elsevier Science Ltd.
- Whyatt, G.A., W.E. Tegrotenhuis, J.G.H. Geeting, J.M. Davis, R.S. Wegeng, and L.R. Pederson, 2001. *Demonstration of Energy Efficient Steam Reforming in Microchannels for Automotive Fuel Processing*, IMRET 5 – 5th International Conference on Microreaction Technology, May 27–30, Strasbourg, France.

- Wegeng, R.S., 2000. *"Compact Microchannel Reforming Systems,"* Fuel Cells Infrastructure Conference, San Diego, CA, November 30.

Special Recognitions, Awards, and Patents Issued

- *Microcomponent Assembly for Efficient Contacting of Fluid*, U.S. Patent No. 6126723, issued October 03, 2000.
- *Microchannel Laminated Mass Exchanger and Method of Making*, U.S. Patent No. 6129973, issued October 10, 2000.
- *Active Microchannel Fluid Processing Unit and Method of Making*, U.S. Patent No. 6192596, issued February 27, 2001.
- *Active Microchannel Heat Exchanger*, U.S. Patent No. 6200536, issued March 13, 2001.

E. Reformate Fuel Cell System Durability

Rod Borup (primary contact), Michael Inbody, Byron Morton, and José Tafoya
ESA-EPE
Thomas Zawodzinski, Franciso Uribe, and Don McMurray
MST-11
Los Alamos National Laboratory
P.O. Box 1663
Los Alamos, NM 87545
(505) 667-2823, fax: (505) 665-9507, e-mail: Borup@lanl.gov

DOE Program Manager: JoAnn Milliken
(202) 586-2480, fax: (202) 586-9811, e-mail: JoAnn.Milliken@ee.doe.gov

---

Objectives

- Meet DOE target for fuel cell system durability of 5,000 h when operating on reformate.
- Quantify effects of fuel reformate on fuel cell stack/system durability.
  - Determine stack (anode and membrane) durability limits of operation with reformed fuel:
    - Determine effect of reformate on the durability of electrocatalysts and
    - Determine effect of reformate on the durability of proton-exchange membranes.
  - Determine effects of fuel and fuel impurities on the durability of fuel processor catalyst.
  - Identify reformate species that limit anode durability.
  - Examine effects of fuel composition on the durability of stack (and fuel processor components).

OAAT R&D Plan: Task 3; Barriers A, E

Approach

- Construct liquid hydrocarbon fuel processor to generate real reformate.
  - Include modular subsections for optimal and flexible operation:
    - Partial oxidation/steam reforming, High-Temperature-Shift (HTS), Low-Temperature-Shift (LTS), and Preferential Oxidation (PrOx).
  - Analyze fuel processor catalysts to determine structural and elemental changes.
  - Analyze reformate to determine low level of impurities.
  - Measure stack component durability with hydrogen for baseline comparison.
- Test durability of fuel cell stack on hydrogen reformed from liquid hydrocarbons
  - Test small (2-kW_e) stack or single cells.
  - Characterize MEAs during operation on reformate:
    - Electrochemical polarization curves,
    - Hydrogen adsorption/desorption, and
    - High-frequency measurements.
  - Post-characterize MEAs after performance on reformate.
  - Analyze fuel processor catalysts to determine structural and elemental changes in collaboration with Oak Ridge National Laboratory.

Accomplishments

- Designed, constructed, and installed durability test hardware.
  - Incorporated gas composition and emissions analysis instrumentation.

- Automated experiments.
- Made initial measurements of fuel reformate impurities.

Future Directions

- Study stack operation on reformed petroleum-based fuels to evaluate reformate effects on the following:
  - Initial operation on pure fuel components, including pure fuel components and component blends with impurity addition (sulfur compounds and nitrogen compounds) and
  - Operation with real fuels, including standard gasoline and reformulated gasoline.
- Measure fuel cell stack durability with hydrogen fuel
  - Use hydrogen stack durability for baseline comparison with reformate.

Introduction

This report describes our FY 2001 technical progress in examining fuel cell stack operation on reformed hydrogen from liquid hydrocarbons. The goal of this research is to explore the effects of reformed fuels on the durability of the fuel cell system and fuel cell stack, including the effects of fuel constituent and fuel impurity on the durability of on-board hydrogen generation devices and on the fuel cell stack. This project is in support of DOE's target for durability operation of 5,000 h.

In this report, we describe the design and construction of the durability system, including the operating conditions for the system, and the analytical methods that will be used in this project. These methods include fuel processor catalyst characterization and MEA characterization techniques for on-line monitoring of the fuel cell stack system performance and post-characterization of the components.

Approach

To measure durability, a modular system has been designed and constructed. The modular design of the fuel processor allows independent control of the fuel processor subsection to operate the catalysts at optimal temperatures. The advantage of the modular design is that the system has the built-in flexibility to test new and different catalysts as the fuel processing catalysts are improved. An image of the fuel processor subsection is shown in Figure 1.

The fuel processor subsystem has been designed and constructed to simulate traditional fuel cell methods of hydrogen generation for PEM fuel cell stacks. The initial subsection is partial oxidation/ steam reforming for the autothermal reforming of

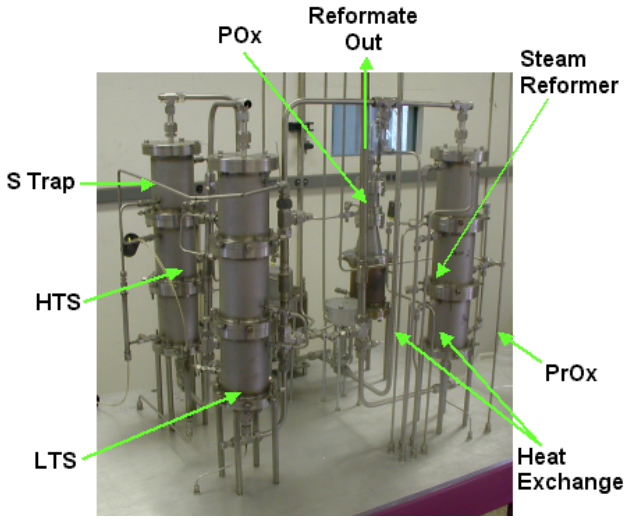

Figure 1. Image of the durability fuel processing subsection system.

liquid hydrocarbons. The operation of this subsection will use typical noble metal oxidation catalysts and noble metal or non-noble metal steam-reforming catalysts. Operation of this subsection also includes the pre-vaporization of fuel and water and pre-heating of air for the fuel oxidation. Typical atomic O/C (oxygen/carbon — O from air) ratios will be from 0.7 to 0.8, while typical S/C (steam/carbon) ratios will be from 1.0 to 2.0 (Krumpelt, DOE OAAT Review Meeting, July 20, 1998).

After the steam reforming section, liquid water injection is used to reduce the effluent temperature of the reformed gas. A heat exchanger is also included before the next subsection of the fuel processor, which involves sulfur sorption and HTS. The addition of water to the reformed gas increases the overall S/C ratio to a typical S/C of 2.5–3.5.

After the HTS, the reformate temperature is reduced through an additional heat exchanger and then enters the LTS stage. After the LTS stage, an additional heat exchanger is used before the preferential oxidation stage. The preferential oxidation subsection is currently capable of three stages of operation, including three air-injection stages. After the final removal of carbon monoxide, a proportional valve is used to control the reformate flow to the fuel cell.

This fuel processing subsection can be used to produce reformate, which can be used to fuel a small stack subsection (approximately 2 kW_e) or multiple single cells. Currently, 50 cm^2 of single-cell components is planned for the single-cell measurements, which include the use of AC impedance, periodic polarization curves, Hydrogen Adsorption/Desorption (HAD) measurements to monitor the anode catalyst surface area, and continual monitoring of the voltage/current performance of the fuel cell.

Operation with pure fuel components can be expensive because of their relative high cost. Fuel consumption in the fuel processing subsection has been calculated (see Table 1). For operation with pure fuel components at approximately 50 kW_e, constant power operation would require about 575 gal of fuel per week. The commercial cost of pure isooctane has been about $27/gal, which makes operation with pure isooctane at this power level expensive. To limit fuel consumption, this system has been designed to operate at between 5 and 1 kW low-heating-value (LHV) fuel.

Tests of fuel cell stack durability using pure hydrogen as the fuel will be conducted to provide a baseline comparison for reformate durability. This operation with pure hydrogen as the stack fuel will provide a direct comparison of the effect that the fuel processing reformate has on stack durability.

Table 1. Fuel usage and cost for various power levels.

LHV Fuel kW Fuel In	80% FP 50% Stack KW(e)	L/day	168 h/week gal/week	Fuel Cost/week @ $1.5/gal $$	Fuel Cost/week @ $27/gal $$
1	0.4	2.5	4.6	15	278
2	0.8	5.0	9.2	31	555
5	2	12.5	23.0	76	1388
10	4	25.0	46.1	153	2777
20	8	50.0	92.1	305	5553
30	12	75.0	138.2	458	8330
50	20	125.0	230.3	764	13883
100	40	250.1	460.7	1527	27767
125	50	312.6	575.9	1909	34709

Results

In support of the DOE targets for reducing the cost of fuel cell components, MEA catalyst loadings are being reduced. The reduction in anode catalyst loading makes the electrocatalyst more susceptible to poisoning species. These species can be produced in the fuel processor or can be present in the fuel used in the fuel processor. To examine the reformate stream for potential MEA electrocatalyst poisons, sample calculations have been made to determine the resolution to which reformate analysis must be made. These are presented in Table 2. Using the various assumptions presented in the table, we calculate that, if irreversible poisons are present in the reformate stream, they will totally saturate the anode electrocatalyst within about 5,000 h at a concentration of only 10 ppb (parts per billion, or 0.01 ppm). Thus, to adequately understand the reformate stream composition, potential poisoning species must be measured to this level of concentration.

To understand the reformate composition, initial analysis of reformate gas composition has been conducted by equilibrium gas modeling and by experimental gas analysis of real reformate to try to detect low levels of contaminants. Modeling has been conducted to identify various species that may be present because of thermodynamic equilibria.

Table 2. Calculation of allowable irreversible reformate impurity concentration.

MEA Assumptions	**Value**	**Units**
Catalyst Surface area	120	m^2/g Pt
Anode Loading	0.1	mg/cm^2
MEA Pt Surface area	0.012	m^2 Pt/cm^2 membrane
MEA Pt Surface area	120	cm^2 Pt/cm^2 membrane
EC Charge for Pt surface	210	microCoulombs/cm^2 Pt
Pt Surface sites	1.31E+15	Pt surface sites/cm^2 Pt s.a.
MEA Pt Surface sites	1.57E+17	# Pt sites/cm^2 membrane
Pt utilization	50	%
Available surface sites	7.87E+16	# Pt sites/cm^2 membrane
Stack Assumptions:		
Anode Stoich	1.2	
Current Density	0.5	Amp/cm^2
Hydrogen flowrate	1.56055E+18	molecules H^2/s-cm^2 MEa
Hydrogen flowrate	0.003484017	SLPM/cm^2 MEA
Hydrogen Concentration	40	%
Total Molecular Flow	3.90E+18	molecules/s – cm^2 MEA
Contaminant Flowrate	3.90E+10	molecules/s – cm^2 MEA
Contaminant sticking coefficient	0.1	
Time for saturation	2.02E+07	s
Time for saturation	**5,600.0**	**h**
Contaminant Conc.	**0.01**	**ppm**

Experimental analysis has been conducted by taking gas samples after a partial oxidation/steam reformer and analyzing by using FTIR. The results from the equilibrium modeling and the gas analysis for several components are shown in Table 3. Results show that equilibrium predicts relatively high concentrations of HCN and NH_3 (high compared with the calculated allowable concentrations). However, the initial experimental measurements did not detect these species. The theoretical limit for HCN and NH_3 detection by the FTIR method is about 1–2 ppb; however, this limit is without interference from other species. Figure 2 shows an enlargement of the FTIR wavelength range where HCN is present. There is no evident HCN peak present in the FTIR spectra. However, the residual peaks from the carbon dioxide (CO_2) make the identification of small concentrations (<1 ppm) of HCN difficult. Although some species are expected to be present from the equilibrium modeling and have not been identified, others — such as ethylene (C_2H_4) and acetylene (C_2H_2) — have been measured.

Table 3. Various contaminant concentrations by equilibrium modeling and by experimental measurement.

Equilibrium Modeling	**Value**	**Units**
HCN (Hydrogen Cyanide)	0.4	ppm
NH_3 (Ammonia)	89	ppm
C_2H_2 (Acetylene)	0.03	ppb
C_2H_4 (Ethylene)	12	ppb
Experimental		
HCN (Hydrogen Cyanide)	ND	
NH_3 (Ammonia)	ND	
C_2H_2 (Acetylene)	100	ppm
C_2H_4 (Ethylene)	250	ppm

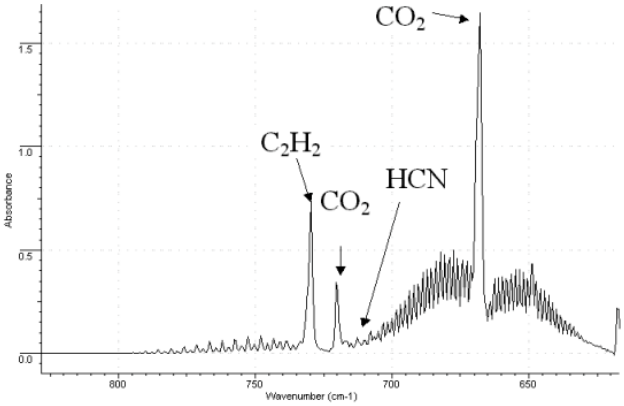

Figure 2. FTIR spectra of reformate with enlarged wavelength region to observe HCN.

Conclusions

Test capabilities have been developed that are capable of testing the durability of fuel cell stacks and fuel processor components with liquid fuels. These capabilities provide the ability for unattended reforming of liquid hydrocarbons and operation of fuel cell stack components. The fuel processor subsystem has the capability to operate with partial oxidation, iso-thermal HTS, iso-thermal LTS, and preferential oxidation. The fuel processor system consists of a modular design for operation at variable temperatures so that newly developed fuel processing catalysts can be included. Analytical instrumentation to characterize operation has been included with the supervisory controls required for the unattended operation.

Initial impurity measurements have not indicated the presence of HCN and NH_3, even though equilibrium calculations indicate they should be present. Others — such as ethylene (C_2H_4) and acetylene (C_2H_2) — have been measured experimentally, even though modeling indicates that they should be absent.

F. R&D of a Novel Breadboard Device Suitable for Carbon Monoxide Remediation in an Automotive PEM Fuel Cell Power Plant

Nguyen Minh (primary contact) and Stan Simpson (co-principal investigator)
Honeywell Engines and Systems
2525 W. 190th Street, MS-36-1-93140
Torrance, CA 90504-6099
Minh, (310) 512-3515, fax: (310) 512-3432, e-mail: Nguyen.Minh@Honeywell.Com
Simpson, (310) 512-4804, fax: (310) 512-3432, e-mail: Stan.Simpson@Honeywell.Com

Di-Jia Liu (co-principal investigator)
Honeywell Des Plaines Technology Center
50 E. Algonquin Road
Des Plaines, IL 60017-5016.
(847) 391-3703, fax: (847) 391-3750, e-mail: Di-Jia.Liu@Honeywell.com

DOE Program Manager: Patrick Davis
(202) 586-8061, fax: (202) 586-9811, e-mail: patrick.davis@ee.doe.gov

ANL Technical Advisor: William Swift
(630) 252-5964, fax: (630) 252 4176, e-mail: swift@cmt.anl.gov

Contractor: Honeywell Engines and Systems, Torrance, California
Prime Contract No. DE-FC02-99EE50578, October 1999–December 2001

Objectives

- Develop, implement, and demonstrate a new CO-removal process for use in polymer electrolyte membrane fuel cell (PEMFC) systems that provides high CO removal efficiency, low parasitic hydrogen consumption, and tolerance to CO input variation in an easily controlled manner.
- Design a system for removal of CO from a continuous reformate flow sized for a 10-kW PEMFC stack with a CO input level of 5,000–8,000 ppm.

OAAT R&D Plan: Task 3; Barrier E

Approach

- In a 27-month program, Honeywell will research and develop a novel technology to selectively remove CO from reformate fuel for use in PEMFCs. Two approaches to CO removal will be explored and developed: adsorption/catalytic oxidation of CO (ACO) and adsorption/electrocatalytic oxidation of CO (ECO). Following an initial R&D phase, the two approaches will be evaluated critically, and one will be chosen on the basis of efficiency, system compatibility, and cost criteria. A breadboard CO remediation system sized for a 10-kW PEMFC stack will then be constructed and tested on synthetic reformate as well as reformate obtained from an operating fuel processor.
- The program consists of four major tasks:
  - Research and development of two potentially viable approaches to remove CO from reformate,
  - Selection of the most promising technique based on performance and cost,
  - Design and fabrication of a breadboard CO-removal device based on the selected technology, and
  - Testing of the CO-removal system.

Accomplishments

- Proof-of-principle experiments for both technologies have been successfully executed.
- A test plant for the rapid evaluation of catalyst/support materials has been constructed.
- Laboratory-scale working devices for both ACO and ECO have demonstrated CO reductions from 8,000 ppm to ≤100 ppm in synthetic reformate formulations.
- Both ACO and ECO have been shown to be tolerant to CO transients.
- In-tandem operation with a PEMFC has been demonstrated for both ACO and ECO hardware.
- Parasitic hydrogen consumption has been characterized for both ACO and ECO techniques in laboratory-scale hardware.

Future Directions

- Conduct device lifetime studies (in progress).
- Design a working prototype for operation at the 10-kW PEMFC level.
- Fabricate and test the prototype.

Introduction

The PEMFC continues to benefit from intense development efforts for its potential application in automobiles. Its success is attributable to a number of inherent advantages, including high efficiency, low noise and chemical emissions, and low operating temperature. Hydrogen is the most energetic fuel for the PEMFC, but the lack of an existing infrastructure for the routine handling and distribution of hydrogen severely limits its utility. Alternatively, hydrocarbon fuels (such as gasoline or methanol) can be reformed to hydrogen-containing fuel mixtures known as reformate via a fuel processor. Unfortunately, a typical reformate consists of a mixture of gaseous products that include CO at concentrations near 1% (10,000 ppm); the detrimental effect of CO at even a ppm-concentration level on the performance of a PEMFC operating with platinum catalysts is well documented. One approach to solving the CO problem is to incorporate a pretreatment device or process in the fuel line between the fuel processor and the fuel cell that significantly decreases the CO concentration in the reformate. This device or process can be based either on physical removal (as in membrane separation) or chemical reaction (as methanation or preferential oxidation). These techniques suffer from various disadvantages, including high cost and complexity, high parasitic hydrogen consumption, and an intolerance to large CO transients without complicated and expensive control processes.

Approach

The goal of this program is to develop and demonstrate a novel, easily controlled CO-removal system that provides high CO removal efficiency with an increased tolerance to CO input variation. This system will be incorporated into a working PEMFC system between the fuel processor and the PEMFC stack. The system will be based on the use of a selective CO removal device that can be regenerated periodically when saturated with CO. Potential advantages of this approach include a high tolerance for CO transients, low parasitic hydrogen consumption, relative operational simplicity, and the ability to control and operate during the "cold-start" condition.

Two innovative approaches to selective CO removal and regeneration are being investigated in this project. Both approaches make use of multiple, CO-selective adsorption surfaces that can be regenerated quickly, simply, and efficiently with minimum consumption of the hydrogen fuel in the reformate stream. The methods, called the ACO and the ECO techniques, differ in the manner in which the active adsorption surfaces are regenerated. In ACO, CO is adsorbed over a bifunctional material bed and subsequently oxidized chemically to CO_2. In ECO, the adsorbed CO is removed through electrocatalytic oxidation.

Results

Removal of CO at 5,000–8,000-ppm Concentration Level

One of the primary goals of this research effort is to develop hardware that is capable of CO removal at concentrations in the 5,000–8,000-ppm range. Honeywell reached this goal last year by using both the ACO and ECO approaches.

As an example, the continuous removal of CO using a laboratory-scale ECO device is demonstrated in Figure 1 for a synthetic reformate stream containing 8,000 ppm CO. In the figure, the CO concentration at the exit of the ECO device is plotted as a function of time. The figure clearly shows that the CO concentration at the exit of the device can be reduced to 100 ppm — a CO concentration that is acceptable for current PEM fuel cell catalyst technology — when the ECO unit is activated.

Similar performance has been achieved for the ACO technique. In this experiment, a laboratory-scale hybrid ACO device was constructed and tested by using a synthetic reformate stream containing approximately 8,000 ppm CO. Following processing by the ACO device, the reformate was found to contain a near- zero CO concentration. This performance is illustrated in Figure 2.

Tolerance to Changes in CO Concentration

Often, variations in fuel processor output that follow adjustments in system load are accompanied by changes in the CO content of the reformate. Thus, tolerance to abrupt increases in CO concentration is a highly desirable attribute of any CO removal system.

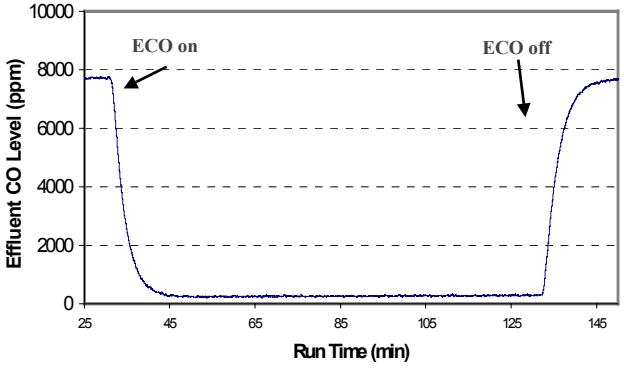

Figure 1. Demonstration of continuous CO removal from reformate using an ECO cell.

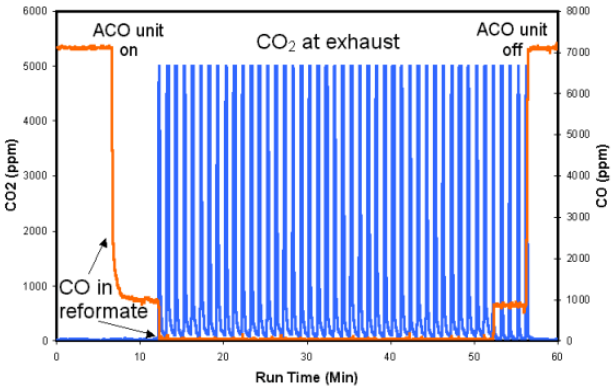

Figure 2. Demonstration of continuous CO removal using an ACO approach.

Because both the ACO and ECO technologies are based upon a passive adsorption approach, these devices should be more tolerant to dynamic variations of input CO level. During the previous year, tolerance to increases in CO concentration was confirmed for both the ACO and ECO technologies.

In Figure 3, we provide data from an experiment in which a reformate mixture containing 900 ppm CO was directed into a single-cell ECO device. A CO detector was incorporated into the experiment and configured to measure the CO concentration either before or after the ECO device. Periodically, a high-concentration CO spike was injected into the fuel stream to simulate a CO transient. Shown in the upper traces of Figure 3 is the CO detector output during a simulated CO transient when the detector was positioned before the ECO device. The CO injections represent changes in CO concentration ranging from 80% (Experiment 1) to 100% (Experiment 2) over the baseline CO concentration

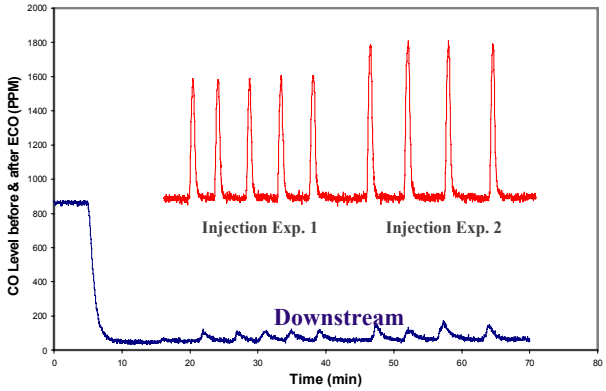

Figure 3. Demonstration of CO tolerance for the ECO technique.

of 900 ppm. The bottom trace in the figure represents the CO concentration detected downstream of the ECO device during similar injections. During these experiments, the ECO device was operated using a 1-s regeneration pulse that was applied every 30 s, which is equivalent to a duty cycle of 3.3%. As shown in the bottom trace of the figure, the CO concentration is reduced substantially by the ECO device, even with injection of an additional 80% of the input CO level. As discussed in the previous annual report, similar tolerance to CO transients can be achieved by using the ACO approach.

Operation of ACO and ECO Devices in Tandem with a PEMFC

To demonstrate that the ACO and ECO devices can remove CO effectively from a reformate stream and supply an operating PEMFC, two experiments were conducted in which a standard PEMFC was linked serially to an upstream ACO or ECO device. A synthetic reformate fuel mixture containing CO was then fed to the linked ACO-PEMFC and ECO-PEMFC devices, and the performance of the PEMFC was evaluated for CO poisoning effects. Results from the ACO-PEMFC are presented in Figure 4. Collectively, the results from these two experiments indicate little or no loss in PEMFC performance when using an ACO approach to CO removal.

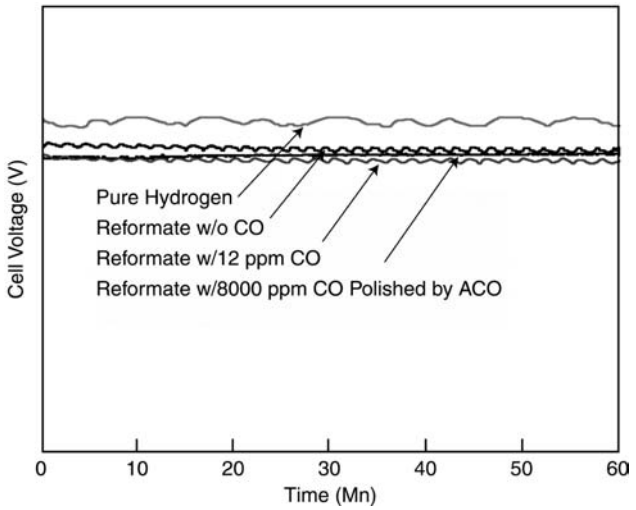

Figure 4. Voltage output of a PEMFC using unprocessed reformate and reformate processed by ACO.

During the previous year, efforts have continued to improve both the materials and the operating parameters of the two techniques to maximize the lifetimes and selectivity characteristics of the catalysts. These efforts have resulted in significant enhancements in the performance of both the ACO and ECO techniques.

One of the key approaches to improving ACO material durability is through improved catalyst synthesis and materials selection. As shown in Figure 5, we have been able to significantly improve the aging character of ACO materials by careful manipulation of selected precursors and addition of critical stabilizing agents. In ECO, the optimization of both MEA fabrication techniques (Figure 6) as well as materials and operating conditions (Figure 7)

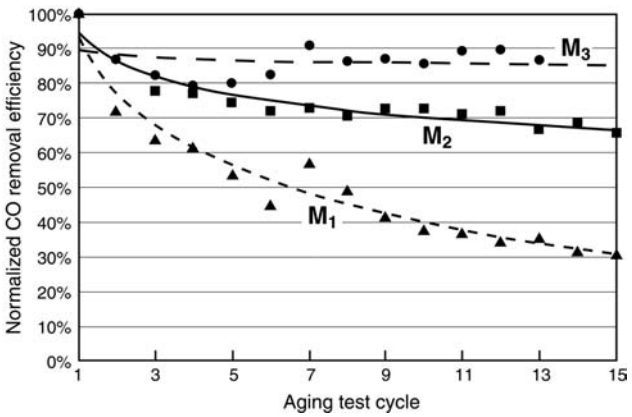

Figure 5. Improvement of the durability of ACO materials.

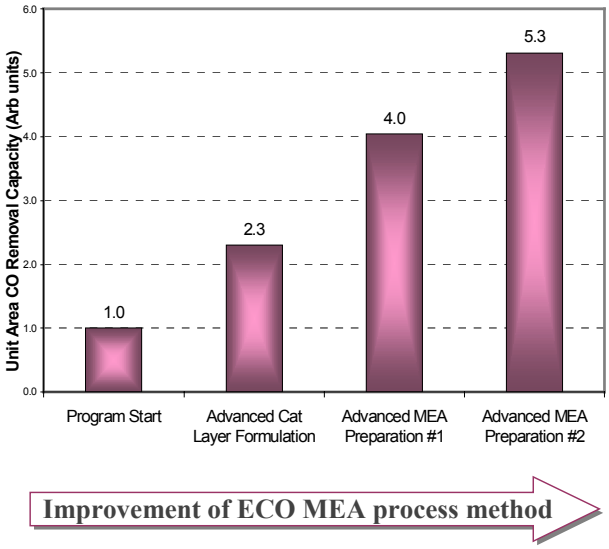

Figure 6. Continuous improvement of CO removal capacity for ECO.

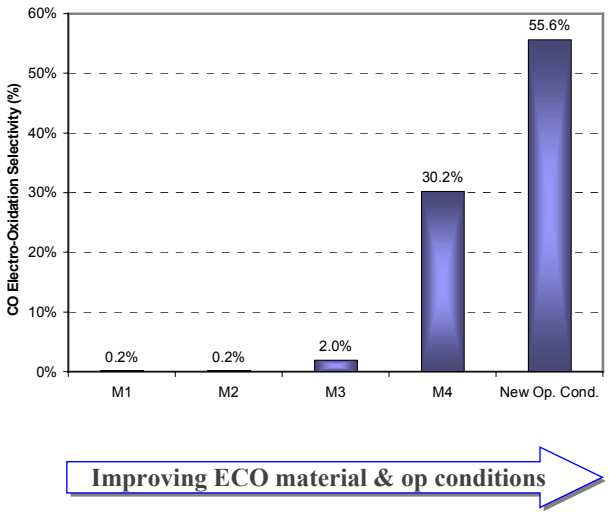

Figure 7. Continuous improvement of CO removal selectivity for ECO.

has led to improvements in both CO removal capacity and selectivity.

Conclusions

On the basis of the results of experiments conducted in the last year, the ACO and ECO technologies for the removal of CO from processed hydrocarbon reformate have been shown to be robust and applicable for use with the PEMFC. Numerous desirable attributes (such as tolerance to CO transients, tolerance to relatively high CO levels, and operation with a PEMFC) were demonstrated for both techniques at the laboratory scale. Following selection of the most promising candidate technology, activities in the coming year will focus on further performance and lifetime improvement as well as design, construction, and testing of the breadboard.

Publications/Presentations/Patents

1. D.-J. Liu, J. Williams, M. Kaiser, D. Winstead, J. Kudart, S. Simpson, and T. Rehg, "Two New Approaches for CO Removal from Reformate Fuel for the PEM Fuel Cell Application," SAE 2000 World Congress, March 2000, SAE Technical Paper Series 2000-01-0379.
2. D.-J. Liu, J. Williams, M. Kaiser, D. Winstead, S. Simpson, and T. Rehg, "Two New Approaches for CO Removal from Reformate Fuel for the PEM Fuel Cell Application," 2000 Fuel Cell Seminar, October 2000, Extended Abstract, pages 102–105.

G. Development of CO Cleanup Technology

Michael Inbody (primary contact), José Tafoya, Lee Perry, and Troy Semelsberger
Los Alamos National Laboratory
ESA-EPE, MS J576
P.O. Box 1663
Los Alamos, NM 87545
(505) 665-7853, fax: (505) 665-9507, e-mail: inbody@lanl.gov

DOE Program Manager: JoAnn Milliken
(202) 586-2480, fax: (202) 586-9811, e-mail: JoAnn.Milliken@ee.doe.gov

Objectives

- Research and develop carbon monoxide (CO) cleanup technology based on preferential oxidation (PrOx) for integration into fuel processor systems to meet technical targets for contaminant removal, transient performance, energy efficiency, cost, volume, weight, and durability.

OAAT R&D Plan: Task 3; Barrier E

Approach

- Transfer PrOx technology to fuel processor/fuel cell system developers.
- Investigate PrOx catalysts on ceramic monoliths and foams and on metal foams.
- Investigate PrOx concepts and behavior for rapid start-up and transient control.
- Develop *in-situ* CO concentration measurements for fast transient response measurements.
- Investigate removal of additional fuel cell stack contaminants.

Accomplishments

- Established technology transfer projects and collaborations with
  - McDermott Technology;
  - Argonne National Laboratory (ANL);
  - H2fuel, LLC; and
  - International Fuel Cells.
- Initiated testing of PrOx catalysts on ceramic monoliths and foams and on metal foams.
- Examined PrOx concepts for rapid start-up.
- Demonstrated a PrOx cold-start with reduction from 5% CO to <10 ppm CO in ~225 s.
- Investigated PrOx response and controls for power transients in multi-stage and single-stage reactors.
- Investigated effects of propane, ethylene, and acetylene on PrOx performance.

Future Directions

- Complete project on CO cleanup.
- Complete work on technology transfer and collaborations.
- In close-out work, address transient CO diagnostics and measurements, catalyst investigations, and impurity effects and removal.

Introduction

This report describes the research conducted during FY2001 to develop CO cleanup technology for fuel cell systems. CO cleanup is a subset of reformate cleanup, which — as the last unit operation in a fuel processor stream — is responsible for removal of contaminants to concentrations that do not compromise performance of the fuel cell stack. The CO cleanup reactor operates in the system context of the fuel processor; for the fuel processor system to meet its technical targets, the final CO cleanup stage must achieve the purity requirements of the system. Key technical targets that apply to the CO cleanup reactor are requirements for contaminant removal (CO <10 ppm steady-state, <100 ppm transient; NH_3 <5 ppm and H_2S <0.2 ppm currently, but these values may be revised to ppb limits based on ongoing research), transient response (<1 s for 10% to 90% power), cold start (<1 minute), and overall energy efficiency. Other technical targets include system cost, volume, weight, and durability.

Ongoing research (FY1996–FY2000) has resulted in the development of laboratory and demonstration PrOx reactor systems to reduce CO to the levels required by the fuel cell for fuel processing systems. This year, the program focused on transfer of the technology base to fuel processor system developers. This year's research also addressed key technical barriers, including implementing catalysts on automotive supports, characterizing and controlling transient response, developing methods for fast *in-situ* CO concentration measurements, and examining removal of contaminants other than CO.

Approach

We have worked to transfer the technology developed during the CO cleanup project by communicating our findings and collaborating with fuel processor developers to incorporate Los Alamos National Laboratory (LANL) PrOx technology into their systems. Knowledge gained from these collaborations also guides future research.

To improve the performance of CO cleanup reactors, we are investigating PrOx catalysts supported on automotive substrates. This work will help to reduce the size and number of stages, reduce the reactor pressure drop, and increase durability. A comparison study will be conducted with PrOx catalysts on monoliths, ceramic foams, and metal foams to quantify advantages and disadvantages of each substrate type.

We are addressing the key technical barriers of PrOx transient response and start-up by measuring the PrOx response to power transients and CO concentration transients and by identifying requirements to control the outlet CO concentration. We are implementing a tunable diode laser absorption system for *in-situ* CO concentration measurements at time scales of <100 ms with a 1-ppm CO resolution for successful CO transient measurements. To meet the overall fuel processor start-up time requirements, we are exploring PrOx concepts for operation at low temperatures with high inlet CO concentrations.

We have evaluated the effects of hydrocarbon contaminants on PrOx performance and examined methods for removal of other contaminants. The effects of other contaminants (such as NH_3 and H_2S) and their removal will be measured in a microscale catalyst test facility.

Results

We are transferring the technology developed during this project by collaborating on PrOx designs for fuel processor systems, contributing models and data from our laboratory hardware, and supporting designs with experimental verification in our PrOx test facility. Technology transfer has also been accomplished by sharing PrOx experience and knowledge through presentations at conferences (see list below) and through direct interactions — such as hosting members of various fuel processing teams. Major collaborations with McDermott Technology and Argonne National Laboratory (ANL) are ongoing. We are assisting McDermott Technology in the design of a 50-kW_e PrOx system for manufacturability and commercialization, with an intermediate goal of providing it with a laboratory 10-kW_e PrOx system. A prototype of the 10-kW_e system is shown in Figure 1. The purpose of the collaboration with ANL is to design and provide a 10-kW_e PrOx system for integration with the ANL-developed fuel processor for subsequent investigation of start-up issues. A 10-kW_e laboratory PrOx system has been supplied to ANL for initial fuel processor integration experiments. The goal of an ongoing collaboration with H2fuel, LLC, is to design a PrOx reactor for integration with that

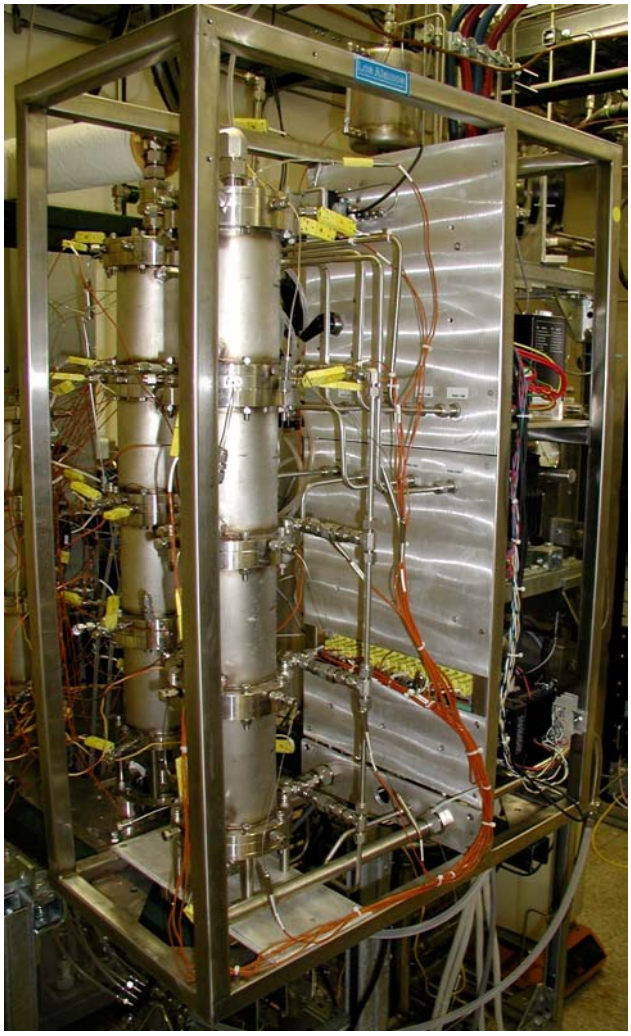

Figure 1. Laboratory 10-kW$_e$ PrOx subsystem.

company's fuel processor. A 10-kW$_e$ laboratory PrOx system has been supplied for preliminary integration experiments with H2fuel's prototype fuel processor.

We began investigation of PrOx catalysts on automotive supports with benchmark testing of PrOx catalysts on 400-cells-per-square-inch (cpsi) cordierite monoliths. Catalysts on a variety of substrates have been obtained from various commercial catalyst vendors. Testing is being conducted in a PrOx single-stage reactor (an adiabatic integral plug-flow reactor) and in a microscale reactor (an isothermal differential plug-flow reactor).

PrOx response to power transients was measured in a four-stage configuration for removal of 2% CO in simulated gasoline reformate and in a single-stage configuration for removal of 2,000-ppm CO. We characterized the transient response of the four-stage reactor as the total flow was varied between 10 and 30 kW. The response and CO control was complicated by the interactions between the stages and will be fully reported in a later publication. To better characterize the response of PrOx components to power transients, a PrOx single-stage reactor was subjected to step transients between 10 and 30 kW. Figure 2 shows the CO flow into the reactor, along with injected air flow through two cycles of the step transient. The outlet CO concentration was maintained below 100 ppm peak, as shown in Figure 3, by leading with the air flow by 1 s during the up transient and by lagging with the air flow by 1 s during the down transient.

To meet the technical targets for executing transients in less than a second, the experimental capability to measure CO concentrations must be faster than 1 s. Thus, we are implementing a tunable diode laser absorption system to measure *in-situ* CO concentrations at the interstage locations in the laboratory PrOx test setup. The expected response time is on the order of 100 ms, with a resolution of 1 ppm in CO concentration.

The feasibility of using PrOx reactors to reduce the system start-up time by removing high concentrations of CO was investigated by using a four-stage PrOx reactor starting at room

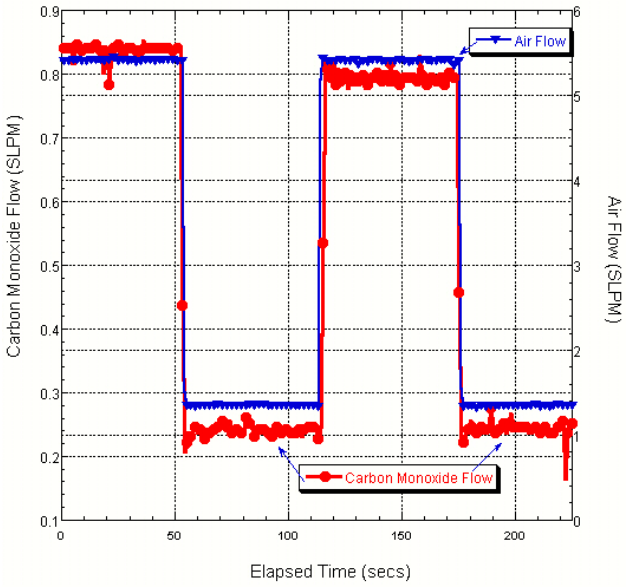

Figure 2. Carbon monoxide and air injection flows during step transients between 10-kW and 30-kW total flows of simulated gasoline reformate.

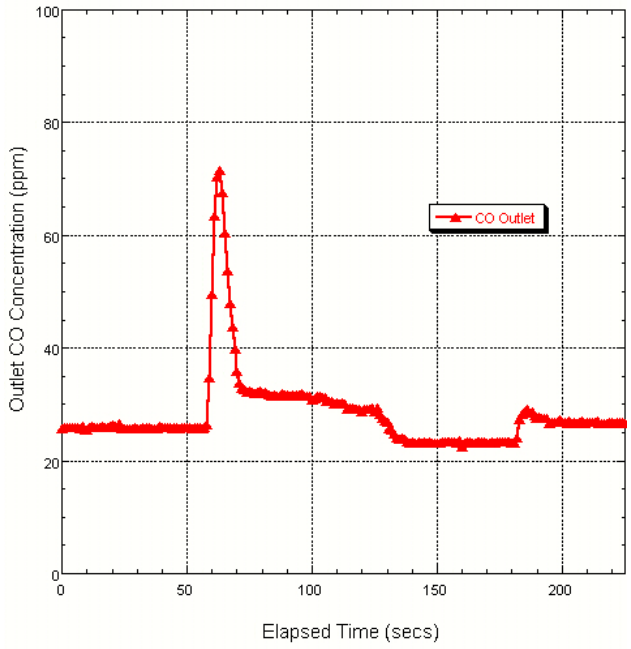

Figure 3. Outlet CO concentration measured during step transients between 10- and 30-kW total flows of simulated gasoline reformate.

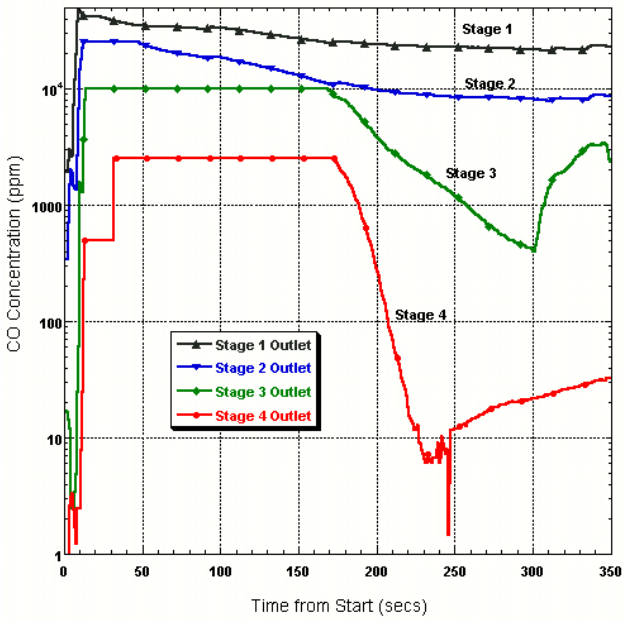

Figure 4. Outlet CO concentrations from each PrOx stage during start-up with an inlet 5% CO concentration in simulated gasoline reformate.

temperature. Start-up flows were set to a 10-kW (lower heating value [LHV] H_2) simulated gasoline reformate with 5% CO. Figure 4 shows the outlet CO concentrations from each stage as a function of time from the start-up. Initial air flows were set to achieve a maximum setpoint temperature at the outlet of each stage. The outlet CO concentration from the last stage dropped below 10 ppm in 225 s from start-up. The 2008 technical target is less than 30 s; thus, further improvement is required.

The effects and removal of other impurities, including propane, ethylene, and acetylene, on PrOx performance have also been investigated. These hydrocarbons have been measured in gasoline fuel processor effluent [2]. Propane, ethylene, and acetylene were injected at 500- and 1,000-ppm concentrations into simulated gasoline reformate in a single-stage PrOx reactor configuration with 2,000 ppm CO. Propane, a saturated hydrocarbon, had no short-term effect on the CO removal, and there was no measurable change in its concentration. The unsaturated hydrocarbons, ethylene and acetylene, also had no short-term effects on PrOx CO removal. However, both were found to partially hydrogenate to ethane. The extent of the conversion is a function of the temperature and the CO concentration. If these unsaturated hydrocarbons prove to be fuel cell poisons, a PrOx reactor may be able to convert them to more benign hydrocarbons.

Conclusions

Collaborations to transfer technology and incorporate LANL PrOx technology into fuel processor systems are ongoing with McDermott Technology, ANL, and H2fuel, LLC. These activities will continue into FY 2002. To improve PrOx reactor performance, we are investigating catalysts and catalyst supports, including comparisons of ceramic foam, metal foam, and high-cpsi monoliths.

The transient response of PrOx reactors to power transients and CO composition transients has been investigated, and options for CO transient control have been identified. A tunable diode laser absorption system to measure *in-situ* CO concentrations is being added to measure transient responses at fast time scales (~100 ms). Future work includes using this apparatus to identify strategies for meeting 1-s transient response requirements. A promising method for reducing fuel processor start-up time has been identified, with demonstration of PrOx reactor start-up to remove CO, from 5% CO to less than 10 ppm within 225 s. The effects and removal of hydrocarbon impurities in PrOx

operation have been investigated, with no degradation of the PrOx catalysts observed. Removal of other major contaminants, including H_2S and NH_3, will be investigated by using a microscale catalyst test facility. Further research into reformate cleanup will be required for the long-term success of fuel cell systems.

References

1. Shabbir Ahmed, et al., *Integrated Fuel Processor Development*, Office of Advanced Automotive Technologies, Transportation Fuel Cell Power Systems FY 2001 Accomplishments Report.
2. Rod Borup, et al., *Reformate Fuel Cell System Durability*, Office of Advanced Automotive Technologies, Transportation Fuel Cell Power Systems FY 2001 Accomplishments Report.

Presentations

- M.A. Inbody, R.L. Borup, J.C. Hedstrom, J.I. Tafoya, and B. Morton, "Transient Carbon Monoxide Control-PrOx Reactor Strategies," 2000 AIChE Annual Meeting, November 12–17, 2000, Los Angeles, CA.
- M.A. Inbody, R.L. Borup, J.C. Hedstrom, J.I. Tafoya, and B. Morton, "Transient Carbon Monoxide Control for PEMFC Automotive Applications," 2000 Fuel Cell Seminar, October 30–November 2, 2000, Portland, Oregon.

H. Evaluation of Partial Oxidation Fuel Cell Reformer Emissions

Stefan Unnasch
Arthur D. Little, Inc.
10061 Bubb Rd.
Cupertino, CA 95014
(408) 517-1563, fax: (408) 517-1553, e-mail: unnasch.stefan@adlittle.com

DOE Program Manager: Nancy L. Garland
(202) 586-5673, fax: (202) 586-9811, e-mail: nancy.garland@ee.doe.gov

ANL Technical Advisor: Walter Podolski
(630) 252-7558, fax: (630) 972-4430, e-mail: Podolski@cmt.anl.gov

Contractor: Arthur D. Little, Cupertino, CA
Prime Contract No.: DE-FC02-99EE50585, September 1999–December 2001.
Subcontractors: Nuvera Corp., Air Toxics, Ltd., Clean Air Vehicle Technology Center

---

Objectives

- Measure the emissions from a partial oxidation/autothermal fuel processor for a polymer electrolyte membrane (PEM) fuel cell system under both cold-start and normal operating conditions.
- Assess the feasibility of meeting emissions standards for automobiles and light-duty trucks through the use of a fuel cell vehicle with a multi-fuel reformer.

OAAT R&D Plan: Task 5; Barriers F and G

Approach

- Define a representative test cycle consisting of both cold-start and normal operating conditions.
- Use the established test cycle to quantify emissions from a partial oxidation reformer before and after anode-gas-burner treatment.
- Measure emissions with continuous monitor measurements supplemented with laboratory analyses of speciated hydrocarbons.
- Use reasonable approximations and estimates to convert emissions data from a gram/unit fuel basis to a predicted gram/mile basis.

Accomplishments

- Measured emissions from a fuel processor (without fuel cell) over several operating conditions, including cold start.
- Speciated total hydrocarbon data before and after the anode gas burner.
- Assessed the sensitivity of monitoring equipment over a range of operating conditions.
- Analyzed data to report emissions on a gram/kilogram fuel basis.

Future Directions

- Perform extensive analysis of a fuel cell/reformer system exhaust to include particulates, formaldehyde, and ammonia, as well as NO_x, HC, and CO.
- Develop control strategies to minimize emissions.

Introduction

The operation of partial oxidation reformers is generally divided into two operating modes: start-up and normal partial oxidation. During start-up, the fuel processor burns fuel at near stoichiometric conditions until critical system temperatures and pressures stabilize at target values. Once the target conditions are reached, the reformer operates in normal mode, in which the fuel processor burns fuel at very rich conditions. Since these modes consist of considerably different operating conditions, it follows that the emissions associated with each of these modes are also considerably different.

Since the combustor is typically cold under start-up conditions, the emissions produced during this brief period (target times are under 30 s) can be substantially higher than those produced during the remaining, and much longer, portion of the driving cycle. The pollutant emissions produced during the start-up mode include NO_x, CO, formaldehyde, and organic compounds. These organic compounds, which include hydrocarbons, alcohols, and aldehydes, are referred to as non-methane organic gases (NMOG) in California and are regulated.

Under normal operating conditions, in which the combustor is sufficiently warm and operated under fuel-rich conditions, virtually no NO_x is formed, although the formation of ammonia is possible. Most hydrocarbons are converted to carbon dioxide (or methane if the reaction is incomplete); however, trace levels of hydrocarbons can pass through the fuel processor and fuel cell. The shift reactors and the preferential oxidation (PrOx) reactor reduce CO in the product gas, resulting in a feed concentration to the fuel cell that can be less than 20 ppm CO. The fuel cell may also convert CO to CO_2, thereby further reducing exhaust CO levels. Thus, of the criteria pollutants (NO_x, CO, and hydrocarbons [NMOG]), NO_x and CO levels are generally well below the most aggressive standards. NMOG concentrations, however, can exceed emission goals if these are not efficiently eliminated in the catalytic burner.

Approach

In this study, a gasoline fuel processor was operated under conditions simulating both cold-start and normal operation. Under these conditions, emissions were measured before and after treatment by an anode gas burner to quantify the effectiveness of the burner catalyst in controlling start-up emissions. The emissions sampling system included continuous emissions monitors (CEMs) for O_2, CO_2, CO, NO_x, and total hydrocarbons (THC). Also, integrated gas samples were collected in Tedlar bags for hydrocarbon speciation analysis via gas chromatography (GC). This analysis will yield the concentrations of the hydrocarbon species required for the California NMOG calculation. In subsequent tests, the particulate concentration in the anode burner exhaust will be measured through either isokinetic sampling or the placement of a filter in the exhaust stream.

Concentrations of the aforementioned species were obtained by using an emission sampling system shown schematically in Figure 1. Since emissions from a PrOx system vary significantly between start-up and normal operation, a wide range of analyzer capability will be required.

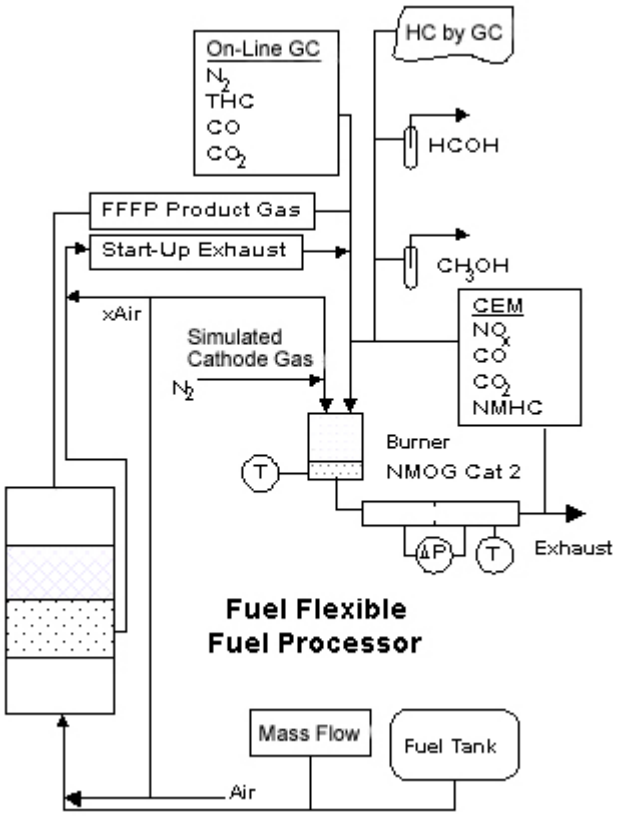

Figure 1. Emission testing setup.

Results

This report summarizes the results of a preliminary test of a fuel processor operating with a fuel cell. The test focused on NO_x and hydrocarbon emissions, including speciation of hydrocarbon components. Figure 2 shows NO_x and THC emissions from the Nuvera gasoline-fueled autothermal fuel processor. The figure indicates emission levels as the reformer was started up and operated over a duty cycle. The testing did not attempt to follow a driving cycle but rather followed a series of steady-state conditions with load changes. THC emissions were quite high during start-up and then varied during the test, with spikes occurring when the load was increased.

Figure 3 compares the composition of the hydrocarbons starting with the gasoline fuel, then during start-up, and finally under reforming conditions before and after an anode gas burner (Tail Gas Combustor, TGC). During reforming, over 90% of the THC emissions are methane. The speciation of the hydrocarbons was also analyzed to determine the presence of toxic contaminants (benzene, formaldehyde, and 1,3 butadiene can occur in gasoline vehicle exhaust). Benzene concentrations were 300 ppbv during start-up and less than 10 ppbv during steady-state reformer operation. More analysis is required to present the benzene and other toxics on a gram/mile basis.

Figure 4 shows the non-methane hydrocarbon (NMHC) emissions on a gram/kilogram fuel basis. The mass fraction of the NMHC after it is burned in the anode gas burner is a very small fraction of the fuel entering the fuel processor. For a fuel cell

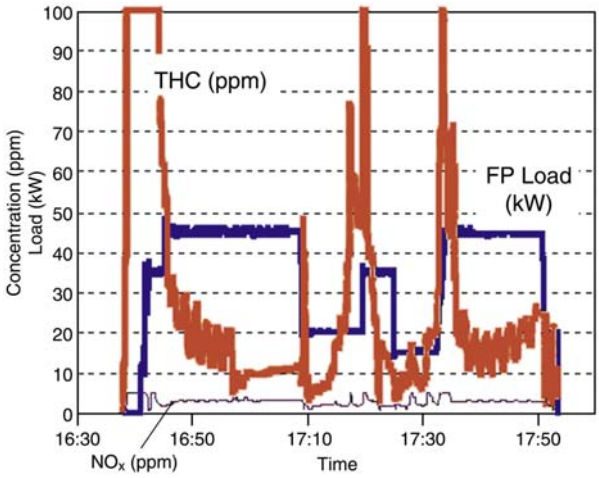

Figure 2. Reformer load and emissions.

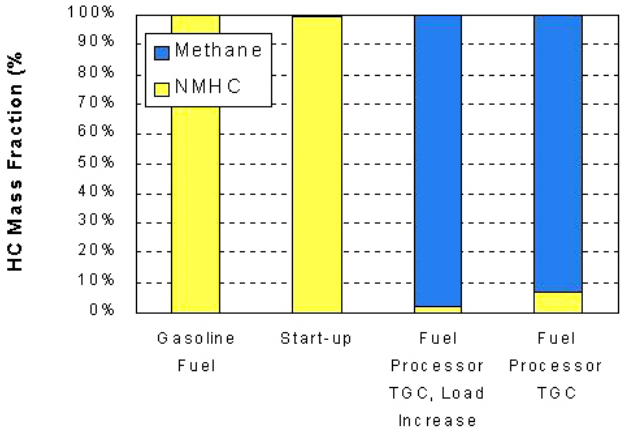

Figure 3. NMHC emissions.

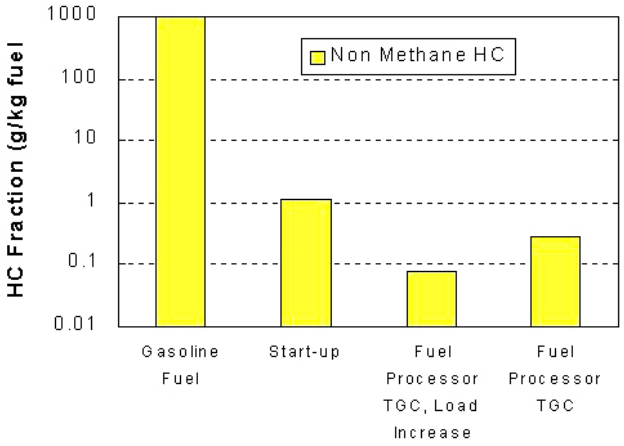

Figure 4. NMHC emissions per unit gasoline fuel.

vehicle with a fuel economy of 60 miles per gallon, an emission rate of 0.2 g/kg fuel translates into 0.01 g/mi of NMOG. A more significant source of emissions occurs during start-up. Emission rates, for the configuration that was tested, are higher during start-up, and the emissions are primarily NMOG with little methane. Determining approaches for controlling NMOG during start-up will be essential for meeting the most stringent emission standards.

To make quantitative conclusions regarding the impact of fuel composition on reformer emissions, the measured volumetric exhaust concentrations of each pollutant were converted to a gram/unit fuel basis. To make further conclusions regarding the feasibility of meeting California SULEV emissions standards, appropriate assumptions and estimates regarding the powertrain of a fuel cell vehicle were used to convert the measured emissions levels to a predicted gram/mile basis. These results will be

presented in a final report, which evaluates the reformer and anode gas burner configurations.

Conclusions

An initial test of the Nuvera fuel processor took place in October 2000. Because additional time is required to complete the integration of the fuel processor and fuel cell, final testing of an integrated system will not occur until the end of 2001. This information will provide information to identify research needs for controlling fuel processor emissions and estimating on-road emissions from fuel-cell-powered vehicles.

Reference

1. Unnasch, S., "Evaluation of Fuel Cell Reformer Emissions," Final Report for Contract 95-313, prepared for California Air Resources Board, Sacramento, California, August 1999.

I. Catalytic Autothermal Reforming

Michael Krumpelt (primary contact), Theodore Krause, J. David Carter, Jennifer Mawdsley, Joong-Myeon Bae, Shabbir Ahmed, and Cecile Rossignol
Argonne National Laboratory
9700 South Cass Ave.
Argonne, IL 60439
(630) 252-8520, fax: (630) 252-4176, e-mail: krumpelt@cmt.anl.gov

DOE Program Manager: JoAnn Milliken
(202) 586-2480, fax: (202) 586-9811, e-mail: JoAnn.Milliken@ee.doe.gov

---

Objectives

- Improve catalytic activity and reduce the cost of autothermal reforming (ATR) catalyst to decrease the size of the fuel processor and start-up time.
- Minimize hydrocarbon breakthrough.

OAAT R&D Plan: Task 3; Barrier E

Approach

- Synthesize materials that meet Argonne National Laboratory (ANL) selection criteria and DOE cost goals.
- Determine H_2, CO, CO_2, CH_4, and C_nH_m yields versus temperature and space velocity.
- Work with catalyst manufacturers.

Accomplishments

- Licensed ATR catalyst technology to Süd-Chemie, Inc.
- Obtained evidence that individual platinum ions on the surface of ceria play a role in the oxidation reaction.
- Reduced the metal loading to meet the DOE cost goals.
- Obtained data on hydrocarbon breakthrough.

Future Directions

- Continue to improve the performance of non-precious metal catalysts.
- Continue catalyst characterization and explore catalysts favoring partial oxidation mechanism.
- Improve the stability of structured forms of catalysts.
- Provide technical support to Süd-Chemie, Inc.
- In collaboration with academia, develop a better understanding of reaction mechanisms.

Introduction

Catalytic autothermal reforming (ATR) of hydrocarbon fuels was first proposed by Argonne National Laboratory (ANL) several years ago and has been widely accepted as the most promising route to meet the efficiency, volume, and cost goals of the DOE Fuel Cells for Transportation Program. ANL has developed and licensed a new class of catalysts that are modeled after the internally reforming anode materials used in solid oxide fuel cells. Unlike typical industrial steam-reforming and oxidation catalysts of nickel or platinum supported

on alumina substrates, the substrate for the ANL catalysts is an oxide ion-conducting material. The preferred formulation for the substrate is ceria doped with rare earth oxides. The surface of the substrate is then coated with a Group VIII metal. In the past twelve months, we have more fully characterized the effects of different dopants for ceria and metals on the catalytic activity and the selectivity.

Approach

Doped ceria substrates are prepared from nitrate salt precursors by either coprecipitation or glycine-nitrate combustion techniques. Metals are loaded onto the doped ceria substrates by using the incipient wetness process. The catalysts are tested for methane or isooctane reforming under ATR conditions. For methane reforming, ~50 mg of catalyst are exposed to CH_4, O_2, H_2O, and N_2 at the desired feed ratios over a temperature range of 400–800°C by using a Zeton Altamira Chemisorption Instrument Model AMI-100. The product gas composition is determined by mass spectroscopy. For isooctane reforming, ~2 g of catalyst are exposed to C_8H_{18}, O_2, H_2O, and N_2 at the desired feed ratios over a temperature range of 400–800°C by using a microreactor system consisting of a 0.5-in. O.D. 316 SS tube heated in a temperature-controlled furnace. The product gas composition is determined by gas chromatography. Characterization studies of several Pt catalysts by using x-ray photoelectron spectroscopy (XPS) were performed at the University of Alabama at Tuscaloosa.

Results

Effect of Substrate

Figure 1 shows the product gas yield as a function of temperature for methane ATR for 0.5 wt% Pt supported on two different doped-ceria substrates: gadolinium-doped ceria with a composition of $Ce_{0.8}Gd_{0.2}O_{1.9}$ (CGO-20) and zirconium-doped ceria with a composition of $Ce_{0.8}Zr_{0.2}O_{2.0}$ (CZO-20). For the CGO-20 substrate, H_2 and CO, both products of partial oxidation reforming reactions involving CH_4, O_2, and H_2O, are observed in the product gas at a temperature of 400°C, with the equilibrium concentration being achieved at a temperature of ~600°C. For the CZO-20 substrate, H_2 and CO are not observed in the product gas at temperatures <550°C, with the equilibrium concentration being achieved at ~800°C.

The higher reforming activity exhibited by the CGO substrate at lower temperatures (compared to CZO) suggests that a different reaction mechanism may be occurring on the two substrates. Figure 2 shows how doping ceria with Gd^{3+} leads to the formation of oxygen ion vacancies, whereas doping ceria with Zr^{4+} introduces lattice stress and distorts the lattice but does not lead to the formation of oxygen ion vacancies. We believe that it is the presence of the oxygen ion vacancies in the CGO

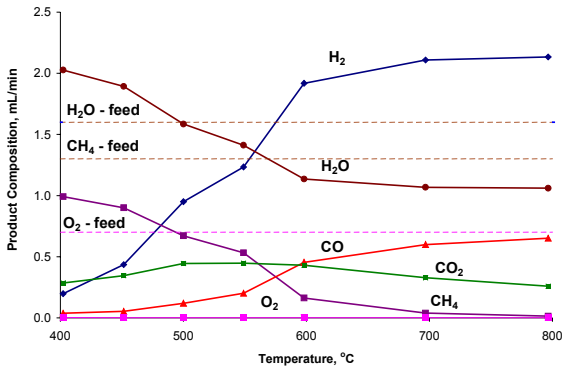

(a) 0.5 wt% Pt on CGO-20.

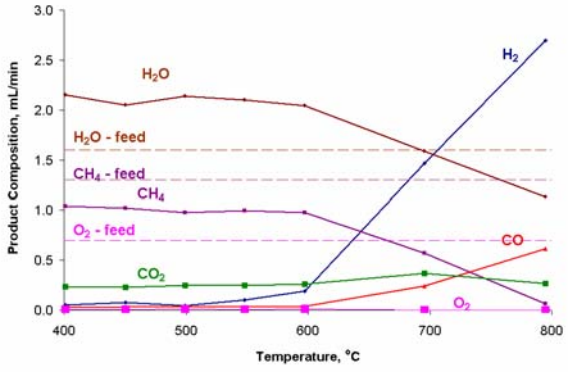

(b) 0.5 wt% Pt on CZO-20.

Figure 1. Product gas yield as a function of temperature for methane reforming for 0.5 wt% Pt supported on (a) CGO-20 and (b) CZO-20. Conditions: CH_4 feed rate = 1.4 mL/min; O_2:CH_4 ratio = 0.55; H_2O:CH_4 ratio = 1.2; balance N_2, GHSV = ~50,000 h^{-1}.

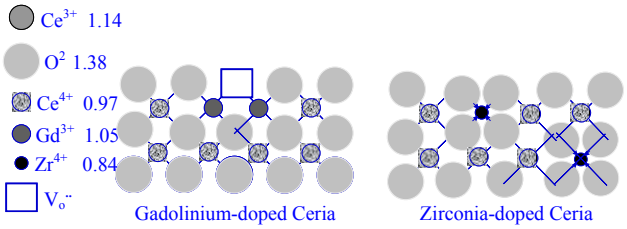

Figure 2. Comparison of the defect structures of gadolinium-doped ceria and zirconium-doped ceria.

that is responsible for the differences in activity observed between the two substrates.

For CGO, the oxygen vacancies ($V_o^{\cdot\cdot}$) can interact with Pt^0 on the surface and O_2 in the gas phase to form individual platinum ions:

$$Pt^0 + 2V_o^{\cdot\cdot} + O_2 = Pt^{4+} + 2O^{2-} \quad (1)$$

Once formed, Pt^{4+} can oxidize methane to methanol. In solution, Pt^{4+} ions are known to oxidize methane to methanol [1,2]. On the ceria surface, such a reaction can be written as:

$$Pt^{4+} + 2O^{2-} + 2CH_4 = Pt^0 + 2V_o^{\cdot\cdot} + 2CH_3OH \quad (2)$$

While we have not yet shown unequivocally that methane is oxidized to methanol on a Pt^{4+} site, XPS analysis (Table 1) clearly shows that the Pt:Ce ratio on the surface decreases as the concentration of gadolinium dopant increases, as would be expected if Pt^0 interacts with the oxygen ion vacancies, as shown in Equation (1).

Oxygen ion vacancies may also play an important role in the decomposition of water [3]. Water molecules can interact with an oxygen ion vacancy, as shown in Equation (3):

$$H_2O + V_o^{\cdot\cdot} + 2e^- = O^{2-} + H_2 \quad (3)$$

Table 1 XPS data for 0.5 wt% Pt supported on various gadolinium-doped cerias with varying Ce:Gd ratios.

Composition	Ce:Gd Bulk	Ce:Gd Surface	Pt:Ce Surface
CeO_2	N.A.	N.A.	5
$Ce_{0.95}Gd_{0.05}O_{1.975}$	19:1	4:1	0.32
$Ce_{0.90}Gd_{0.10}O_{1.95}$	9:1	1:1	1
$Ce_{0.85}Gd_{0.15}O_{1.925}$	5.7:1	0.9	0.6
$Ce_{0.80}Gd_{0.20}O_{1.90}$	4:1	0.9	0.6

This reaction would occur near the isolated Pt^0, which would provide the electrons, as shown in Equation (4):

$$Pt^0 = Pt^{4+} + 4e^- \quad (4)$$

Pt^{4+} can then be reduced by the methanol that was formed in Equation (2):

$$2CH_3OH + Pt^{4+} + 2O^{2-} = 2CH_2O + Pt^{2+} + 2H_2 + 2V_o^{\cdot\cdot} \quad (5)$$

Adding Equations (3), (4), and (5) yield H_2 and CH_2O in a reaction sequence that involves oxygen ion vacancies. CH_2O is readily oxidized to CO to complete the reaction sequence. Referring to Figure 1, for 0.5 wt% Pt supported on CGO-20, which has oxygen ion vacancies, H_2O and CH_4 can react at temperatures of 400–600°C to produce H_2 and CO. For 0.5 wt% Pt supported on CZO-20, which does not contain oxygen ion vacancies, higher temperatures (>550°C) are required before steam reforming is observed. Future work will focus on identifying reaction intermediates, such as CH_3OH and CH_2O.

Effect of Metal

To refine our earlier results for isooctane reforming over various metals, we have measured the product yields of H_2, CO, CO_2, CH_4, and total hydrocarbon (HCs) (on a basis of per mole product gas per mole of C_8H_{18} feed) for two precious metals — Pt (Figure 3) and Rh (Figure 4) — and two non-precious metals — Co (Figure 5) and Ni (Figure 6) — all supported on CGO-20. At 500°C, the Ni and Rh catalysts each produce ~10 moles of H_2/mole of C_8H_{18}, which is higher than the Pt catalyst (~3 moles of H_2/mole of C_8H_{18}) or the Co catalyst (<2 moles of H_2/mole of C_8H_{18}). At 700°C, the Pt and Rh catalysts each produce ~12 moles of H_2/mole of C_8H_{18}, which is the equilibrium H_2 yield for the reaction conditions. The Ni and Co catalysts each produce a high H_2 yield (~10 moles of H_2/mole of C_8H_{18}); however, significant quantities of CH_4 are observed (~1 mole of CH_4/mole of C_8H_{18}). Future work will focus on eliminating the noble metal or significantly reducing the weight loading of the noble metal through the use of bimetallic compositions to reduce the cost of the catalysts.

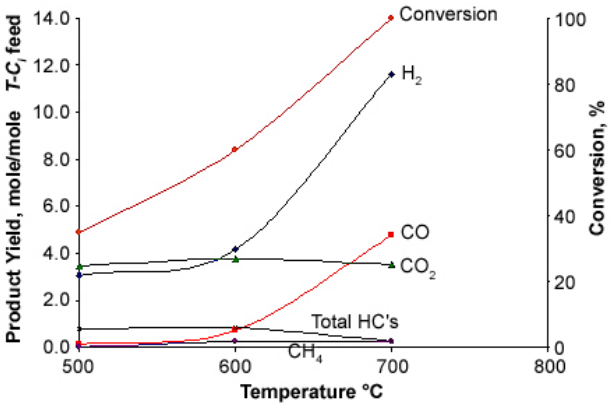

Figure 3. H_2, CO, CO_2, CH_4, and total hydrocarbon yield as a function of temperature for isooctane reforming for 0.5 wt% Pt supported on CGO-20. Conditions: O_2:C_8 = 4; H_2O:C_8 = 9.2; GHSV = 10,000 h^{-1}.

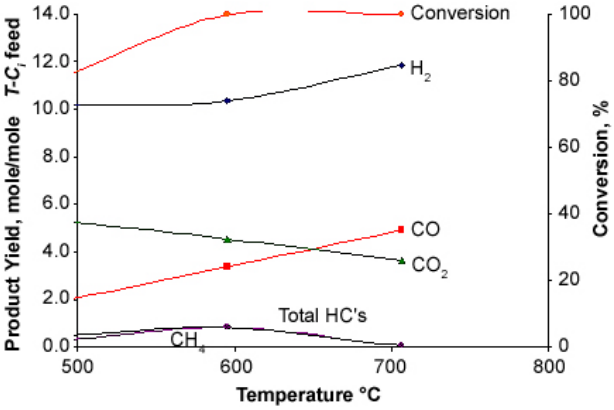

Figure 4. H_2, CO, CO_2, CH_4, and total hydrocarbon yield as a function of temperature for isooctane reforming for 0.5 wt% Rh supported on CGO-20. Conditions: O_2:C_8 = 4; H_2O:C_8 = 9.2; GHSV = 19,000 h^{-1}.

Hydrocarbon Breakthrough

One of the concerns with any fuel processor is whether any hydrocarbon products, other than CH_4, are contained in the reformate gas. Hydrocarbons in the reformate gas not only reduce the overall efficiency of the processor, but they may also poison the water-gas shift and preferential CO oxidation catalysts. This concern is not just a question of catalytic activity, but it relates to the design of the fuel processor. Ideally, fuel, air, and steam would be mixed homogeneously in the gas phase without undergoing any gas phase reactions before being exposed to the catalyst. In reality, the mixture will

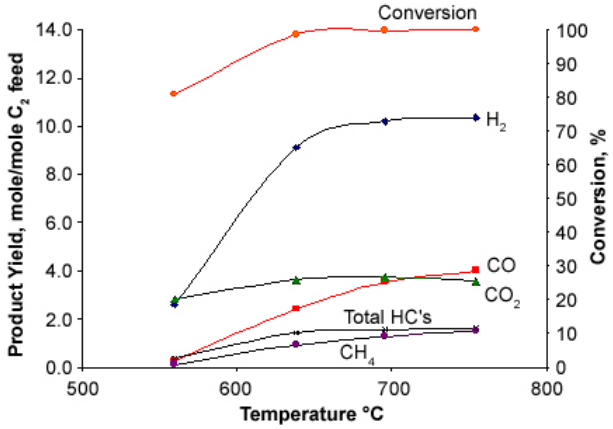

Figure 5. H_2, CO, CO_2, CH_4, and total hydrocarbon yield as a function of temperature for isooctane reforming for 0.34 wt% Co supported on CGO-20. Conditions: O_2:C_8 = 4; H_2O:C_8 = 9.2; GHSV = 5,000 h^{-1}.

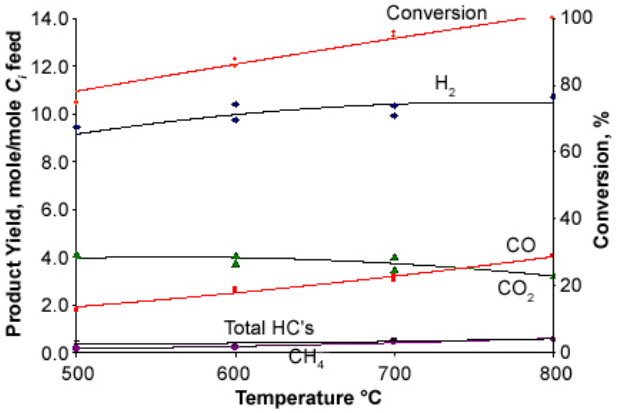

Figure 6. H_2, CO, CO_2, CH_4, and total hydrocarbon yield as a function of temperature for isooctane reforming for 1.0 wt% Ni supported on CGO-20. Conditions: O_2:C_8 = 4; H_2O:C_8 = 9.2; GHSV = 19,000 h^{-1}.

be exposed to hot surfaces before reaching the catalyst, which may lead to pre-ignition or thermal decomposition.

To begin addressing these issues, we have analyzed the product gas composition for hydrocarbon components after passing a mixture of isooctane, O_2, and H_2O under ATR conditions over three different materials in a microreactor system: silicon carbide (Figure 7), CGO-20 (no metal) (Figure 8), and 0.5 wt% Pt-supported CGO-20 (Figure 9).

On silicon carbide, which is considered to be catalytically inert, the principal reaction products were CO, CO_2, and (presumably) H_2O, which was

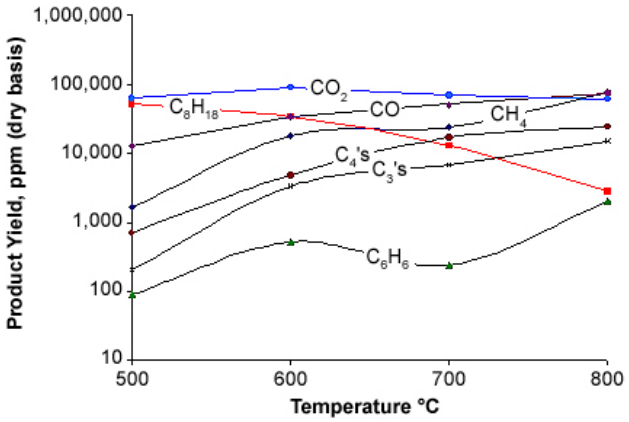

Figure 7. Product gas composition as a function of temperature for isooctane reforming for silicon carbide. Conditions: O_2:C_8 = 4; H_2O:C_8 = 9.2; GHSV = 5,000 h^{-1}.

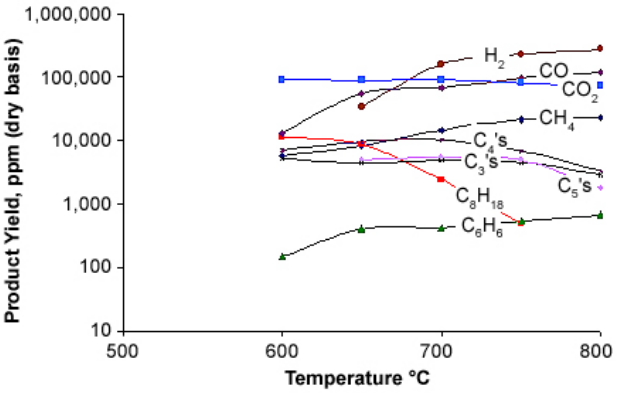

Figure 8. Product gas composition as a function of temperature for isooctane reforming for CGO-20 (no metal). Conditions: O_2:C_8 = 4; H_2O:C_8 = 9.2; GHSV = 5,000 h^{-1}.

not measured. No H_2 was observed. Substantial yields of CH_4, C_3s, and C_4s, which are believed to be products of isooctane thermal decomposition, C_6H_6, as well as unconverted C_8H_{18}, were observed over the temperature range (500–800°C) investigated. A small amount of C_6H_6 (<1,000 ppm) was observed, which is believed to result from gas-phase reactions.

On CGO-20 (no metal), the principal reaction products were H_2, CO, CO_2, and (presumably) H_2O, which was not measured. Substantial yields of CH_4, C_3s, C_4s, C_5s, C_6H_6, and unconverted C_8H_{18} were observed over the temperature range (500–800°C) investigated. At >700°C, the yields of C_3s, C_4s, and C_5s were observed to decrease, suggesting that these compounds were undergoing additional reactions, probably cracking to CH_4. The C_6H_6 yield

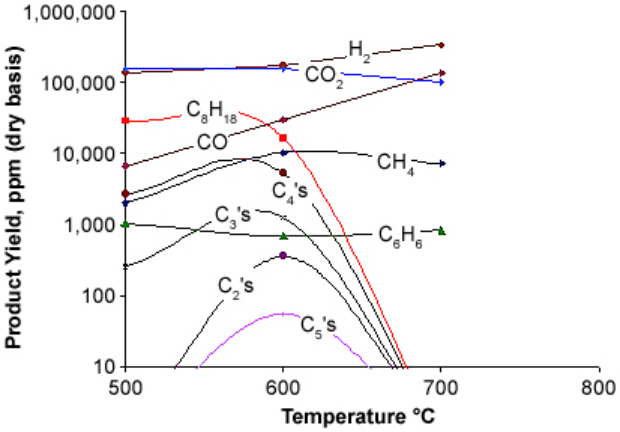

Figure 9. Product gas composition as a function of temperature for isooctane reforming for 0.5 wt% Pt supported on CGO-20. Conditions: O_2:C_8 = 4; H_2O:C_8 = 9.2; GHSV = 5,000 h^{-1}.

(<1,000 ppm) was similar to that observed with silicon carbide.

On 0.5 wt% Pt supported on CGO-20, the principal reaction products were H_2, CO, CO_2, and (presumably) H_2O, which was not measured. At <650°C, lower yields of CH_4, C_2s, C_3s, C_4s, C_5s, and unconverted C_8H_{18} were observed compared with the yields observed for these compounds on both silicon carbide and CGO-20 (no metal). At >650°C, only CH_4 and C_6H_6 were observed. The C_6H_6 yield was similar to that observed with silicon carbide.

The presence of C_6H_6 in the product gas generated over the three materials tested is of concern because of the potential problems associated with C_6H_6 emissions. However, the observation that the C_6H_6 yield was nearly identical over the three materials tested indicates that *the catalyst is not producing C_6H_6* and that a better reactor design, which eliminates gas-phase reactions before the gaseous feed mixture reaches the catalyst, should not produce C_6H_6.

Cost

Meeting the cost goals set by DOE is a critical consideration for catalyst development, especially when noble metals are involved. As discussed, efforts are under way to develop a catalyst that either completely eliminates the noble metal or significantly reduces the noble metal weight loading through the use of bimetallics to reduce the cost of the catalyst. Table 2 shows a cost comparison for

Table 2. ATR catalyst materials cost estimate for three single metal and two bimetallic catalysts. DOE technical target is < \$5/kW_e.

Metal	\$/kg cat	\$/kW_e
A	\$19.39	\$1.94
B	\$118.99	\$11.90
C	\$23.66	\$2.37
AB	\$85.57	\$8.56
AC	\$20.13	\$2.01

three different metals and two different bimetallic compositions that we have developed. The data suggest that, through the use of bimetallics, we are very close to meeting the DOE target of < \$5/kW_e.

Conclusions

The ATR catalyst developed at ANL is commercially available and is being used in several industrial programs. We have increased our understanding of how these catalysts work and are making progress toward replacing the noble metals with less-expensive catalyst formulations to meet DOE cost targets.

References

1. A.E. Shilov and G.B. Shul'pin, 1997, *Chem. Rev.* Vol. 97, p. 2879.
2. R.A. Periana, D.J. Taube, S. Gamble, H. Taube, T. Satoh, and H. Fuji, 1998, *Science,* Vol. 280, p. 560.
3. K. Otsuka, M. Jatang, and A. Morikawa, 1983, *J. Catal.*, Vol. 79, p. 493.

J. Alternative Water-Gas-Shift Catalysts

Deborah J. Myers (primary contact), John F. Krebs, Theodore R. Krause, J. David Carter, and Michael Krumpelt
Argonne National Laboratory, Argonne, IL 60439-4837
(630) 252-4261, fax: (630) 252-4176, e-mail: myers@cmt.anl.gov

DOE Program Manager: JoAnn Milliken
(202) 586-2480, fax: (202) 586-9811, e-mail: JoAnn.Milliken@ee.doe.gov

Objectives

- The water-gas-shift (WGS) reaction is used to convert CO in reformate to CO_2 and additional hydrogen. The objective of this effort is to develop alternatives to commercial WGS catalysts that:
  - eliminate the need to sequester catalyst during system shutdown,
  - eliminate the need for careful *in situ* catalyst activation,
  - increase tolerance to temperature excursions,
  - reduce size and weight of the shift reactor(s), and
  - extend lifetime of the catalyst.

OAAT R&D Plan: Task 3; Barriers E and G

Approach

- Develop metal-support combinations to promote the bifunctional mechanism of catalyst action:
  - one component to adsorb CO (e.g., metal with intermediate CO adsorption strength) and a second component to adsorb and dissociate H_2O (e.g., oxides with redox properties or oxygen vacancies under reformate conditions).

Accomplishments

- Developed an air-stable, temperature-stable copper catalyst that may allow the WGS reactor to meet DOE's volume and cost targets.
- Developed an air-stable cobalt catalyst with higher activity than commercial iron-chrome (325–400°C).
- Increased activity of Pt catalyst by 50% with a new mixed-oxide substrate.
- Increased activity of the nonprecious metal catalyst by 500% (at 230°C).
- Demonstrated <1% CO at 250–300°C with simulated gasoline reformate by using copper/oxide and cobalt/oxide catalysts.

Future Directions

- Determine lifetime and durability of catalysts under actual reformate conditions.
- Determine sulfur tolerance of copper and cobalt catalysts.
- Fabricate copper and cobalt catalysts in a structured form (i.e., pellets, extrudates, monoliths).
- Continue to explore metal/oxide combinations and oxides to achieve higher space velocities at lower temperatures.
- Explore the fabrication of homogeneous WGS catalysts into a supported form for use as a low-temperature heterogeneous catalyst.
- Provide samples of newly developed WGS catalysts to industry for performance evaluation.

Introduction

The water-gas-shift (WGS) reaction,

$$CO + H_2O \rightarrow CO_2 + H_2,$$

is used to convert the bulk of CO in the raw reformate to CO_2 and additional H_2. In the chemical process industry (e.g., in the manufacture of ammonia), the shift reaction is conducted at two distinct temperatures. The high-temperature shift (HTS) is carried out at 350–450°C by using an iron-chrome catalyst. The low-temperature shift (LTS) is carried out at 160–250°C with the aid of a copper/zinc oxide catalyst.

The commercial HTS and LTS catalysts require activation by careful pre-reduction *in situ* and, once activated, lose activity very rapidly if they are exposed to air. Further, the HTS catalyst is inactive at temperatures <300°C, while the LTS catalyst degrades if heated to temperatures >250°C. The automotive application, because of its highly intermittent duty cycle, requires alternative WGS catalysts that (1) eliminate the need to sequester the catalyst during system shutdown, (2) eliminate the need for careful *in-situ* catalyst activation, (3) increase tolerance to temperature excursions, and (4) reduce the size and weight of the shift reactors.

Approach

We are investigating bifunctional catalysts where one component of the catalyst adsorbs or oxidizes CO and the other component dissociates water. Our present research is focused on metal-support combinations to promote this bifunctional mechanism. The metallic component is chosen to adsorb CO at intermediate adsorption strengths (Pt, Ru, Pd, PtRu, PtCu, Co, Ag, Fe, Cu, and Mo). The support is chosen to adsorb and dissociate water, typically a mixed-valence oxide with redox properties or oxygen vacancies under the highly reducing conditions of the reformate.

Tests of the candidate catalysts' activities were conducted with simulated reformate by using a micro-reactor. The micro-reactor was operated as a differential reactor for determining kinetic parameters. The concentrations of reactant gases were chosen to simulate the composition and concentrations of gases exiting an autothermal reformer (dry composition: 10% CO, 13% CO_2, 43% H_2, balance N_2). A water concentration of 31% was chosen to simulate the additional amount of water necessary to cool the autothermal reforming gases to 400°C.

Results

Early in this project, a platinum/mixed-oxide catalyst was identified as a potential WGS catalyst with several desirable properties. As opposed to copper/zinc oxide, this catalyst does not have to be reduced *in situ*, does not lose activity upon exposure to air at 21–550°C, and is active over the 180–400°C temperature range. Over the first three years of the project, the WGS activity of the platinum/mixed-oxide catalyst was quadrupled, while the platinum loading was reduced by an order of magnitude from 1 wt% to 0.14 wt%. The catalyst was also supported on an alumina extrudate. This year, an improved mixed oxide support was developed. As shown in Figure 1, the new mixed oxide support (MO-2) increased the activity of the powdered catalyst by 50%. The doubling of activity when supporting the catalyst on alumina, as was seen with the original mixed oxide (MO-1), is also expected with MO-2.

This year, we also developed perovskite catalysts and catalysts consisting of cobalt supported on transition metal oxides. As shown in Figure 2, these catalysts are more active than commercial iron-chrome at 400°C. The activity of the cobalt/transition metal oxide catalysts was not changed after exposure to air at 400°C, and the activity of the perovskite catalysts could be recovered after reduction in 4% hydrogen. The only catalyst to exhibit methanation activity was the

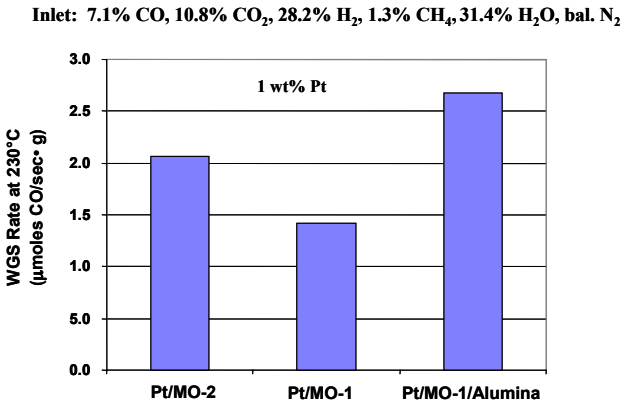

Figure 1. A new mixed-oxide substrate has improved the activity of the platinum catalyst by 50% (MO-2 vs. MO-1).

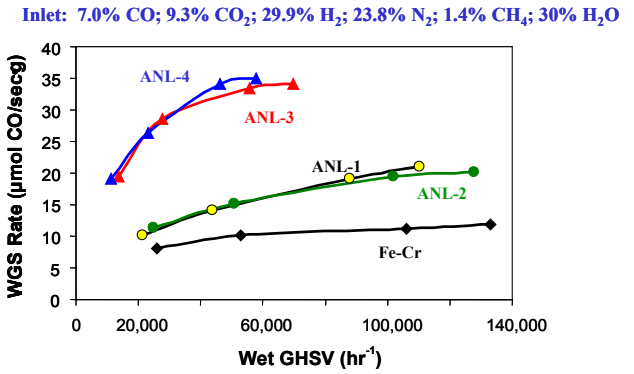

Figure 2. Argonne's cobalt and perovskite catalysts are more active than commercial Fe-Cr at 400°C. ANL-1, 7.5 wt% Co/transition metal oxide; ANL-2, 3.8 wt% Co/transition metal oxide; ANL-3, perovskite; and ANL-4, 0.8 wt% Pt/perovskite. GHSV = gas hourly space velocity.

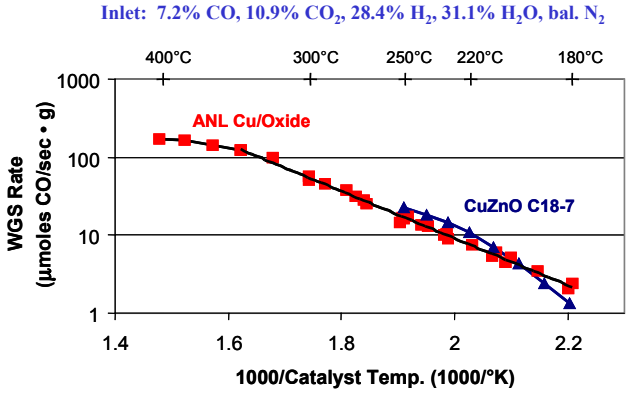

Figure 3. Argonne's copper/oxide catalyst has activity comparable with that of commercial copper/zinc oxide and is not limited to temperatures <250°C.

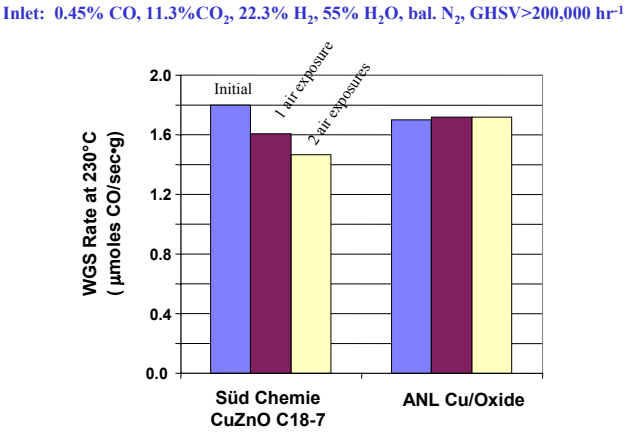

Figure 4. Argonne's copper/oxide catalyst retains activity when exposed to air at 230°C.

cobalt/transition metal oxide, but this was eliminated by decreasing the cobalt loading from 7.5 to 3.8 wt%. X-ray diffraction analysis of the perovskite catalysts revealed structural degradation caused by the exposure to simulated reformate. These catalysts also showed higher WGS activity than the commercial Fe-Cr catalyst at 325°C; however, the activity is dramatically decreased below this temperature. These results indicate that the cobalt/transition metal oxide catalyst would be a suitable replacement for Fe-Cr as an HTS catalyst.

We also developed a copper/oxide catalyst that has the same activity as copper/zinc oxide, the commercial LTS catalyst (Figure 3). Unlike copper/zinc oxide, the Argonne copper/oxide catalyst can operate above 250°C without deactivation and retains activity after exposure to air at 230°C (Figure 4). The higher operating temperature range of the Argonne copper/oxide catalyst allows it to be used in both the HTS and LTS stages. This catalyst also has higher WGS activity than iron-chrome; therefore, it can dramatically reduce the size and weight of the HTS stage. The temperature stability of the copper/oxide catalyst allows the LTS stage to run at a higher inlet temperature (e.g., 300°C) than would be possible with copper/zinc oxide (200°C). The improved kinetics afforded by a higher operating temperature will reduce the size and weight of the LTS.

The catalyst volumes needed for a 50-kW_e reactor were calculated on the basis of the measured intrinsic reaction rates and activation energies for the Argonne catalysts, as well as the published kinetic data for the commercial catalysts. The HTS and LTS stages were assumed to operate adiabatically. The calculated amount of catalyst is that needed to reduce the exit CO concentration to 1% (dry basis) from an inlet reformate gas consisting of 10% CO, 10% CO_2, 34% H_2, 33% N_2, and 13% H_2O (wet basis). As shown in Figure 5, for the commercial HTS and LTS catalysts operating at 400°C and 200°C, respectively, a total catalyst volume of 19.2 L is needed for a 50-kW_e fuel cell system. With the Argonne platinum catalyst

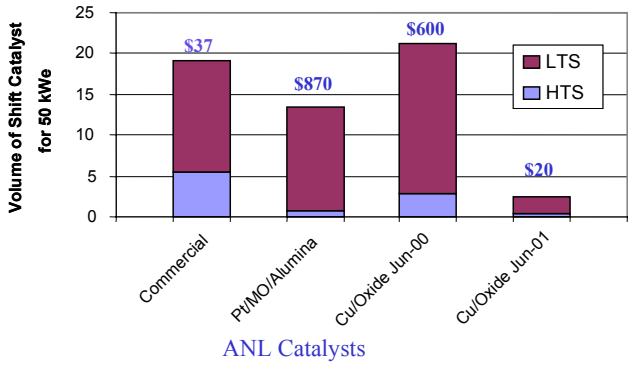

Figure 5. Argonne's copper/oxide catalyst reduces the WGS catalyst volume for a 50-kW_e reactor to 13% the volume of the commercial iron-chrome and copper/zinc oxide catalysts (2.4 L vs. 19.2 L). Commercial LTS is Cu/ZnO at 200°C, and commercial HTS is Fe-Cr at 400°C. ANL LTS operating at 300°C and ANL HTS at 400°C.

operating at 400°C and 300°C, respectively, the total required catalyst volume is 13.5 L, which is a 30% reduction compared to the commercial catalysts. As of June 2000, Argonne's copper/oxide catalyst was less active than commercial copper/zinc oxide with a total catalyst volume of 21.2 L. This year's improvements in Argonne's copper/oxide catalyst resulted in a reduction of the total catalyst volume to 2.4 L for a 50-kW_e system. The estimated costs of these catalysts, based on materials' costs only, are also shown in Figure 5. Argonne's copper/oxide catalyst reduces the WGS catalyst cost by 46% as compared to the commercial catalysts. These results demonstrate the potential of the Argonne copper/oxide catalyst to meet or exceed DOE's catalyst volume and cost goals for the WGS reactor of < 1 L/kW_e and < $1/kW, respectively.

Conclusions

In the past year, we have developed a temperature-stable copper/oxide catalyst. Estimates based on isothermal kinetic data show that the copper/oxide catalyst has the potential to reduce the WGS catalyst volume to 13% of the commercial iron-chrome-copper/zinc oxide combination. In addition, the Argonne copper/oxide catalyst does not lose activity after exposure to air. We have also developed an air-stable cobalt catalyst with higher activity than commercial iron-chrome (325–400°C). Reactors based on Argonne's cobalt and copper catalysts were shown to reduce the carbon monoxide level in simulated reformate from 10.4% to <1% (dry gas basis).

IV. FUEL CELL STACK SUBSYSTEM[1]

A. R&D of a 50-kW, High-Efficiency, High-Power-Density, CO-Tolerant PEM Fuel Cell Stack System

Tim Rehg (principal investigater) and Nguyen Minh (project manager)
Honeywell Engines and Systems
2525 W. 190th Street, MS-36-1-93193
Torrance, CA 90504-6099
Rehg, (310) 512-2281, fax: (310) 512-3432, e-mail: Tim.Rehg@Honeywell.com
Minh, (310) 512-3515, fax: (310) 512-3432, e-mail: Nguyen.Minh@Honeywell.com

DOE Program Manager: Patrick Davis
(202) 586-8061, fax: (202) 586-9811, e-mail: patrick.davis@ee.doe.gov

ANL Technical Advisor: William Swift
(630) 252-5964, fax: (630) 972-4473, e-mail: swift@cmt.anl.gov

Contractor: Honeywell Engines and Systems, Torrance, California
Prime Contract No. DE-FC02-97EE50470, October 1997–December 2001

Objectives

- Research, develop, assemble, and test a 50-kW-net polymer electrolyte membrane (PEM) fuel cell stack system:
  - Consisting of a PEM fuel cell stack and the supporting gas, thermal, and water management subsystems and
  - Capable of integration with at least one of the fuel processors currently under development by Hydrogen Burner Technology (HBT) and Nuvera.

OAAT R&D Plan: Task 11; Barriers A, B, C, D, and E

Approach

- A phased R&D program that includes the fabrication and testing of three 10-kW subscale PEM fuel cell stacks leading up to the final 50-kW system.
  - Conduct stack technology development and system analysis iteratively to identify pertinent technology advances to be incorporated into successive subscale stack builds.
  - Define the 50-kW stack and system configuration on the basis of the final system analysis.
- Phase I: PEM stack R&D
  - Demonstrate multifuel capability and CO tolerance.
  - Advance technologies toward U.S. Department of Energy (DOE) targets.
- Phase II:
  - Complete subscale integration.

[1] The DOE draft technical targets for fuel cell stack systems running on hydrogen-rich fuel from a fuel-flexible fuel processor can be found in Table 3, Appendix B. Because the targets in Appendix B were updated after the reports were written, the reports may not reflect the updated targets.

  - Develop electronic control system.
  - Characterize transients.
  - Conduct durability testing.
- Phase III:
  - Test the 50-kW PEM fuel cell stack system.
  - Deliver the 50-kW PEM fuel cell stack system to Argonne National Laboratory.

Accomplishments

- Completed the 50-kW brassboard system balance-of-plant component procurement.
- Completed the major balance-of-plant hardware assembly (minus fuel cell stacks) and subsystem testing.
- Integrated the turbocompressor and its controller with the balance of plant and tested components for performance.
- Designed controls and interfaces for real-time operation of the 50-kW brassboard and completed the hardware/software interface.
- Integrated two 10-kW-class PEM stacks into the balance of plant for shakedown testing of the control system.
- Began component procurement for the third-generation 10-kW-class PEM fuel cell stack with molded composite bipolar plates.
- Tested a 6-cell subscale PEM fuel cell stack with molded plates. Demonstrated simulated reformate stoichiometric flows as low as 1.1.

Future Directions

- Complete and test the third-generation 10-kW-class PEM stack (scheduled for August 2001).
- Build and integrate the 50-kW-class PEM stack into the brassboard system and conduct performance testing.
- Deliver 50-kW-net PEM fuel cell stack system brassboard to Argonne National Laboratory at the conclusion of the project (12/01).
- Continue collaboration with Argonne National Laboratory and fuel processor contractors on system integration issues.
- Continue to drive development toward DOE 2000 technical targets for high-volume production costs ($100/kW for 5,000,000 units/yr).

Introduction

Fuel cell power plants will become viable substitutes for the internal combustion engine (ICE) in automotive applications only when their benefits of increased fuel efficiency and reduced emissions are accompanied by performance and cost comparable with those of the ICE. Meeting these requirements is a significant technical challenge that requires an integrated systems approach. This effort encompasses the technical and developmental activities required to incorporate innovations necessary to develop a 50-kW fuel cell stack system to meet the requirements set forth by DOE. Honeywell is currently nearing the end of Phase II of the three-phase R&D program.

Approach and Results

Fuel Cell Stack System

The PEM fuel cell stack system consists of the fuel cell stack and supporting gas, thermal, and water management systems, as shown in Figure 1. Overall system performance depends on the careful integration of these subsystems.

The design of the 50-kW fuel cell stack brassboard system has been completed. The three-dimensional layout, including six hexagonally shaped stacks, is shown in Figure 2. During this reporting period, all major components have been procured, and the balance of plant has been assembled. A photograph of the system is shown in Figure 3. The brassboard has been designed for

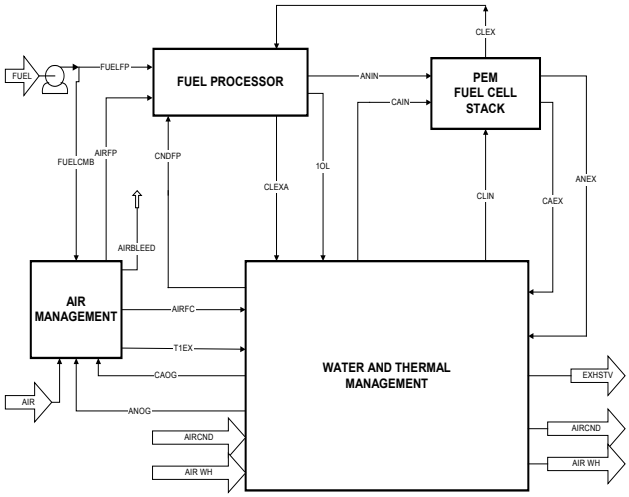

Figure 1. Diagram of PEM fuel cell stack system.

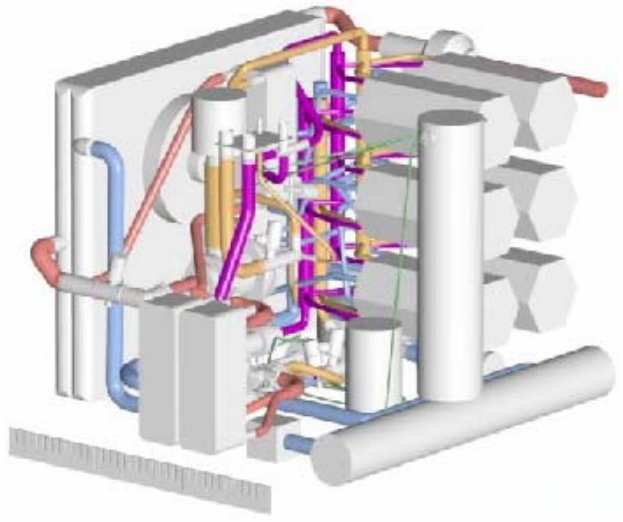

Figure 2. Design of 50-kW brassboard system.

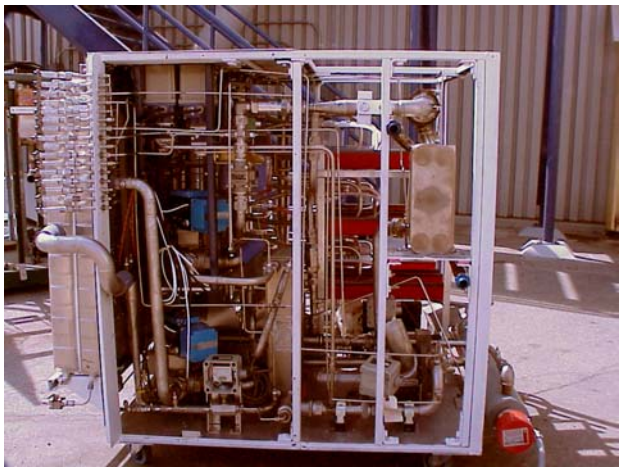

Figure 3. 50-kW brassboard system (without the stacks).

50-kW-net electric power output, operating at high efficiency on gasoline reformate. It incorporates full integration and management of on-board thermal, water, and air subsystems and makes use of off-the-shelf components to minimize cost and assembly time.

For air delivery, the fuel cell stack system is equipped with a Honeywell turbocompressor developed under DOE funding (see Figure 4). The turbocompressor delivers enough air for the fuel cell stack system and the fuel processor at an operating pressure of up to 3 atmospheres at peak power condition. During this reporting period, the turbocompressor and its controller have been integrated into the balance-of-plant, and proper functionality has been verified through subsystem testing.

To verify the operation of the system, two PEM fuel cell stacks taken from an internal Honeywell program were integrated into the system and tested. The key objective for this test was to validate the functionality of the balance-of-plant and the system controller with integrated fuel cell stacks.

During open-circuit operation, the balance-of-plant was checked for stable operation. After reaching thermal equilibrium in all gas streams and the coolant loop, the current was increased stepwise by using a ramp time between steps of one minute, and the system showed stable behavior during all ramps, as well as at the steady power levels.

The results from this test illustrate that the system operates safely and is stable during steady-state and slow transient operation.

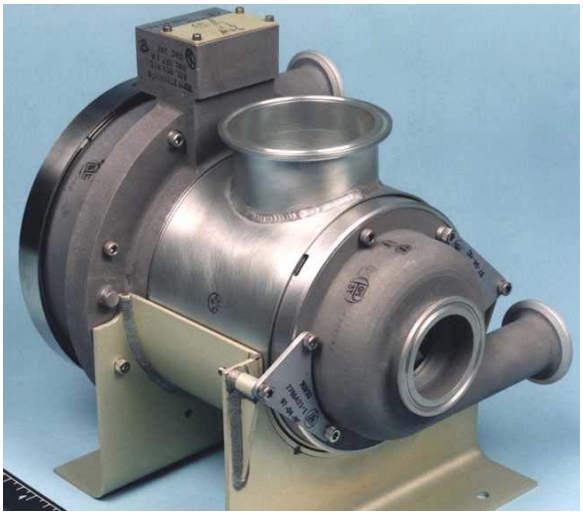

Figure 4. Honeywell Phase II Turbocompressor.

Control System

Controls have been designed by assuming a full dynamic control capability, but provisions have been made for a variety of actuation schemes. The hardware/software interface has been completed, and all actuators are controlled via a Rapid Prototype System (RPS).

All thermal loops are under automatic control, including the cathode inlet temperature, water cooling loop temperature, and humidification of the cathode stream. Figure 5 shows the response of the cathode inlet temperature to a system disturbance. Even with a large temperature disturbance, the inlet cathode temperature does not exceed the 1% error band.

The cathode air flow control loop has been developed, but further work remains on mapping the turbocompressor performance over the entire operating range. Reformate flow is controlled by setpoint command to the fuel processor test stand.

A power control architecture has been simulated and will be implemented in the next phase of testing. Communication between the RPS controller and the cell performance monitors has been established and tested.

Molded Bipolar Plates

For the fabrication of the 50-kW PEM fuel cell stack, it is planned to use compression-molded composite bipolar plates. These plates are made in a single step, which will help to reduce the manufacturing cost substantially. During this reporting period, Honeywell has received the first iteration of molded bipolar plates.

By using the initial molded plates, a 6-cell stack was built and tested in excess of 50 h at the nominal system operating point (12.5 kW) (see Figure 6). The detailed test conditions are described in Table 1.

The 6-cell stack performed very well at the nominal system operating condition at a stoichiometric anode flow as low as 1.1. When 100 ppm of CO was introduced into the anode flow, the stoichiometric flow was raised to 1.15. Overall, the performance of the molded stack in terms of stoichiometric flows is superior to that previously accomplished. The low anode flow has a potentially large effect on overall system efficiency, as is shown in Table 2.

The molding process faces a number of challenges that still need to be overcome. These challenges include thickness tolerance, flatness, and

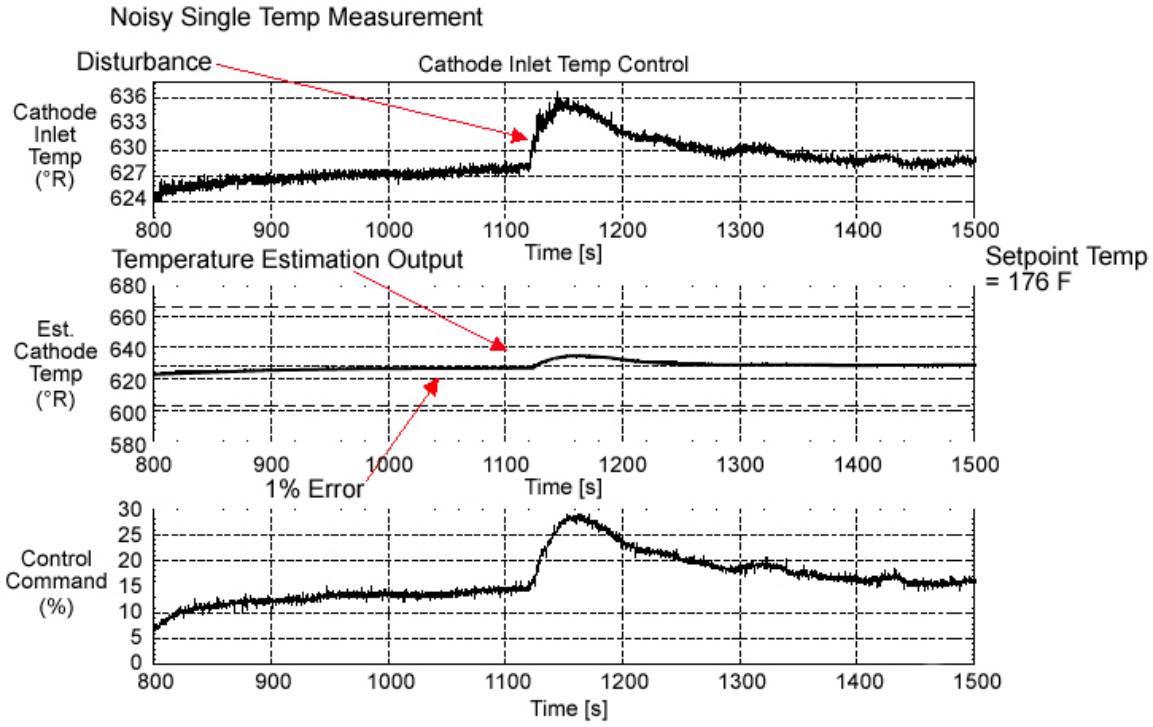

Figure 5. Signal for automated cathode inlet temperature control.

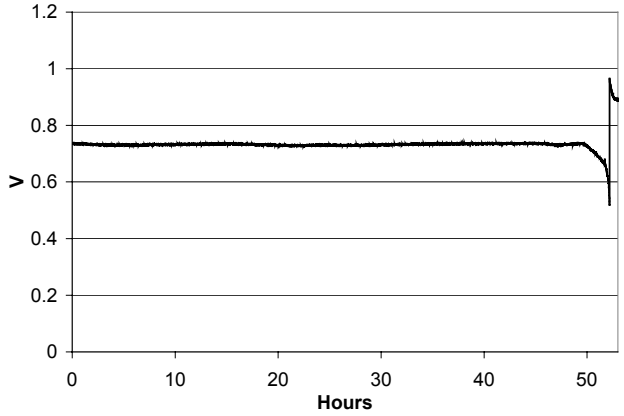

Figure 6. Single-cell voltage for 6-cell PEM FC stack with molded composite bipolar plates.

Table 1. Test conditions for 6-cell PEM FC stack with molded composite bipolar plates.

	Anode	**Cathode**
Gas	Reformate	Air
Stoich	1.1	2.0
RH	100%	50%
Temperature	80°C	80°C
Pressure	1.25atm	1.25atm

Table 2. System performance for different anode stoichiometry.

Load %	**100**	**25**	**25**	**25**
PEM Performance	**3 atm**	**1.278 atm**	**1.278 atm**	**1.278 atm**
FUEL PROCESSOR INTERFACE:				
FUEL FLOW lb/min	0.62	0.12	0.10	0.11
AIR FLOW lb/min	3.35	0.63	0.63	0.63
COND FLOW lb/min	1.87	0.35	0.35	0.35
FUEL CELL STACK SYSTEM:				
COMPRESSOR FLOW OUT lb/min	9.88	2.42	2.42	2.42
SHAFT SPEED rpm	101727	46246	46246	46246
COMP EFFICIENCY	0.78	0.73	0.73	0.73
HYDROGEN STOICS	**1.50**	**1.25**	**1.10**	**1.20**
OXYGEN STOICS	1.71	2.00	2.00	2.00
CATHODE RH IN %	50	50	50	50
TURB TEMP IN deg F	525	525	353	494
TURB EFFICIENCY	0.81	0.51	0.51	0.51
TURB PR	2.06	1.16	1.16	1.16
TURBOCOMPRESSOR MOTOR POWER kW	4.09	0.40	0.44	0.41
PARASITE POWER kW	0.50	0.50	0.50	0.50
FC STACK POWER kW	54.59	13.39	13.43	13.40
NET POWER OUT kW	50.00	12.50	12.50	12.50
FC STACK AREA cm^2	191196	191196	191196	191196
SINGLE CELL V volts/cell	**0.68**	**0.75**	**0.75**	**0.75**
AVRG CRNT DENS A/cm^2	0.42	0.09	0.09	0.09
FCSS EFFICIENCY %	**34**	**45**	**49**	**47**

parallelism of the individual plates. During the following months of this program, Honeywell is focusing on resolution of these challenges and building the 50-kW PEM fuel cell stack for the brassboard system.

Conclusions

In this reporting period, Honeywell has built the balance of the plant with the turbocompressor. Attention is now focused on incorporating the third-generation 10-kW stack with molded composite bipolar plates into the system. Results from a subscale (6-cell) PEM fuel cell stack test with compression-molded composite bipolar plates demonstrated a low-anode stoichiometric flow of 1.1 at nominal conditions. The current projected brassboard system nominal efficiency is 48% (assuming 1.15X stoichiometric flow of reformate), and the projected power densities are ~0.2 kW/kg and ~0.15 kW/L, versus the PNGV/DOE targets of 55%, 0.35 kW/kg, and 0.35 kW/L, respectively. Note that the above numbers include contributions from off-the-shelf components for the brassboard (i.e., oversized heat exchangers and valves).

FY 2001 Publication/Presentation

- D. Tourbier, J. Ferrall, T. Rehg, 2000, "Automotive PEM Fuel Cell System Development at Honeywell," Fuel Cell Seminar, Portland, OR, October.

B. Development of Advanced, Low-Cost PEM Fuel Cell Stack and System Design for Operation on Reformate

Michel Fuchs
Teledyne Energy Systems, Inc.
1501 Northpoint Parkway, #101
West Palm Beach, FL 33407
(561) 688-0506 x239, fax: (561) 688-0766, e-mail: fuchs@teledynees.com

DOE Program Manager: Donna Lee Ho
(202) 586-8000, fax: (202) 586-9811, e-mail: donna.ho@ee.doe.gov

ANL Technical Advisor: William Swift
(630) 252-5964, fax: (630) 972-4473, e-mail: swift@cmt.anl.gov

Contractor: Teledyne Energy Systems, Inc. (formerly Energy Partners), West Palm Beach, Florida
Prime Contract No. DE-FC02-97EE50476, October 1, 2001–June 30, 2002

Objectives

The acquisition of Energy Partners by Teledyne Energy Systems, Inc., has resulted in a change in the overall direction of this project. Specifically, the revised objectives of this project are to:

- Design and demonstrate a reformate-capable fuel cell stack, utilizing CO-tolerant membrane electrode assemblies (MEAs) and low-cost bipolar collector plates.
- Design, integrate, and demonstrate a natural-gas-fueled, 7-kW_{net} fuel cell power system.

OAAT R&D Plan: Task 8; Barrier J

Approach

- Phase I: Demonstration and delivery of a polymer electrolyte membrane (PEM) 10-cell stack with reformate capability and 10 additional bipolar plates manufactured by the compression-molding process.
- Phase II: Demonstration and delivery of a high-efficiency, reformate-tolerant, 7-kW_{net} fuel cell stack and power system utilizing molded bipolar plates, power conditioning, and a natural gas fuel processor to Argonne National Laboratory for independent testing and verification.

Accomplishments

- Built and operated a 3-kW_{net} fuel cell system with integrated natural gas reformer.
- Achieved target performance with four-cell Model NG3000™ on reformate/air.
- Completed nearly 2,000 h of endurance testing.

Future Directions

- Continue evaluations of new MEA materials for reformate performance.
- Fabricate, assemble, and test 7-kW_{net} system and prepare it for delivery.

Introduction

As a result of change in ownership (formerly, Energy Partners, Inc.), the focus of the contract has been updated to coincide with current company objectives. Future work will concentrate on the development of a 7-kW_{net} fuel cell system with an integrated natural gas reformer and power conditioning based on Teledyne Energy Systems' 3-kW_{net} prototype stationary power plant. The development effort will focus on a systems approach, but it will be broken down into three areas: PEM fuel cell stack, natural gas reformer, and integrated system.

PEM Fuel Cell Stack

A stack design capable of meeting automotive requirements was developed and then evaluated through "short" stack testing. The new stack, designated the NG3000 series (Figure 1), will be considered, along with its predecessor, the NG2000, for use in the 7-kW_{net} system. Both stacks have been proven on reformate, and the final selection will depend on overall system performance and packaging considerations. In either case, Teledyne Energy Systems' advanced compression-molded collector plates will be utilized to minimize cost.

The NG3000 has an active area twice the size of its predecessor (600 cm^2 vs. 300 cm^2) and is specifically designed to operate on reformate (40% H_2, 40% N_2, 20% CO_2). The NG3000 exhibited comparable performance to an NG2000 (Figure 2) and satisfied load demands with excellent cell-to-cell consistency (Figure 3). Operating on reformate, the NG3000 can be scaled to meet a variety of power requirements, from 490 W to 61 kW.

Figure 1. NG3000™ 10-cell stack.

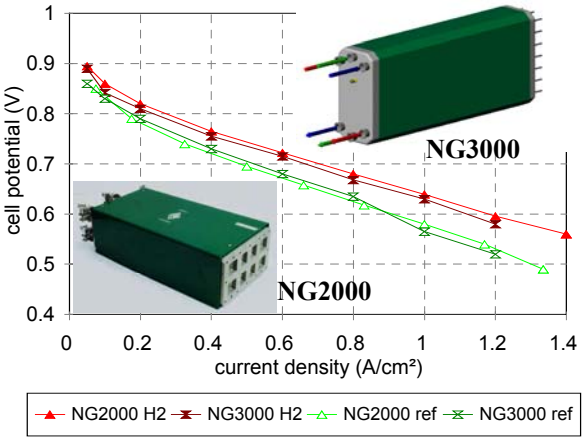

Figure 2. Comparison of NG2000™ and NG3000™ stacks on hydrogen and on reformate.

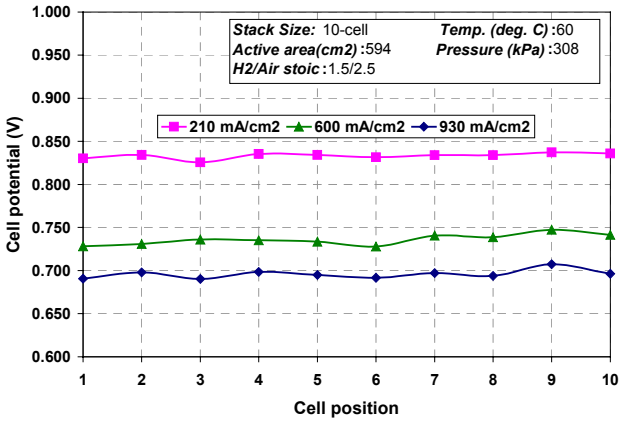

Figure 3. Cell voltage variation in NG3000 10-cell stack.

The NG2000, although initially configured to run on pure hydrogen, has been updated and is now the NG2000R, which has better performance on reformate. Even though its performance might be slightly lower than that of the newer series stack, the NG2000R has an active area better suited for small power systems (i.e., systems less than 10kW_{net}).

Both fuel cell designs are capable of operating between 0.2 and 3 atm and are able to tolerate steady-state CO levels of up to 100 ppm. Durability so far is based on the results of a four-cell NG2000 stack, running on hydrogen, which operated continuously for nearly 2,000 h (Figure 4).

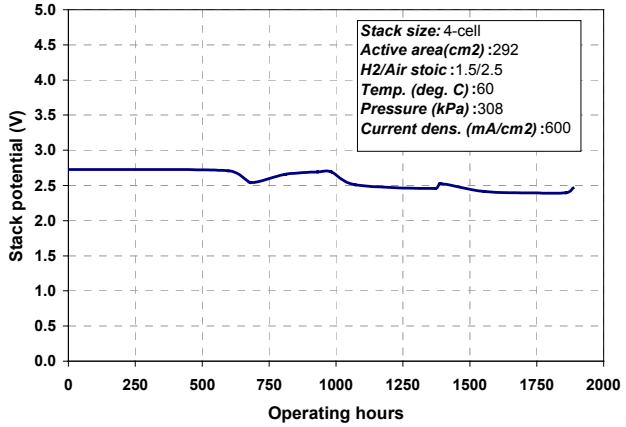

Figure 4. Durability of a four-cell stack at 0.6 A/cm^2 at 100% humidification on H_2/air.

In-situ evaluation of the NG2000R was demonstrated in the successful testing of Teledyne Energy Systems' 3-kW$_{net}$ prototype stationary power plant (Figure 5), which incorporates a natural gas reformer.

Reformer

A natural gas fuel processor able to supply sufficient hydrogen to allow the fuel cell to meet all system load demands, including parasitic loads, will be integrated into the system. The reformer is expected to be a re-sized version of the unit used in the 3-kW$_{net}$ stationary system, which has demonstrated good transient response and low CO output (less than 50 ppm throughout its operating envelope).

Integrated System

The 7-kW$_{net}$ system will consist of the fuel cell, reformer, power conditioning system, and balance-of-plant subsystems. The final packaged system will be optimized for laboratory use and outfitted with an extensive PC-based data acquisition system for in-depth performance testing.

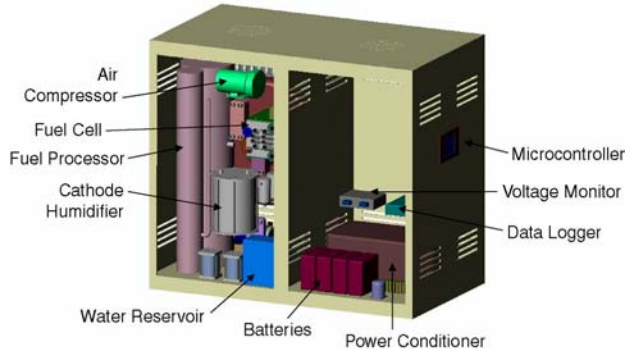

Figure 5. Conceptual view of the 3-kW$_{net}$ stationary power plant.

Incorporated into the 7-kW$_{net}$ package will be a power conditioning system, which will provide the option to test with AC power (the 7-kW$_{net}$ is based on the net system DC power output before conditioning).

The subsystems will be designed to track the load demands placed on the power plant. For instance, compressors, pumps, and fans will be operated to provide the necessary conditions to enable the system to satisfy power demands without excessively contributing to parasitic losses. This will minimize the effects of partial load operation on the overall system efficiency. In addition, a model corrected for test results obtained from the 3-kW$_{net}$ stationary unit will be developed to aid in the design of the subsystems. The model will also assist in minimizing the overall system cost.

Conclusion

Teledyne Energy Systems, Inc., will develop a 7-kW$_{net}$ stationary fuel cell system that will utilize natural gas and enable an in-depth evaluation of a fuel cell and reformer package. The design of the system will be based on Teledyne Energy Systems' 3-kW$_{net}$ prototype stationary power plant, which is currently undergoing testing.

Presentations/Publications

- M. Fuchs, F. Barbir, and M. Nadal, "Performance of Third Generation Fuel Cell Powered Utility Vehicle #2 with Metal Hydride Fuel Storage," presented at the 2001 European Polymer Electrolyte Fuel Cell Forum, Lucerne, Switzerland, July 2001.
- F. Barbir and J. Braun, "Development of Low Cost Bi-Polar Plates for PEM Fuel Cell," Proc. Fuel Cell 2000 Research & Development, Strategic Research Institute Conference, Philadelphia, September 2000.
- M. Fuchs, F. Barbir, and M. Nadal, "Fuel Cell Powered Utility Vehicle with Metal Hydride Fuel Storage," presented at the GlobeEx 2000 Conference, Las Vegas, Nevada, July 2000.
- V. Gurau, F. Barbir, and H. Liu, "An Analytical Solution of a Half-cell Model for PEM Fuel Cells," Journal *of Electrochemical Society*, Vol. 147(7), 2000.

C. Direct Methanol Fuel Cells

Piotr Zelenay (primary contact), Bryan Pivovar, François Guyon, Xiaoming Ren, Cynthia Rice, John Davey, John Ramsey, and Shimshon Gottesfeld
Materials Science and Technology Division
Los Alamos National Laboratory
Los Alamos, New Mexico 97545
(505) 667-0197, fax: (505) 665-4292, e-mail: zelenay@lanl.gov

DOE Program Manager: JoAnn Milliken
(202) 586-2480, fax: (202) 586-9811, e-mail: JoAnn.Milliken@ee.doe.gov

---

Objectives

Develop materials, components, and operation conditions to prove the potential of direct methanol fuel cells (DMFCs) for transportation applications in terms of power density, energy-conversion efficiency, and cost. In particular:

- Optimize membrane-electrode assemblies (MEAs) to enhance cell performance,
- Lower the total precious metal loading in single-cell and short-stack operation, and
- Prove the viability and stability of cell components in long-term operation of single cells and stacks.

OAAT R&D Plan: Task 14; Barriers B, F, H, and I

Approach

- Operate single cells and DMFC stacks with a variety of catalysts and membrane materials to optimize performance and demonstrate stability.
- Design, fabricate, and test various cell components, such as bi-polar plates, flow-fields, and gas-diffusion layers, to optimize performance of single cells and short stacks.

Accomplishments

- *Catalyst optimization*: Optimized composition of low-Pt DMFC anode as a function of catalyst loading.
- *Lowering of the total Pt loading in a short DMFC stack*: Demonstrated 45-cm^2 five-cell stack with a total Pt loading of 0.5 mg cm^{-2} and peak power of 26 W.
- *Membrane research*: Identified new, promising low-crossover and high-efficiency membranes.

Future Directions

- Further develop novel catalysts and alternative membranes for DMFCs.
- Implement a system for automated and reproducible fabrication of quality MEAs for direct methanol fuel cells.
- Design, fabricate, and test hardware for higher-power DMFC stacks.
- Scale up the DMFC stack to 0.3–0.4 kW, which is relevant to auxiliary power applications (in collaboration with the U.S. Communication Electronics Command [CECOM]).

Introduction

The main goal of the direct methanol fuel cell research at Los Alamos National Laboratory (LANL) has been to develop materials, components, and operation conditions relevant to the potential application of DMFCs in automotive transportation. In particular, our intent has been to show that direct methanol fuel cells stand a good chance of meeting the program goals in terms of power density, overall energy-conversion efficiency, and cost. DMFCs combine unique properties of the liquid fuel feed to the anode with system simplicity and possible zero-emission status. In addition to being considered for the main source of vehicular power (in a longer time horizon), DMFCs stand a good chance to be used in on-board auxiliary power units (APUs).

Results

In FY 2001, we have made significant progress in demonstrating operation of direct methanol fuel cells with greatly reduced platinum loading. We have built and successfully tested a 45-cm^2 five-cell DMFC stack with total platinum loading of 0.53 ± 0.02 mg cm^{-2} (equally distributed between the anode and the cathode, at 0.26 ± 0.01 mg cm^{-2} and 0.27 ± 0.01 mg cm^{-2}, respectively). When operated on pressurized air at 100°C, the stack has generated almost 0.2 A cm^{-2} at 2.0 V. The maximum power of 26 W has been achieved at a current density of *ca.* 0.45 A cm^{-2} (Figure 1). For comparison, power accomplished with a similar stack at a Pt loading of nearly 12 mg cm^{-2}, which we built earlier, was 48 W.

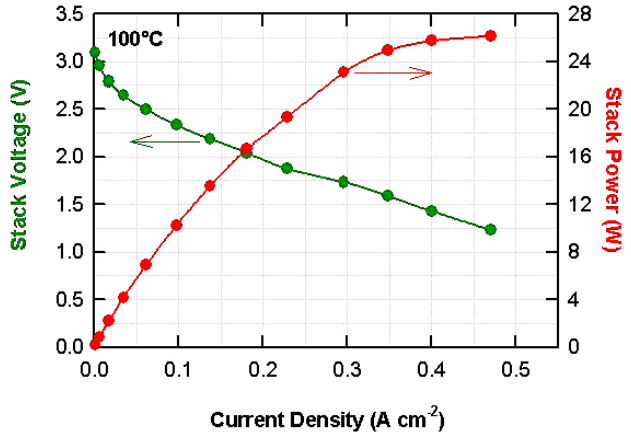

Figure 1. Five-cell stack polarization and power plots for a very low total Pt loading of 0.53 mg cm^{-2} at 100°C (45-cm^2 cells).

Thus, a very significant reduction in the stack platinum loading by more than 95% has led to a reduction in the maximum power of the stack of less than 50%. The performance obtained with the short stack corresponds to 5 g of Pt required to generate 1 kW of power, which fulfills a major project milestone in FY 2001.

Achieving good cell/stack performance with low catalyst loadings has required very careful selection of the anode and cathode catalysts, together with a thorough optimization of the catalyst composition and structure. We have found that fuel cells operating at reduced catalyst loadings seem to benefit from the use of carbon-supported catalysts (see anode data in Figure 2). Comparison of the activity of unsupported 1:1 Pt-Ru anode catalyst with the activity of three different formulations using carbon-supported Pt:Ru catalyst (45% carbon by weight) indicates that carbon-supported anodes outperform the unsupported anode as long as Pt loading remains below *ca.* 1 mg cm^{-2}, probably because of better catalyst utilization.

Another important conclusion from the anode research in FY 2001 is that optimization of the catalyst layer composition and structure is often as important as choosing the right catalyst material. Separate optimization procedures may be required for various intended catalyst loadings. For example, out of the three different Pt-Ru/C catalyst formulations shown in Figure 2, formulation (3) has performed the best in the Pt loading range between

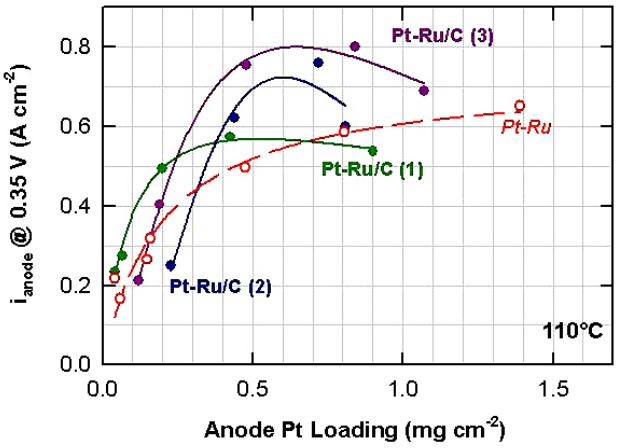

Figure 2. Optimization of the anode performance at low Pt catalyst loadings at 110°C (current density of methanol oxidation determined from the anode polarization plots at a potential of 0.35 V vs. DHE).

0.3 and 1.1 mg cm^{-2}, while formulation (1) has offered an edge at the lowest anode catalyst loadings, which are below 0.2 mg of Pt per cm^2.

In the past year, we have made considerable progress toward the identification of new ionomeric membranes as an alternative to Nafion 117®. A summary of the most important results is given in Table 1. Of several developmental membrane materials tested, some have shown very promising performance, close to or even better than that of the Nafion 117® benchmark. For example, a BPS40 membrane from Virginia Polytechnic Institute and State University exhibited high selectivity and low electro-osmotic drag coefficient λ of water. In this case, substantial reduction in the crossover has resulted in much improved energy conversion efficiency (Figure 3). Membrane A1 is another promising membrane showing reduced methanol crossover without a performance penalty.

We have continued our close collaboration with Ball Aerospace Technologies Corporation (BATC) on the development of a complete DMFC system. In the course of this effort, we have built two more 80-W (gross power) 45-cm^2 30-cell stacks, which were integrated by BATC into a complete brassboard system shown in Figure 4. The system has been capable of running itself for a prolonged time and generating approximately 60 W (net) in power with a total fuel-to-electricity efficiency of 29%.

For most of the fiscal year, we continued the collaboration with Motorola until the completion of our cooperative research and development agreement (CRADA) in May 2001. Aimed specifically at portable electronics application of DMFCs, our collaboration with Motorola has

Table 1. Summary of test data for different alternative membrane materials obtained in a direct methanol fuel cell with 1.0 M methanol at 60°C.

Membrane	Permeability (10^{-6} cm^2 s^{-1})	Conductivity (mS cm^{-1})	Selectivity (10^6 mS s cm^{-3})	Relative Selectivity	λ (H_2O/H^+)
Nafion 117	*2.8*	*85*	*30*	*1.0*	*3.6*
BPS40 (VT)	0.6	38	63	2.1	1.5
BPS45 (VT)	0.8	28	34	1.1	1.9
BPS50 (VT)	0.9	40	46	2.1	2.5
BPS60 (VT)	2.2	52	23	0.8	3.0
IonClad (Pall)	0.6	26	45	1.5	1.1 - 2.5
A1	2.5	89	36	1.2	-
A2	2.7	51	19	0.6	-
N117-TiO_2	2.1	16	7.7	0.3	3.1
N117-SiO_2	2.5	57	23	0.8	3.1

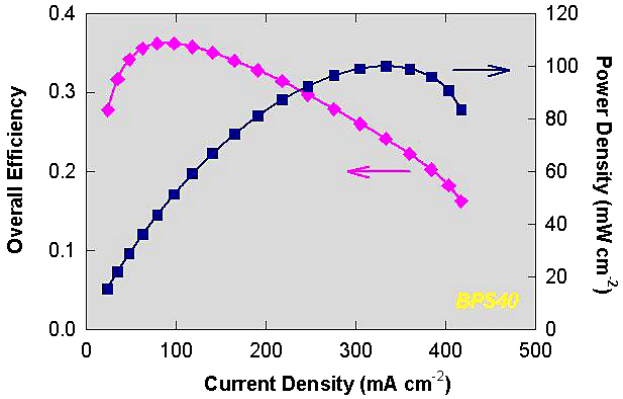

Figure 3. Overall energy-conversion efficiency and power density plots for an experimental BPS40 membrane from Virginia Polytechnic Institute and State University (tested with 1.0 M methanol at 60°C).

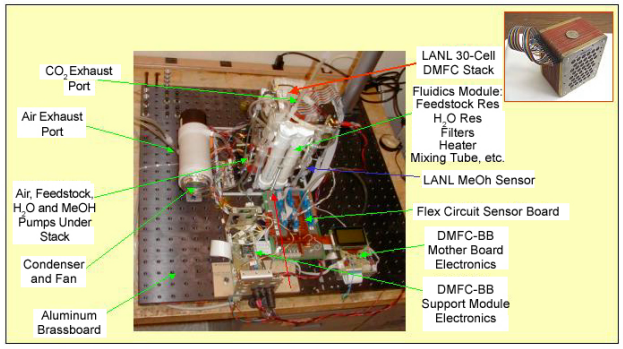

Figure 4. Complete 60-W (net power) DMFC system built by Ball Aerospace Technologies Corporation around 80-W DMFC stack designed and built at LANL.

resulted in building prototype power units using Motorola's ceramic cell technology and LANL's MEAs. When operated at ambient pressure and room temperature, the cells have shown respectable power density and very good stability for 700 h. Future collaborative DMFC research between Motorola and LANL is planned.

Conclusions

DMFC research work at LANL in FY 2001 has concentrated both on fundamental issues, such as catalysts, membranes and electrode structures, as well as on the cell and stack hardware design and testing. Following thorough optimization of the anode and cathode catalysts, we have successfully demonstrated a five-cell DMFC stack with total

MEA platinum loading of only 0.5 mg cm^{-2}. We have identified and characterized several membranes that exhibit reduced crossover of methanol at a performance very similar to that of Nafion 117®. Our collaboration with Ball Aerospace has led to a fully integrated 60-W (net power) brassboard system, which is awaiting final packaging within weeks from the time this report was written. We perceive this success as a firm basis for the scale-up of the DMFC system to the 0.3–0.4-kW level for APU applications. In addition to the planned further hardware/stack development, we intend to continue our research on fundamental aspects of DMFCs, especially on the effect of catalyst composition on the cell performance at different temperatures and on reproducibility and long-term stability of membrane-electrode assemblies utilizing alternative membrane materials.